

Possible depression of canine papillary muscle  
contractility with plasma from aged dogs

ISU  
1980  
G 465  
C. 3

by

Rose Miriam Glassman

A Thesis Submitted to the  
Graduate Faculty in Partial Fulfillment of the  
Requirements for the Degree of  
MASTER OF SCIENCE

Department: Veterinary Physiology and  
Pharmacology  
Major: Veterinary Physiology

---

Signatures have been redacted for privacy

Iowa State University  
Ames, Iowa

1980

Copyright © Rose Miriam Glassman. 1980. All rights reserved.

1268542

## TABLE OF CONTENTS

	Page
INTRODUCTION	1
LITERATURE REVIEW	3
Myocardial Depressant Factor in Shock - a Controversy	3
Characterization of MDF	3
Peptide or salt?	6
Origin of MDF	10
Formation of MDF	14
Transport of MDF	19
Biological action of MDF	22
Blocking MDF formation	26
The separate identity of MDF in light of other proposed cardioinhibitory factors	29
The separate identity of MDF in light of other peptides and substances elevated during shock	37
Human Pancreatic Polypeptide and Age	43
Comparison of Age and Shock	45
Mechanics of Myocardial Contraction	59
A model for muscle	60
Frank-Starling law	61
Preload curve	61
Afterload	64
Force-velocity relation	64
$P_o$	65
$V_{max}$	66
The Hill equation	70
MATERIALS AND METHODS	73
Surgical Procedure for Producing MDF	73
Blood Collection Procedure	74
Dialysis Procedure	74
Lyophilization Procedure	76

	Page
Gel Filtration Chromatography	77
Packing procedure	77
Layering a sample	78
Maintenance of the column	79
Calibration of the column	79
Molecular weight markers	80
Detection of Protein	81
Absorption spectrophotometry	81
Ninhydrin procedure	81
Preparation of Eluted Column Peaks for Papillary Muscle Bioassay	82
Experimental Design	85
Short medical history of two of the dogs	86
Papillary Muscle Bioassay	88
Criteria for judging validity of papillary muscle performance	88
Mounting the papillary muscle	89
Description of the system	92
Measurements	94
Equations used in the computerized mathematical derivation of the preload and afterload curves	97
Statistical Analysis	98
Statistical objectives	99
RESULTS	102
DISCUSSION	204
Discussion of Methods	204
Dialysis	204
Column chromatography	204
Papillary muscle sensitivity	205
Papillary muscle selection	208

	Page
Prestretching the muscle	213
Basis for selecting the preload weight	214
Generating preload and afterload curves backwards	216
Composite force-velocity curves	216
Discussion of Results	217
Conclusions	238
REFERENCES	243
ACKNOWLEDGMENTS	253
APPENDIX	254



## LIST OF TABLES

	Page
Table 1. Assignment of dogs to individual muscle experiments	87
Table 2. Ninhydrin test and average elution volumes of the six peaks of Bio-Gel P-2 chromatograms with an estimate of molecular weight	136
Table 3. Cross-sectional area, muscle length, $L_{\max}$ pre-load, resting tension, and active tension to resting tension ratio values for papillary muscles in the shock and age experiments	138
Table 4. Latency (slope), $P_o$ , $V_{\max}$ , $V_{\max}$ per unit of cross-sectional area, and active tension values for all muscle experiments	139
Table 5. F-values to test for method and age effects and age by method interaction	189
Table 6. Means	192
Table 7. Comparison of the means	193
Table 8. Correlation coefficients	197
Table 9. t-values for latency, $P_o$ , $V_{\max}$ , $V_{\max}$ /cross-sectional area, and active tension for individual muscle experiments	203

## LIST OF FIGURES

	Page
Figure 1. Apparatus for dialysis under pressure	75
Figure 2. Procedure prior to the papillary muscle bioassay	84
Figure 3. Preparation of stainless steel wire with loop for mounting papillary muscles	90
Figure 4. Diagram of statistical design	100
Figure 5. Bio-Gel P-2 column elution pattern of processed shock plasma ultrafiltrate obtained from a young male mongrel dog with experimental pancreatic vessel ischemia	104
Figure 6. Bio-Gel P-2 column elution pattern of processed shock plasma ultrafiltrate obtained from a young male mongrel dog with experimental pancreatic vessel ischemia	106
Figure 7. Bio-Gel P-2 column elution pattern of processed plasma ultrafiltrate obtained from a young male mongrel dog (Y1)	108
Figure 8. Bio-Gel P-2 column elution pattern of processed plasma ultrafiltrate obtained from a young male mongrel dog (Y2)	110
Figure 9. Bio-Gel P-2 column elution pattern of processed plasma ultrafiltrate obtained from a young male shepherd (Y3)	112
Figure 10. Bio-Gel P-2 column elution pattern of processed plasma ultrafiltrate obtained from a young male shepherd (Y3)	114
Figure 11. Bio-Gel P-2 column elution pattern of processed plasma ultrafiltrate obtained from a young female shepherd (Y4)	116
Figure 12. Bio-Gel P-2 column elution pattern of processed plasma ultrafiltrate obtained from a young male mongrel dog (Y5)	118

	Page
Figure 13. Bio-Gel P-2 column elution pattern of processed plasma ultrafiltrate obtained from a young female mongrel dog (Y6)	120
Figure 14. Bio-Gel P-2 column elution pattern of processed plasma ultrafiltrate obtained from an aged female dachshund (15 years) (O1)	122
Figure 15. Bio-Gel P-2 column elution pattern of processed plasma ultrafiltrate obtained from an aged male beagle (13.5 years) (O2)	124
Figure 16. Bio-Gel P-2 column elution pattern of processed plasma ultrafiltrate obtained from an aged male Weimaraner (14 years) (O3)	126
Figure 17. Bio-Gel P-2 column elution pattern of processed plasma ultrafiltrate obtained from an aged male collie (16 years) (O4)	128
Figure 18. Bio-Gel P-2 column elution pattern of processed plasma ultrafiltrate obtained from an aged female beagle (17 years) (O5)	130
Figure 19. Bio-Gel P-2 column elution pattern of processed plasma ultrafiltrate obtained from an aged female dachshund (15 years) (O6)	132
Figure 20. Bio-Gel P-2 column elution pattern of dextran blue (molecular weight 2,000,000)	133
Figure 21. Composite Bio-Gel P-2 column elution pattern of molecular weight markers	135
Figure 22. Typical preload curve	137
Figure 23. Force-velocity curve	141
Figure 24. Force-velocity curve	142
Figure 25. Force-velocity curve	144
Figure 26. Force-velocity curve	145
Figure 27. Force-velocity curve	146

	Page
Figure 28. Force-velocity curve	147
Figure 29. Force-velocity curve	148
Figure 30. Force-velocity curve	149
Figure 31. Force-velocity curve	150
Figure 32. Force-velocity curve	151
Figure 33. Force-velocity curve	153
Figure 34. Force-velocity curve	155
Figure 35. Composite of Krebs-Henseleit force-velocity curves where velocity is plotted against $P/P_0$	157
Figure 36. Composite of processed plasma peak D-young force-velocity curves where velocity is plotted against $P/P_0$	159
Figure 37. Composite of processed plasma peak D-old force-velocity curves where velocity is plotted against $P/P_0$	161
Figure 38. Composite of whole plasma-young force-velocity curves where velocity is plotted against $P/P_0$	162
Figure 39. Composite of whole plasma-old force-velocity curves where velocity is plotted against $P/P_0$	164
Figure 40. Composite Krebs-Henseleit, peak D-young and peak D-old force-velocity curves from age muscle experiments where mean velocity is plotted against $P/P_0$	166
Figure 41. Composite Krebs-Henseleit, plasma-young and plasma-old force-velocity curves from age muscle experiments where mean velocity is plotted against $P/P_0$	167
Figure 42. Composite Krebs-Henseleit, peak D-young and peak D-old force-velocity curves from age muscle experiments where the mean of velocity per unit of cross-sectional area is plotted against $P/P_0$	169

	Page
Figure 43. Composite Krebs-Henseleit, plasma-young and plasma-old force-velocity curves from age muscle experiments where the mean of velocity per unit of cross-sectional area is plotted against $P/P_0$	170
Figure 44. Load-latency curve	171
Figure 45. Load-latency curve	173
Figure 46. Load-latency curve	175
Figure 47. Load-latency curve	177
Figure 48. Load-latency curve	179
Figure 49. Load-latency curve	180
Figure 50. Load-latency curve	182
Figure 51. Load-latency curve	183
Figure 52. Load-latency curve	184
Figure 53. Load-latency curve	186
Figure 54. Load-latency curve	188
Figure 55. Latency (slope) and age	198
Figure 56. $P_0$ and age	199
Figure 57. $V_{max}$ and age	200
Figure 58. $V_{max}$ per unit of cross-sectional area and age	201
Figure 59. Active tension and age	202
Figure 60. Bio-Gel P-2 column elution pattern of processed plasma ultrafiltrate obtained from an aged female beagle (17 years) (O5)	256
Figure 61. Bio-Gel P-2 column elution pattern of processed plasma ultrafiltrate obtained from an aged female beagle (17 years) (O5)	258

## INTRODUCTION

The role of aging in myocardial depression was investigated. It was hypothesized that some component of blood plasma from aged dogs may depress myocardial contractility in young dogs. The experiments in this study were designed to investigate Myocardial Depressant Factor (MDF) as an aging factor. Previously, MDF has been implicated to have an important role in shock.

Many of the changes which occur in the blood and body during the aging process may be correlated with common elements in the mechanism of shock. The primary element present in both shock and aging is the pancreatic origin of MDF (shock) and human pancreatic polypeptide (hpp) (age). Other components are: lysosomes, hydrolase activity, tissue hypoxia, mitochondrial changes, enzyme changes, neutrophilia, protein globulin changes, inhibitory protein and lipid factors, less efficient homeostasis, organ hypoperfusion, serum copper levels, the role of cysteine, and parameters in muscle mechanics which are similarly affected in age and shock.

Most researchers accept the presence of a myocardial depressant factor during shock. The controversy pertains to the isolation and characterization of the factor. Therefore, to initiate this study, the evidence that MDF is a peptide

which can be induced with experimental shock was first established. The search for MDF in the plasma of aged dogs was conducted with gel filtration chromatography. Semi-purified fractions of canine plasma from both young and aged dogs were tested with isolated young canine papillary muscle.

## LITERATURE REVIEW

Myocardial Depressant Factor in  
Shock - a Controversy

The etiology of irreversible circulatory shock is controversial. Two well-known researchers, Allan Lefer and Stephen Wangenstein, debate over the existence of a myocardial depressant factor (MDF) which has been implicated to have an important role in shock. The controversy stems from the uncertainty of the chemical nature of MDF. Some investigators question the peptidic nature of MDF, claiming it is just a salt; others question the origin, formation, transport, and precise actions. Some of the difficulties in the characterization of MDF are apparent from the inconsistent reports on the molecular charge, elution volume from chromatographic columns, and the reaction rate of MDF in in vitro studies.

Characterization of MDF

MDF was first isolated from feline shock plasma by Brand and Lefer (1966). Since then, MDF has been isolated from many species (man, cat, dog, guinea pig, baboon) in a variety of shock states (endotoxic, cardiogenic, hemorrhagic and burn shock, pancreatitis, and in splanchnic, bowel, and pancreatic ischemia). MDF has been reported to be present in shock plasma at concentrations of 0.5-1.0 nmole/ml



(Greene et al., 1977; Yamada and Pettit, 1977), 10 nmoles/ml (Lefer, 1970), and in the picomolar range (Goldfarb and Weber, 1977b).

MDF has been characterized as a biologically active octapeptide or nonapeptide (Lovett et al., 1971). The following amino acids were found in MDF: alanine, aspartic acid, glycine, glutamic acid, iso-leucine, leucine, serine, threonine, and valine (Okuda and Fukui, 1974). An active myocardial depressant component of shock plasma, which was isolated by Bio-gel filtration chromatography as peak D, was further fractionated into nine components by cation exchange chromatography. The fifth component consisted of free L-isoleucine and L-leucine in a ratio of 1:4 and had high cardiodepressant activity which was comparable to the original shock plasma peak D (Goldfarb et al., 1978). Since L-isoleucine was co-purified with L-leucine, each amino acid was tested individually on the papillary muscle bioassay system. Free L-leucine caused a dose-related depression; free L-isoleucine slightly stimulated the muscle.

The amino acid composition of the MDF fraction from high voltage paper electrophoresis consisted of glutamic acid, glycine, serine, and an unidentified acidic amino acid (Greene et al., 1977).

Twenty common amino acids were assayed for inotropic activity at concentrations of 1 and 10 mM. At 1 mM, none of

the twenty amino acids exerted any significant negative inotropic activity. Leucine, glycine and valine were reported to increase the contractile force by 3-4%. Cysteine, histidine and tryptophan each decreased contractile force by 10-20% at a 10 mM concentration (Greene et al., 1977).

MDF has been reported to be a charged substance capable of being bound to mixed cation-anion exchange resins.

While MDF has been described to contain either a positive or a negative electric charge or both (Brand et al., 1969), most researchers have claimed MDF to be anionic.

MDF contains no sulfur-linked amino acids, and may even be a glycopeptide, since an unidentified carbohydrate substance was found in the Dowex-50 active peak D<sub>1</sub> (a further purified Bio-gel peak D) (Lefer, 1970).

MDF was found in the fourth peak (peak D) of a gel filtration chromatogram in an elution volume of 80-100 ml (Lefer and Inge, 1973). A molecular weight range of 500-1000 was thus assigned to MDF; some researchers reported MDF to be between 500-700 daltons, while others claimed it has a molecular weight between 800-1000 daltons. There is disagreement on the elution volume for MDF. Lefer originally found peak D at the 155 ml elution volume, later reported it at 120 ml, and presently recovers it at 80-100 ml. Yamada and Pettit (1977) found the elution volume of MDF to be between 85-105 ml. Wangenstein et al. (1973a) isolated their peak D at 120-150 ml. Goldfarb and Weber (1977b)

claimed MDF was contained in the peak eluted at 122-150 ml. According to Okuda and Fukui (1974), the elution volume for peak D was 135-154 ml. The elution volume for peak D approximated from one of Lefer and Martin's (1970a) original column elution patterns was actually 131-169 ml with a peak height at 156 ml.

MDF was heat stable at 80C for 30 minutes at neutral pH, water soluble, insoluble in methylene chloride, dialyzable, and ninhydrin positive.

#### Peptide or salt?

The primary biological action of MDF is its negative inotropic effect on the isolated papillary muscle, isolated perfused heart, and in the intact animal. This negative inotropic effect follows a dose-response curve.

Wangensteen attributed this depressant activity to salt. He claimed that this MDF was just an artifact of isolation and assay procedure, namely, excess sodium chloride (NaCl) rather than a peptide. The myocardial depressant activity could be correlated only with changes in  $\text{Na}^+$  concentration and, to a lesser degree, calcium ion ( $\text{Ca}^{++}$ ) concentration. According to Wangenstein et al. (1973a), 200 mEq/l of  $\text{Na}^+$  caused 40% depression, 350 mEq/l caused 80% depression and 500 mEq/l caused 100% depression. Thus, an increase in the sodium ion concentration depressed papillary muscle in a linear fashion (Goldfarb and Weber, 1977b). Wangenstein et al.

(1973a) also claimed that peak D and NaCl were eluted from the column at the same elution volume, 120 ml.

When paper high voltage electrophoresis and thin layer chromatography were performed, all bands causing depression of papillary muscle activity were in positions identical to the NaCl bands. Calculated elution-to-void volume ratios for peak D and for salts were 2.44-2.99 and 2.5 or greater, respectively (Wangensteen et al., 1973a). According to Wangenstein, a peptide with a molecular weight of 800-1000 should appear near the elution volume of 63 ml with a  $V_e/V_o$  ratio of 1.4. However, this is assuming that there is no adsorption to the Bio-gel P-2. Certain charged organic substances are adsorbed to the Bio-gel and are eluted at higher volumes than predicted (Wangensteen et al., 1973a).

Lefer and Glenn (1973) insisted that MDF was not an inorganic salt nor an artifact of column chromatography; peak D contained only 10-20 mEq/l NaCl above that of Krebs-Henseleit solution. In fact, proper elution of gel filtration columns yielded sodium concentrations of 120-150 mEq/liter (Lefer and Inge, 1973). Only when total sodium approached 520 mEq/l, a fourfold concentration of plasma sodium, did the salt effect approximate the negative inotropic effect of MDF (Lefer and Inge, 1973). It is therefore highly unlikely that salt could have interfered with the assay of MDF in column eluates. Lefer and several others

have effectively desalted the MDF peak by column chromatography. MDF was eluted prior to the salt peak which showed up at 115-150 ml (Lefer and Inge, 1973) and at a later volume in Goldfarb and Weber's (1977b) study.

If the negative inotropic action of MDF could be attributed to NaCl, the NaCl concentration would have to be far in excess of that occurring during the shock state. Secondly, one could easily distinguish a MDF effect from that of a high salt concentration effect by looking for any changes in base line tension. MDF depresses developed tension by decreasing active tension without a change in resting tension. High salt concentrations depress developed tension by decreasing active tension and markedly increasing resting (base line) tension (Greene et al., 1977). This large increase in base line tension serves to distinguish a MDF activity response from that of a high salt concentration response. Another distinguishing factor is the time to elicit a response. The reaction rate of sodium was different from that of MDF; the sodium effect being instantaneous (Okuda and Fukui, 1974), whereas the MDF effect would take anywhere from 2-30 minutes.

Further evidence that MDF is a peptide has been questioned. Pronase, a nonspecific proteolytic enzyme isolated from Streptomyces griseus, will inactivate peptides by the cleavage of peptide bonds to form single amino acids when

incubated at 55C for four hours. Lefer (1970) reported almost total inactivation of MDF. Wangenstein et al. (1973a) incubated their shock plasma peak D for six hours at 37C followed by one-half hour at 56C to inactivate the enzyme. The depressant activity was not eliminated, thus suggesting that peak D was not a peptide. Wangenstein eliminated the positive inotropic activity of angiotension II, an octapeptide, by the same procedure. Wangenstein dialyzed the enzyme, protease VI, free of calcium prior to use since it was supplied in 30% calcium acetate. Lefer did not report the presence of calcium with his enzyme. However, if Lefer's pronase was supplied with an excess of calcium as a stabilizing agent, calcium would antagonize any depressant activity. Perhaps Lefer's report that pronase incubation caused a loss of depressant activity, and therefore the depressant substance was a peptide is an incorrect inference. The loss of depressant activity could simply be due to masking by the calcium present with the pronase.

Lefer questioned the techniques of Wangenstein and claimed Wangenstein's results were all based on the use of an incorrect peak, the salt peak, as opposed to the peptide peak that Lefer isolated.

Wangenstein et al. (1973a) even went so far as to claim that plasma depressant activities in normal control animals and human volunteers were as high or higher than plasma

activities from those dying in shock.

Goldfarb and Weber (1977b) investigated the problem using different techniques. They obtained a salt-free peptide peak which they purified to obtain one cardio-depressant active peak. They believed MDF to be a single peptide rather than a mixture of different active compounds (Goldfarb and Weber, 1977a; Okuda and Fukui, 1974).

It is of interest that no other known peptide with negative inotropic action has been found in mammals. Eledoisin, an endecapeptide which has been isolated from the salivary gland of the mollusk, is the only known peptide in the entire animal kingdom which will depress the myocardium. A  $10^{-5}$  Molar concentration of eledoisin has decreased the developed tension of papillary muscle in a 10 ml muscle bath by 55% (Lefer and Inge, 1973).

Thus, if MDF is indeed a peptide with negative inotropic action, it will be the first one to be isolated from the vertebrates.

#### Origin of MDF

There is evidence to claim that the ischemic pancreas is the origin of MDF. A marked decrease in the splanchnic blood flow has been reported in various types of shock. Other shock factors which appeared to originate in the splanchnic region were: endotoxin, hemochromogen, RDS (reticuloendothelial depressant substance) from the intestine,

Fukuda's factor from the liver, Clowes' factor and Thal's factor from the splanchnic region.

Pancreatectomy, which was performed prior to the induction of hemorrhagic shock or splanchnic vessel occlusion (SVO), prevented MDF activity in the plasma. Incubated homogenates of pancreas without the presence of plasma or any other tissue constituents produced large amounts of MDF, whereas incubated homogenates of liver, spleen, or intestine failed to produce MDF.

Chromatographic patterns from homogenates of various visceral organs (pancreas, liver, spleen, small intestine, heart) were compared with plasma from animals in shock. Every peak from only the pancreatic elution profile was much higher than the corresponding peaks from plasma. The decrease in papillary muscle contraction was much more severe with MDF from the pancreas peak than with MDF from the plasma peak. Peak D from the liver was higher than peak D from the heart. Peak D from the spleen was higher than peak D from the small intestine. A possible explanation for slightly increased peaks in liver and spleen was that the reticuloendothelial system in these two organs permitted accumulation of MDF in shock animals.

The fractional distribution of cardiac output for several principal organs (heart, brain, gastrointestinal tract, kidneys, skin, muscle, spleen, pancreas) was determined



during hypotension. The most pronounced reduction in blood flow was found in the spleen and pancreas (Okada et al., 1977). This is perhaps another indication that the pancreas is the source of MDF formation.

A review of the conflicting reports on whether MDF is formed in the oligemic phase or postoligemic phase of shock, splanchnic vessel occlusion-no release shock or splanchnic vessel occlusion-release shock, early shock or late shock will further support our reasoning for the ischemic-pancreatic origin of MDF.

Early shock plasma decreased developed tension by 26%, and late shock plasma decreased developed tension by 43% (Lefer, 1970). Splanchnic arterial occlusion (SAO) with release of the occlusive clamps results in high MDF activities in both the plasma and pancreas. Splanchnic arterial occlusion-no release is characterized by a low plasma MDF activity with a very high pancreatic MDF level. This indicates that MDF was produced but not released into the plasma. MDF transport is dependent to a large degree on the splanchnic circulation. This is also evidence that MDF is continuously produced during the entire SAO shock process, since a high residual pancreatic MDF activity was found both in non-released and released SAO shock cats.

Some researchers have shown MDF to accumulate in the oligemic phase before reinfusion of the shed blood, in

contrast to the majority of studies demonstrating high plasma MDF activities only in the postoligemic period after reinfusion (Wangensteen et al., 1970; Glenn and Lefer, 1970).

In those studies where MDF appeared in the plasma during the occlusive period of splanchnic ischemia shock, MDF was transported from the splanchnic bed to the systemic circulation via collateral circulation. In these studies, only the superior mesenteric artery was occluded allowing the celiac axis and inferior mesenteric artery to be the primary collaterals. This explains the discrepancy in the literature concerning the presence of MDF during the occlusive period and postrelease of the occlusion. To reiterate, MDF is formed in the ischemic splanchnic region, the pancreas in particular, during the occlusive period, and probably enters the circulation in large quantities only after release of the occlusion.

Occlusion of just the vessels supplying the pancreas (superior and inferior pancreaticoduodenal arteries) for two hours resulted in high MDF activity comparable to that seen with splanchnic vessel occlusion or hemorrhagic shock. Induced-pancreatitis caused plasma MDF activity to reach shock levels. These studies thus point to the ischemic and/or inflamed pancreas as the origin of MDF.

### Formation of MDF

A generalized scheme for the formation of MDF in the pancreatic acinar cell will introduce the various components and their interactions in shock.

Hypoxia is the primary trigger mechanism for MDF formation. This hypoxia acts on the zymogen granule; trypsinogen, kallikreinogen and phospholipase A are activated. Activation and release of trypsin, which requires calcium ions, serves to initiate proteolysis. Trypsin activates phospholipase A. Trypsin may also partially hydrolyze free protein which makes it available to lysosomal cathepsins. The hypoxia acts on the lysosome causing membrane disruption. Lysosomal proteases such as cathepsins, peptidases, glucuronidases, acid phosphatases are released. The phospholipase A lyses subcellular membranes to release compartmentalized protein. The lysosomal proteases then hydrolyze these compartmentalized protein substances to produce peptide fragments like MDF.

This hypoxia can be induced experimentally by creating a hypotensive condition with splanchnic vessel occlusion, hemorrhagic shock, or cardiogenic shock. A significant decrease in cardiac output develops soon after superior mesenteric artery occlusion. An abrupt decline in mean arterial blood pressure occurs after release of the occlusive clamps in splanchnic arterial occlusion shock due to release

of both MDF and lysosomal enzymes. A fall in systemic arterial blood pressure will result in vasoconstriction of the splanchnic vascular bed. This is a homeostatic attempt to shunt the blood to vital organs. However, this vasoconstriction will create pancreatic ischemia, acidosis, and lysosomal membrane disruption. Lysosomes play an important role in the cellular changes leading to the irreversibility of shock states. Lysosomes of the splanchnic region are more sensitive to ischemia than the lysosomes of other regions of the body, and the pancreatic lysosomes are much more sensitive to ischemia than those of the spleen or intestine.

As a result of pancreatic hypoperfusion, the pancreatic acinar cells underwent severe autolytic changes. Peripheral margination and clumping of chromatin material were evident in the nuclei of the acinar cells. The orderly arrangement of endoplasmic reticulum was lacking. Irregular dilatation of the smooth endoplasmic reticulum resulted in large vesicles. The zymogen granules were not as dense. Advanced degenerative changes in mitochondria were an indication of the cessation of oxidative phosphorylation (Okuda and Fukui, 1974). The pancreatic lysosomes were vacuolated and enlarged which indicated fragility and a less stable membrane. The percent of lysosomal area occupied by autophagic vacuoles in splanchnic arterial occlusion

shock was 25% compared to 7.1% in sham SAO (Lefer and Barenholz, 1972). Autolysosomes were present in pancreatic cells undergoing cellular digestion.

It is speculated that there is a two-component system for MDF production: lysosomal proteases and enzymes of zymogen-granule origin. A cell fractionation scheme for pancreatic homogenates explained how two constituents,  $P_{2A}$  and  $P_{2B}$ , were derived from a particulate  $P_2$  component in an attempt to separate zymogen activity from that of the lysosome (Litvin et al., 1973). The sum of the constituent activities of  $P_{2A}$  and  $P_{2B}$  for cathepsin D was very close to the activity in the parent  $P_2$  fraction. Neither  $P_{2A}$  nor  $P_{2B}$  produced significant amounts of MDF activity when incubated separately; when they were recombined,  $P_{2(A+B)}$ , the MDF activity equalled that of the parent fraction  $P_2$ . A two component system is thus implied.

The unique role of the pancreas in the pathogenesis of circulatory shock is evident. Intracellular acidosis present from the pancreatic ischemia provides an optimal environment for active enzymes. Maximal MDF activity in pancreatic homogenates was found at a pH of 5-6.

Pancreatic trypsin activity increased fourfold and phospholipase A activity increased sevenfold in SAO shock. A decrease in the total pancreatic acid phosphatase specific activity suggests a release of hydrolases from the pancreas

into the plasma. The plasma enzyme activity for acid phosphatase was 594% of control at the termination of SAO shock (Lefer and Barenholz, 1972). Within fifteen minutes after splanchnic arterial occlusion, there was a significant increase in  $\beta$ -glucuronidase and cathepsin activities. Release of the occlusion created an additional rise in the plasma activities of these enzymes; this was actually a washout of enzyme that had accumulated in the ischemic splanchnic bed during the occlusive period. The rise in  $\beta$ -glucuronidase activity peaked within thirty minutes after release of the clamps, but the cathepsin activity continued to increase throughout the entire postrelease period. Final enzyme activities were 3-4 times pre-SAO values (Glenn and Lefer, 1970; Leffler et al., 1973).

Cathepsin B and/or C seem(s) to be the most likely enzyme(s) responsible for MDF production (Litvin et al., 1973).

Pancreatic chymotrypsin activities did not increase in the plasma of SAO shock due to endogenous inhibitors of this protease. Amylase activity correlated with MDF activity; succinate neotetrazolium reductase activity did not (Litvin et al., 1973). A high plasma cathepsin activity was always closely correlated with a high plasma MDF activity, whereas plasma  $\beta$ -glucuronidase activity did not correlate as well (Lovett et al., 1971). Cathepsins B and C, which require

thiol groups for action, are inhibited by parachloromercuribenzoate (PCMB), a sulfhydryl blocking protease inhibitor. PCMB-treatment has been shown to prevent MDF formation (Lefer, 1978).

Plasma amino nitrogen activity, which represents the total end product of all proteolysis, increased 175% above the control value two hours after superior mesenteric artery occlusion and 920% after release of the occlusive clamps (Leffler et al., 1973).

The increase in lysosomal protease activity in the plasma occurred before the plasma appearance of MDF (Glenn and Lefer, 1970), which confirms the scheme for MDF formation. The infusion of just lysosomal enzymes into healthy dogs has been shown to depress cardiac function. Thus, all the necessary ingredients for MDF production are present within the pancreas.

There appears to be some ionic requirement for the MDF-producing reaction. Low MDF activities were found when pancreatic homogenates were prepared in distilled water rather than in Krebs-Henseleit solution, and incubated. Homogenates incubated in Krebs-Henseleit solution had the usual high MDF activities (Litvin et al., 1973). Phospholipase A requires calcium ions for activity, which suggests that ions may serve as enzyme activators in MDF formation (Litvin et al., 1973).

MDF production has been shown to proceed at equal rates in an aerobic or anaerobic environment (Litvin et al., 1973). Mitochondria are therefore not essential for MDF production. Hypoxia, the trigger mechanism for MDF formation, therefore has an action which does not inhibit aerobic metabolism. This further confirms the scheme for MDF formation; pancreatic lysosomes and zymogen granules, which are extremely sensitive to a lowered  $P_{O_2}$ , release the enzymes necessary for MDF formation.

Systemic hypotension is not a prerequisite for MDF formation; however, the pancreas must be rendered ischemic (Lefer and Martin, 1970b). An inverse relationship exists between superior mesenteric artery blood flow and MDF activity. There is some degree of specificity for the production of MDF since femoral ischemia, which was produced by ligation of the common iliac arteries at the descending aorta, did not produce MDF.

#### Transport of MDF

Similar MDF activities were found in both arterial and venous blood (Brand et al., 1969) indicating that MDF was present throughout the blood stream.

In 1943, it was reported that thoracic duct lymph from dogs in traumatic shock contained toxic substances (Lefer, 1973; Lefer, 1978). A transient spikelike increase in lymph flow was shown to occur immediately upon initiation



of hemorrhage (Glenn and Lefer, 1970).

Many proteins including enzymes are known to be transported via lymph. It would be difficult for large molecular weight enzymes (lysosomal enzymes: molecular weight = 25,000-200,000) to cross capillary membranes. Indeed, a significant lymphatic transport of lysosomal enzymes in hemorrhagic shock has been shown (Glenn and Lefer, 1970).

An experiment was conducted with cats in which the thoracic lymph duct was cannulated during shock to divert the lymph. A threefold increase in postligemic survival time was found. In the lymph, MDF activity was high, and plasma cathepsinlike and  $\beta$ -glucuronidase activity were increased three- to fourfold. In the plasma, MDF activity was negligible and the lysosomal enzyme activity was low (Lefer, 1970).

MDF thus appears to be in part transported to the systemic circulation via the lymphatics, which may indicate that it is bound to a larger molecule sometime during its formation. The splanchnic region almost solely provides the thoracic duct lymph in anesthetized cats (Lefer, 1970). The proteases, which are released into the extracellular fluid, are taken up by the lymphatic vessels and transported by the thoracic lymph duct to the systemic circulation. While in the lymph, these proteases may hydrolyze lymphatic proteins to make "preformed" MDF (Lefer, 1970).

Thus, the question exists whether MDF is transported to the systemic circulation via splanchnic collaterals or the lymphatic system. MDF is formed primarily in the plasma, since the volume of lymph is much smaller than the blood volume. However, part of the MDF may be formed in the lymph from lymphatic protein substrate. Additional MDF is formed once the lysosomal enzymes reach the systemic circulation.

It may be concluded that cardiac depression occurs as a consequence of a humoral factor (Gomez and Hamilton, 1964; Okada et al., 1977).

In the hemodynamically protected canine heart, cardiac output, intraventricular, proximal aortic and coronary artery pressures, coronary blood flow, and venous return were maintained at preshock levels, whereas the rest of the body was in shock. Any change in cardiac function would therefore occur only as the composition of the blood changed which was returning from the shocked body to perfuse the coronary arteries. Bradycardia was observed and attributed to the shock-induced metabolic acidosis. Acidosis depresses heart contractility by interfering with normal ionic cycles (Rogel and Hilewitz, 1978). The bradycardia was prevented by normalizing the acidic pH with sodium bicarbonate. The force of contraction of the heart decreased in shock, but this decline could not be prevented by pH adjustment. If the blood from the dog in shock was exchanged with the blood

of a normal healthy dog, the recipient's heart rate decreased and myocardial tension fell just as it had in the shock dog prior to the exchange. Thus, all of the responses to shock occur in control animals if their blood is exchanged with the blood of animals in prolonged shock.

#### Biological action of MDF

MDF seems to play a role in the pathogenesis of circulatory shock by exerting its effects in a positive feedback fashion. This humoral substance depresses the heart and further aggravates the splanchnic ischemia which results in the production of additional MDF to continue the cycle. MDF has reticuloendothelial depressing properties which impair phagocytosis in fixed macrophages (Lefer and Blattberg, 1968).

Thus, with the reticuloendothelial system malfunctioning, a reduced liver blood flow, a depletion of plasma opsonins, and a depressed kidney with oliguria, the animal has few pathways which will remove MDF from the circulatory system. Consequently, MDF accumulates in the plasma.

MDF-induced depression in developed tension is completely reversible. This was shown in the papillary muscle bioassay system by simply washing out the muscle chamber with fresh Krebs-Henseleit solution (Lefer and Blattberg, 1968; Harden and Garrett, 1973). The contractility of muscles returned to the base line level (Okuda and Fukui,

1974).

When the external calcium concentration was increased in the papillary muscle system from 2.54 mM to 6.5 mM, the negative inotropic effect of MDF was also completely reversed. When the test medium containing MDF with the high 6.5 mM calcium concentration was replaced with Krebs-Henseleit solution, there was at first a rapid decline in contractility to the level of previous depression elicited by the MDF. This was followed by a gradual increase in contractility to the base line level. A concentration gradient of MDF was created across the cell membrane of the papillary muscle by washing out the external medium in the muscle chamber. The contractile force of the papillary muscle recovered after washout of the MDF sample with fresh Krebs-Henseleit solution; this indicated that MDF acted intracellularly and diffused out of the myocardial cells according to its concentration gradient (Okuda and Fukui, 1974). Repeated washout of the MDF sample with fresh buffer increased the diffusion rate and recovery of contractility of the muscle to base line level (Okuda and Fukui, 1974).

MDF exerts several other biological actions. A 35% increase in coronary flow by a coronary vasodilation may possibly be due to an increase in myocardial metabolic activity which is brought about by the factor. MDF decreased contractile force 83%, and caused cardiac arrest followed by

arrhythmias (premature ventricular contractions and A-V conduction block) in an isolated perfused cat heart with constant heart rate, coronary perfusion pressure and resting cardiac tension. MDF has been postulated to play a primary role in the development of heart failure during circulatory shock by having a direct depressant effect on the myocardium.

In a study by Harden and Garrett (1973), the reversible nature of MDF may make it unreasonable to assume that this peptide per se could produce irreversible heart failure during circulatory shock. However, an elevated plasma level of metabolic end products and substances which are released during shock may potentiate the cardiotoxic action of the peptide in vivo.

MDF has a hypotensive effect. MDF exerts a selective vasoconstrictor effect on splanchnic vascular strips, and it depresses contractility of isolated intestinal strips. There is an inverse relationship between plasma MDF activity and survival time during shock.

There seems to be a discrepancy in the reaction rate of MDF. A fast acting MDF has been reported to exert maximal depressant action within fifteen to twenty minutes. A slower acting MDF required thirty minutes or longer to cause maximal depression (Okuda and Fukui, 1974). MDF has also been reported to decrease cardiac contractility by 83%

within one to two minutes (Glenn and Lefer, 1970; Harden and Garrett, 1973).

The mechanism of the myocardial depressant effect is hypothesized. The negative inotropic effect is a decrease in developed tension rather than in the time to peak tension or in the resting tension. MDF does not interfere with the electrophysiological properties of isolated papillary muscles. There is no alteration of the magnitude of the transmembrane resting or action potential of the muscle cells. This was determined by the use of intracellular microelectrodes. However, a slight but statistically significant decrease in the time to peak tension was demonstrated in a study using three-hour shock plasma. Control plasma and two-hour shock plasma had no effect on time to peak tension (Lundgren et al., 1976).

This leads us to conclude that the mechanism of the negative inotropic effect is possibly an interference with the process of excitation-contraction coupling or a direct depression of contractile proteins. The mechanism of MDF action may involve binding of calcium in the sarcoplasm, sarcoplasmic reticulum, or at contractile components. This is speculated since MDF depression was reversed by an increment of 4 mM/L of calcium.

It has been deduced that the negative inotropic effect is due to a reduction in active state intensity of the myo-

cardial contractile element (Lefer, 1970; Williams et al., 1969). The contractile element of the myocardium is the active factor which is capable of both shortening and tension development. Changes in peak active state intensity reflect changes in the shortening properties of the contractile element. Changes in peak active state duration indicate changes in the time allotted to the contractile element to produce tension. Thus, the change in peak developed tension by MDF could possibly be brought about by changes in either peak active state intensity or peak active state duration. Since there is no real change in time to peak tension, the negative inotropic action of MDF must therefore be associated with changes in peak active state intensity of the contractile element.

#### Blocking MDF Formation

Pretreatment of animals with high concentrations of glucocorticoids, protease inhibitors, local anesthetics,  $\alpha$ -adrenergic blockers, prostaglandins, sulfhydryl containing compounds, or surgical interventions such as pancreatectomy, diversion of thoracic duct lymph, hemodialysis, pancreatic duct ligation will prevent the accumulation of MDF in the plasma.

Glucocorticoids are the most beneficial, since they stabilize the lysosomal membrane to prevent the release of

those lysosomal enzymes which act in concert with the zymogenic enzymes to form MDF. This was also shown by adrenalectomizing cats to deplete their endogenous glucocorticoids and increase the fragility of pancreatic lysosomes. In fact, the free pancreatic  $\beta$ -glucuronidase activity in adrenalectomized cats was comparable to that found in SAO shock cats (Glenn and Lefer, 1970). Methylprednisolone, a synthetic glucocorticoid, prevented changes in lysosomal hydrolase activity and ultrastructure, mucosal lesions, MDF activity, and prolonged survival time fourfold.

Zymogenic protease inhibitors such as aprotinin inhibit the action of proteases (pancreatic trypsin, chymotrypsin, phospholipase A) when they are released from the zymogen granule. Therefore, the proteases can no longer cleave the protein substrate to form peptide fragments. The MDF level in shock plasma is significantly lowered and survival time is prolonged.

Local anesthetics such as lidocaine cause celiac ganglionic blockade. This partially prevents splanchnic ischemia by maintaining normal splanchnic blood flow to prevent an increase in plasma lysosomal enzymes and MDF (Glenn and Lefer, 1970; Lefer, 1970). Alpha adrenergic blocking agents, such as phenoxybenzamine, maintained splanchnic blood flow during shock (Lovett et al., 1971).

Products formed by the prostaglandin synthetase system



either directly stabilize lysosomal membranes to prevent MDF formation or preserve liver phagocytic cell integrity so cathepsins and MDF may be cleared from the circulation. Prostaglandins increase four- to fivefold in the circulating blood in a variety of shock states (Flynn and Lefer, 1977). Arachidonic acid, a twenty carbon fatty acid, is the primary substrate for the production of prostaglandins. Significant increases in circulating plasma prostaglandins  $\text{PGE}_2$  and  $\text{PGF}_{2\alpha}$  were demonstrated in dogs in hemorrhagic shock after the administration of arachidonic acid. This in turn prevented the plasma accumulation of cathepsin D and MDF while mean arterial blood pressure was maintained.

Prostacyclin ( $\text{PGI}_2$ ), a prostaglandin formed in blood vessel walls, is an anti-ischemic agent. It was five to ten times more potent than  $\text{PGE}_1$  in preventing lysosomal hydrolase release (Lefer and Ogletree, 1978).  $\text{PGI}_2$ , a vasodilator, reduced total peripheral resistance and coronary vascular resistance, and inhibited platelet aggregation and thromboxane  $\text{A}_2$  formation.

Sulfhydryl containing compounds, such as glutathione and cysteine, also stabilize cellular and lysosomal membranes to decrease plasma cathepsin D and MDF activities. An angiotensin converting enzyme inhibitor was also found to have protective action in hemorrhagic shock. Circulating lysosomal hydrolase activity, total plasma proteolysis, and

MDF formation were much less in converting enzyme inhibitor-treated shock than in untreated shock (Trachte and Lefer, 1978).

Dopamine (3,4-dihydroxyphenylethylamine), a unique splanchnic dilator, was found to have only transient beneficial effects on mean arterial blood pressure, renal arterial flow and superior mesenteric arterial flow. MDF formation was only delayed. At high concentrations of dopamine,  $\beta$ -glucuronidase release was reduced, but not cathepsin D (Galvin and Lefer, 1978a). This may imply that cathepsins do play a significant role in MDF formation.

The ability to block MDF formation at specific sites is an indication that our hypothesis that lysosomal and zymogenic proteases are the two major components in the mechanism for MDF production is valid.

#### The separate identity of MDF in light of other proposed cardioinhibitory factors

Pancreatic MDF and plasma MDF are eluted at essentially the same elution volume. Canine MDF also appears at the same elution volume as feline MDF, suggesting some universality among species. MDF produced during splanchnic vessel occlusion is identical to the MDF produced during hemorrhagic shock. In fact, of all the known shock factors, only MDF and endotoxin have been identified in the plasma of human patients in many forms of shock (Lefer, 1973).

Several cardiodepressant factors have been proposed to occur in circulatory shock. We do not know if they are identical, exist as a family of related substances, or are totally unrelated. The similarities among these factors may help to elucidate the identity of MDF.

There are basically fourteen factors, none of which can be precisely characterized: PTLF (passively transferable lethal factor-Nagler-McConn's factor), Goldfarb-Weber's factor, Okuda-Hosono's factor, Okada-Kosugi's factor, Rogel-David's factor, McArdle-Ledingham's factor, Clowe's factor, Thal's factor, Fukuda's factor, hemochromogen, endotoxin, lysosomal hydrolases, RDS (reticuloendothelial depressant substance-Blattberg-Levy's factor), Haglund-Lundgren's factor.

PTLF is a negative inotropic peptide with a molecular weight greater than 10,000. It occurs in rat and man during hemorrhagic and cardiogenic shock. It originates in the blood cells, and its appearance is prevented by the administration of glucocorticoids (Lefer, 1978).

Goldfarb-Weber's factor is a negative inotropic factor with a molecular weight between 250-1000. It possibly occurs in splanchnic ischemia in the dog, originating in the pancreas (Lefer, 1978).

Okuda-Hosono's factor is a negative inotropic factor of 1000 daltons which originates in the canine pancreas

during cardiogenic shock. The administration of glucocorticoids prevents its formation (Lefer, 1978).

Okada-Kosugi's factor is a negative inotropic factor and a reticuloendothelial depressant with a molecular weight between 700-1000. It originates in the canine pancreas during hemorrhagic and endotoxic shock. Protease inhibitors prevent its formation (Lefer, 1978; Okada et al., 1977).

Rogel-David's factor is a negative inotropic factor of unknown molecular weight which occurs in the canine splanchnic region during hemorrhagic shock. Protease inhibitors prevent its formation (Lefer, 1978; David and Rogel, 1976).

McArdle-Ledingham's factor is a negative inotropic factor with a molecular weight of 500-700 which occurs in the dog during hemorrhagic shock. The origin of this factor is unknown (Lefer, 1978).

Clowe's factor is possibly a peptide of 1000-3000 daltons which originates in the canine splanchnic region during septic shock. Its activity is free of endotoxin; it increases pulmonary vascular resistance, induces focal alveolar collapse and right heart failure. Its formation is prevented by glucocorticoids, and aprotinin is partially effective (Lefer, 1973).

Thal's factor has an unknown molecular weight and originates in the canine ischemic splanchnic region during SAO shock. It induces lesions in the lung and stimulates vascular

smooth muscle. Thal's factor may not be a single factor (Lefer, 1973).

Fukuda's factor is probably of large molecular weight, water soluble and heat labile. It originates in the canine ischemic splanchnic region, the liver, during hemorrhagic and endotoxic shock. It causes hypotension and its formation is prevented by glucocorticoids (Lefer, 1973).

Hemochromogen has a large molecular weight of 68,000 and is nondialyzable. It is found in blood absorbed by damaged intestinal mucosa during SAO shock, hemorrhagic shock, and acute pancreatitis in the dog. This hemoglobin derivative causes hypotension, but does not depress the myocardium (Lefer, 1973).

Endotoxin is a lipopolysaccharide of molecular weight 200,000-2,000,000, is nondialyzable, originates in the ischemic intestine, but does not depress the myocardium (Lefer, 1973).

Lysosomal hydrolases have a molecular weight between 25,000-200,000, are heat labile and nondialyzable. They sensitize the heart to other toxic factors (Lefer, 1973).

Hemochromogen, endotoxin, and lysosomal enzymes appear to act indirectly by releasing other agents which act as toxic factors. Since these factors have high molecular weights, they may be degraded further to produce a toxic factor. No endotoxin was found in hepatic portal venous blood of SAO shock animals.

RDS has a molecular weight of nearly 700, is a peptide-sugar with a negative inotropic effect, impairs phagocytosis, originates in the splanchnic region (intestine) during hemorrhagic shock and splanchnic ischemia in the rat, cat, and dog. Although RDS and MDF share some properties (both are reticuloendothelial depressants, dialyzable, small molecules, heat stable, show linear dose-response relationships) they can be distinguished from each other. RDS is methylene chloride soluble and MDF is not. RDS does not show distinct absorbance in ultraviolet light. In RDS there is an unidentified amino acid which does not appear to be acidic, whereas in MDF, an unidentified amino acid which is acidic has been reported. Neither MDF nor RDS can be endotoxin, since endotoxin is not dialyzable, nor does it have a negative inotropic effect on isolated papillary muscles (Lefer, 1978; Blattberg and Levy, 1966).

Haglund-Lundgren's factor is a negative inotropic factor with an unknown molecular weight. It possibly occurs in feline splanchnic ischemia originating in the intestine. Its formation is prevented by glucocorticoids (Lefer, 1978).

Thus, most of these factors appear to be small peptides; most originate in the splanchnic region and exert a negative inotropic effect.

An acute burn serum inhibitor (ABSI), isolated from thermally injured patients, depressed developed tension

and decreased the rate of rise of tension of rat and human heart papillary muscles (Hakim, 1975). This was reversed by digitoxin, a cardiac glycoside. Digitoxin attaches to and activates a glycoside specific receptor,  $Mg^{++}$ ,  $Na^+$ ,  $K^+$  activated transport ATPase, in or on the plasma membrane of cardiac muscle. It was therefore suggested that ABSI may have depressed this ATPase.

The presence of a myocardial depressing substance in dogs subjected to 50% third-degree burns was described. This factor was suggested to have a higher molecular weight than MDF and may be clinically significant only in burns above 80% (Lefer and Glenn, 1973; Wangenstein et al., 1973a).

The presence of an intestinal factor in irreversible shock has been debated. According to Lundgren, MDF is not involved in the intestinal shock model; the intestinal venous blood contained a depressant even though the pancreas had been removed (Lundgren et al., 1976). Haglund also tried to convince us that the shock factor is an intestinal factor and not MDF. Williams demonstrated that experimental cardiac depression could be prevented by an intestinal extirpation (Haglund, 1973). However, in another report, surgical removal of the small intestine did not improve survival in dogs subjected to hemorrhagic shock, whereas chronic ligation of the pancreatic ducts did increase survival. This implies the intestine is not the primary

source of the toxic material in shock.

In 1957, Lillehei suggested the existence of an intestinal factor in irreversible hemorrhagic shock and correlated this factor with mucosal lesions (Haglund, 1973). A causal relationship between these mucosal lesions and irreversibility in shock was suggested. Mucosal lesions have been reported in both man and experimental animals dying in various types of shock. The pathogenesis of these lesions is debated also.

A marked intestinal congestion, a net increase of regional blood volume, has been reported after hemorrhagic hypotension (Haglund, 1973). However, the pooling of blood in the intestinal capacitance vessels was not more than 1-2 ml/100 g intestinal tissue. This small reduction, 1.5%, of the total blood volume could not explain the development of irreversible shock.

Hypoxia is the key factor in the pathogenesis of the mucosal lesions. A hypothesized countercurrent exchange mechanism between the central arterial vessel and the subepithelial network of capillaries of the villi can explain how hypoxia and mucosal lesions develop without any change in villous blood flow (Haglund, 1973; Haglund and Lundgren, 1978). An arterio-venous concentration difference is necessary for substances to diffuse from the central arterial vessel to the nearby subepithelial capillary network.

In severe regional hypotension, mean transit time in



the villi is increased up to five times that of the control. The chances for extravascular shortcircuiting of oxygen in the villi are increased, and the villous tips become anoxic despite an almost unchanged volume flow of blood. Thus, with a low pressure head, dilated villous blood vessels, and a reduced linear blood flow rate, villous lesions result. Destroyed villous cells will allow protein leakage. An increased tissue colloid osmotic pressure and mean hydrostatic capillary pressure will upset the Starling equilibrium across the capillary wall. This explains the increased intestinal tissue fluid volume seen in late hypotension.

The injured intestinal mucosal tissue possibly releases products of tissue destruction such as enzymes, hormones, polypeptidelike substances forming cardiotoxic material (Haglund, 1973). This cardiotoxic material has been isolated and consists of two heat stable fractions; one is water soluble, 500-1000 daltons, and the other is lipid soluble with an unknown molecular weight (Haglund and Lundgren, 1978). A direct relationship has been shown between the degree of mucosal damage and cardiovascular collapse.

The separate identity of MDF in light of other peptides and substances elevated during shock

Other peptides and substances which increased in the plasma of animals during shock were compared with MDF in attempt to elucidate its identity.

It was suggested that MDF may represent an undescribed kinin, since MDF is of the same molecular weight as these vasoactive peptides and is released by proteases (Lovett et al., 1971).

Naturally occurring peptides, such as angiotensin II, arginine vasopressin, and bradykinin, were considered, since they were significantly elevated in shock plasma. Angiotensin exerted a marked positive inotropic effect; vasopressin and bradykinin caused a very small positive inotropic effect. Vasopressin depressed the heart only in very high concentrations and only indirectly via coronary constriction. Angiotensin and vasopressin are vasoconstrictors which constrict the splanchnic, renal, and coronary vascular beds. Bradykinin, a vasodilator, increases capillary permeability and damages the microcirculation. Thus, MDF could not be any one of these three vasoactive peptides, but it is not difficult to see how they might potentiate the action of MDF. Angiotensin, vasopressin, and bradykinin are released early in the course of shock, and are to a large extent metabolized or cleared prior to

the late stages of shock. MDF appears more slowly in the plasma and gradually accumulates during shock. The clearance of MDF is then impaired.

Several synthetic bradykinin and kallidin derivatives were studied, but none significantly altered developed tension of papillary muscles (Lefer and Inge, 1973). Serotonin, a potent intestinal vasodilator, which is released by the intestine after periods of local or hemorrhagic hypotension, was also considered (Haglund, 1973).

It has been concluded that these vasoactive substances along with norepinephrine, acetylcholine, histamine, ferritin, and lactic acid do not appear to be primary toxic factors. The release of these neurohumors is more likely a compensatory response to maintain mean arterial blood pressure or blood flow in shock.

MDF activity was further determined not to be due to the presence of nucleotides or nucleosides (Brand et al., 1969). Charcoal, a highly efficient binding agent for nucleotides, failed to remove MDF activity from shock plasma ultrafiltrate. Inosine and hypoxanthine levels increased in the coronary sinus blood after hypoxia, but neither of these compounds depressed myocardial contractility (Brand et al., 1969).

Several other nitrogenous compounds which increased in the plasma of animals during shock have low molecular weights,

are water soluble, and have charged groups (properties similar to MDF), but they are not myocardial depressants.

Uric acid, urea, creatine, creatinine, and kynurenic acid were some of these nitrogenous compounds (Brand et al., 1969).

It is interesting to note that MDF was associated with a spectrophotofluorometric peak with maximum excitation and emission wavelengths of 330 and 428 m $\mu$ , respectively (Brand et al., 1969). The reduced form of nicotinamide adenine dinucleotide (NADH) and kynurenic acid (a normal metabolite of tryptophan) are the only obvious metabolites which have excitation and emission characteristics similar to this peak and are elevated in shock plasma. The presence of NADH in this peak may be discounted since the sample was pretreated with charcoal in this study.

Plasma cations exert a profound effect on myocardial contractility. Most cations, however, are well-regulated and their plasma concentrations change only slightly in circulatory shock. The plasma concentration of sodium decreased slightly and calcium remained unchanged during shock (Lefer and Inge, 1973). A significantly higher K<sup>+</sup> concentration was found in shock plasma, but this was not of sufficient magnitude to depress myocardial contractility (Lundgren et al., 1976). Intracellular K<sup>+</sup> may have been released from damaged intestinal mucosa accounting for the

elevation in plasma.

Thus, by studying peptides, compounds with an amino nitrogen, amino acids, ions, and other substances that markedly increase in plasma during shock, we can eliminate possibilities of what MDF might be.

A plasma elution profile from a Bio-Gel P-2 gel filtration chromatographic column usually has six peaks which are designated A through F. By comparing profiles from control and shock plasma, the effect of shock on the elevation of certain peptides may be seen. Since each elution volume corresponds to a molecular weight, the presence of known substances may be identified.

Angiotensin and bradykinin were found in peak C. Catecholamines and serotonin, if not inactivated by processing, appeared in peak F. None of the commonly occurring cardio-active substances usually found in plasma were present in peak D which was shown to contain MDF.

Sequential changes in column elution patterns in hemorrhagic shock were studied. As shock progressed, peaks C and D increased while peak A, containing the largest molecular weight molecules decreased (Okada et al., 1974; Okada et al., 1977).

In one study, it was determined that peaks A, B, C had molecular weights greater than 1050, while peaks D, E, F

had molecular weights between 130 and 1050 (Lefer and Martin, 1970a). Glycylglycine (130 daltons) and angiotensin (1050 daltons) were used as molecular weight markers.

The reported approximate molecular weights of peaks A through F were: peak A > 1600, peak B = 1300, peak C = 1100, peak D = 800-1000, peak E = 500-700, peak F = 200-300 (Lefer and Martin, 1970a). Peak A was characterized as consisting of large peptides and proteins. Peak B corresponded to unknown component(s); peak C contained a normal component of plasma; peak D contained MDF; peak E consisted of small peptides; and peak F contained very small peptides (Lefer and Martin, 1970a).

However, there are discrepancies as to the number of peaks obtained, the elution volumes for the peaks, the ninhydrin result for one peak, and even which peak contained the myocardial depressant activity.

Okada et al. (1977) obtained seven distinct peaks instead of the six isolated by Lefer and Martin. Elution volumes for each of the peaks which were approximated from a chromatogram were: A 31-50 ml, B 56-81 ml, C 90-112.5 ml, D 131-168.5 ml, E 181-206 ml, F 225-244 ml with angiotensin at 100-128 ml and glycylglycine at 237-268 ml. The flow rate was 9-12 ml/hr (Lefer and Martin, 1970a).

In another study, peak A began at 90 ml; the flow rate was 10 ml/hr (Okuda and Fukui, 1974). Vitamin B<sub>12</sub> (molecular

weight 1355) was eluted at approximately 84-113 ml and oxytocin (molecular weight 1007) was eluted at approximately 126-131 ml. These values were calculated from a chromatogram (Okuda and Fukui, 1974).

The discrepancy concerning the elution volume for peak D was discussed earlier in this review.

All the peaks were described as ninhydrin positive except for peak B (Lefer and Martin, 1970a). However, according to Okuda and Fukui (1974), peak B was ninhydrin positive.

Peak C in control plasma was reported to have slight myocardial depressant activity, while peak D in the shock animal had a marked myocardial depressant effect which accounted for all of the activity of shock plasma. Harden and Garrett (1973) used the same chromatographic media, but their results differed. Peaks C and E were larger during shock; peak C showed appreciable depression. The flow rates of the columns were 9.6-13.8 ml/hr.

A comparison of ultraviolet absorption spectra between normal and shock ultrafiltrates was made at wavelengths of 220 nm to 320 nm. When optical density was plotted against wavelength, the curve for shock ultrafiltrates peaked at 285 nm where the curve for normal ultrafiltrates remained low (Okada et al., 1977). This again indicates that there

is an increase in circulating peptides during shock, since protein is detected at absorption readings at 280 nm.

#### Human Pancreatic Polypeptide and Age

We have questioned the separate identity of MDF in light of other proposed cardioinhibitory factors, and peptides and substances which are elevated during shock. We can trace the cardiac depression which occurs late in the shock state back to splanchnic (pancreatic) hypoperfusion which occurs during early shock. Thus, the pancreas plays the key role in the ultimate myocardial depression.

The pancreas is also the major source of a polypeptide which can be extremely elevated in plasma during aging. A significant positive correlation of the basal plasma level of human pancreatic polypeptide (hPP) with age has been shown (Floyd et al., 1977; Taylor et al., 1978; Bloom et al., 1978). According to Taylor et al. (1978), there is no obvious explanation for this relation.

Human pancreatic polypeptide can be detected consistently in the plasma of healthy subjects. Pancreatic polypeptide has also been isolated from four additional species: avian, bovine, ovine, and porcine. This polypeptide has thirty-six amino acid residues with an average molecular weight of 4200 (Floyd et al., 1977). The four mammalian



polypeptides have nearly identical amino acid sequences. An amidated carboxyl-terminal residue (tyrosine amide) is present in pancreatic polypeptide from all five species. This is significant; amidated carboxyl-terminal residues appear only in polypeptide hormones which suggests that pancreatic polypeptide may have hormonal properties. Removal of the amidated carboxyl-terminal residue markedly reduces some biological effects of bovine pancreatic polypeptide (bPP). According to Floyd et al. (1977), bPP may be a precursor molecule acted on by another enzyme system.

The physiologic function of pancreatic polypeptide is unknown although a gastrointestinal function is suggested. Bovine pancreatic polypeptide when administered to dogs will inhibit the pancreatic enzyme secretion which is induced by cholecystokinin, and the pancreatic hydrelatic secretion which is regulated by secretin. The in vivo plasma half-life of hPP is estimated to be about five minutes (Floyd et al., 1977).

Human pancreatic polypeptide was undetectable in the plasma of pancreatectomized patients, thus confirming the pancreas as the origin of this polypeptide. Taylor et al. (1978) showed that portal blood contained 1080 pmol hPP/l compared with 176 pmol/l in peripheral blood of a patient with Zollinger-Ellison Syndrome.

The plasma concentration of hPP was also high in genetic and experimental diabetes, pancreatitis, and islet cell tumors. MDF activity was also elevated in pancreatitis.

#### Comparison of Age and Shock

There seem to be several similarities in the mechanisms of shock with that of the aging process.

The deposition of lipofuscin pigment is one of the best characterized age changes in the myocardium. Lipofuscin, a yellow, green, brown pigment, accumulates intracellularly in myocardial cells, spleen, liver, adrenals, thyroid, pituitary, nerve cells, smooth, skeletal, and cardiac muscle (Andrew, 1971; Finch and Hayflick, 1977). The possible origin, development, and significance of lipofuscin is under investigation.

The origin of lipofuscin age pigment is unknown although four possibilities have been suggested. The first possibility is that lipofuscin may represent the remains of lysosomes. The lipofuscin granules are sites of acid phosphatase activity. Acid phosphatase is a lysosomal protease which increases 594% in SAO shock. Several other enzymes have been associated with lipofuscin:  $\beta$ -glucuronidase, esterase, alkaline phosphatase, ATPase, succinic dehydrogenase (Finch and Hayflick, 1977; Strehler, 1964).  $\beta$ -

glucuronidase is another lysosomal protease correlated with shock and MDF activity. Lipofuscin may occur as dense aggregates of very small granules or as organelles containing lucent vacuoles. Lysosomes enlarge and develop vacuoles during shock. Increased numbers of lysosomes have been reported in myocardial cells in aging rats (Finch and Hayflick, 1977). The proposed lysosomal origin of lipofuscin is favored.

The second hypothesis is that lipofuscin may be a byproduct of mitochondrial breakdown. Nonfunctional mitochondria may undergo slow degradation in autophagic vacuoles. Areas of cytoplasm containing mitochondria may be acted on by lytic enzymes. Lipofuscin pigment bodies have been observed to occur in regions of human cardiac muscle with many mitochondria (Strehler, 1964). Advanced degenerative changes occur in pancreatic mitochondria as a result of pancreatic ischemia and other shock conditions which suggests another correlation between shock and age.

Thirdly, lipofuscin is also postulated to be formed by the cross-linking of elements of the endoplasmic reticulum (Kohn, 1971).

The fourth possibility is that lipofuscin granules represent secretory bodies which sequester harmful substances from the cytoplasm (Strehler, 1964).

The linear relationship of accumulation of lipofuscin

with age was indicated by Strehler in 1959 in man. In the human the rate of lipofuscin accumulation was 0.067% pigment volume per myocardial volume per year. Pigment accumulated in the canine myocardium at a rate 5.5 times faster (0.36% per year). There is a definite similarity between the rate of accumulation of lipofuscin pigment in the dog and man, since man has a life span which is approximately five times longer than the dog (Munnell and Getty, 1968; Andrew, 1971). This linear relationship was best seen beginning at 3.5 years of age in the dog. In a twelve year old dog, the pigment volume was 9.7% of the myocardial volume (Munnell and Getty, 1968). There is no adequate mechanism of removal of the accumulation of lipofuscin.

Lipofuscin is a heterogeneous pigment which is composed of lipid, carbohydrate, lipoprotein, and protein. Several amino acids which have been identified in age pigment are: arginine, tryptophan, histidine, lysine, tyrosine, cysteine, cystine (Strehler, 1964; Finch and Hayflick, 1977). Acidic groups with strong acid characteristics are present in lipofuscin. It is hypothesized that lipofuscin is a favored site of absorption of lytic enzymes. It should be noted that hydrolase activity is important in the mechanism of MDF formation. In addition to accumulating with age, lipofuscin will appear with longstanding tissue hypoxia and vitamin E deficiency. It should be remembered that hypoxia

is the trigger mechanism for MDF formation.

Oxidative polymerization of unsaturated lipids is the critical initiating reaction in lipofuscin formation. Vitamin E, a biological antioxidant, inhibits lipid peroxidation. Vitamin E deficiency and aging processes parallel each other (Finch and Hayflick, 1977).

Lipofuscin may impair cell function by interfering with nerve transmission, cardiac contractility, or reactivity of smooth muscle cells in blood vessels. This could explain many of the debilities of age. At this time, we do not know what effect lipofuscin has on cells; we know only that it accumulates with age.

With age, there is an alteration in the permeability of cellular and subcellular membranes in mitochondrial structure, and a reduction in their stability to harmful factors (Frolkis et al., 1973; Tate and Herbener, 1976). The surface density of mitochondrial cristae per unit of cytoplasm, the volume density of mitochondria, and the number of mitochondria per unit of cytoplasm decreased in the heart and liver as mice aged (Tate and Herbener, 1976). Advanced degenerative changes in mitochondria also occurred during shock (Okuda and Fukui, 1974).

The expected enzyme changes which occurred during shock similarly occur with age.  $\beta$ -glucuronidase and cathepsin, hydrolytic enzymes, increase in arteries of humans with age

(Wilson, 1973). Cathepsin in the rat heart also increases with age. Cathepsin was postulated to play a key role in MDF formation. Monoamine oxidase, a myocardial and serum enzyme; pyrophosphatase, a hydrolytic enzyme in blood erythrocytes, peptidase in blood leucocytes, diamine oxidase in the serum, and alkaline phosphatase in the serum increase with age in man (Finch and Hayflick, 1977; Wilson, 1973). Dopamine- $\beta$ -hydroxylase, an enzyme which is necessary for norepinephrine synthesis, increases with age in man. Increased synthesis of norepinephrine, a vasoconstrictor, can be correlated with reflex sympathetic stimulation during shock.

Age-influenced alterations in blood cellular and protein components have been studied. Hematological changes occur with age in many mammalian species.

The number of blood neutrophils increased with age in cattle, sheep, and rats (Riegler and Nellor, 1966). Acute hemorrhage, coronary thrombosis, or almost any factor that causes tissue destruction will cause neutrophilia. Neutrophils increase in number when degenerative substances are released into the blood from necrosing, ischemic heart muscle in coronary thrombosis. Thus, neutrophilia is associated with both shock and age.

The total leucocyte numbers were decreased with increasing age in cows (Riegler and Nellor, 1966). Lymphopenia

also occurred with age. The decrease in leucocytes may indicate a depression in phagocytosis similar to reticulo-endothelial depression in shock. In the beagle, mean leucocyte values have been reported not to change with age (Andrew, 1971). Time trends, environmental effects of the calendar year, were eliminated to reveal hematological changes caused by aging per se in a study by Dougherty and Rosenblatt (1965). After correction factors were applied, it was concluded that the apparent downward trend of the leucocytes with age disappeared, and only the erythrocytes continued to show a downward trend with aging in the beagle.

No change with age was found in total leucocyte numbers in sheep or goats, and an increase was observed in rats. Eosinophil numbers increased with age in sheep. Changes in blood leucocyte patterns are frequently used as an index of alterations in adrenocortical function (Riegler and Nellor, 1966). Cortisol, a glucocorticoid secreted by the adrenal cortex, decreases the number of lymphocytes and eosinophils in the blood (Guyton, 1976). Thus, an increase in total leucocytes and eosinophils might indicate insufficient production of cortisol. A lack of glucocorticoids would promote lysosomal membrane disruption characteristic of shock. Riegler and Nellor (1966), however, do caution us that there seems to be an inconsistent relationship of the hematological patterns to adrenocortical hypo- or hyperfunction.

A decline in hemoglobin content, hematocrit, erythrocyte count, mean corpuscular volume, mean corpuscular hemoglobin, and mean corpuscular hemoglobin concentration occurred with increased age in mice (Ewing and Tauber, 1964). According to Finch and Hayflick (1977), there are no consistent age-dependent changes in many hematological values from species to species.

Statistically significant increases in total plasma protein with increasing age in cattle, sheep, goats, and rats have been shown (Riegler and Nellor, 1966). The percentage of plasma albumin in rats, and plasma gamma globulins in cows and goats increased with age (Riegler and Nellor, 1966). In man, globulins increased from 36.65% of the total protein at 10 years of age to 48.13% at 70 years of age (Finch and Hayflick, 1977). In aged rats,  $\alpha_1$ -globulins and  $\alpha_2$ -globulins increased by 22.4% and 26.8%, respectively (Frolkis et al., 1973). In shock, proteases act on these  $\alpha_2$ -globulins to make peptides like MDF.

According to Orgel's error theory of aging, an increasing number of errors in protein synthesis occurs with age (Wilson, 1973). An age-dependent accumulation of aberrantly behaving protein molecules is possible (Finch and Hayflick, 1977). According to the autoimmunity theory of aging, abnormal serum globulins and autoantibodies are found



in increasing percentages of an aging population (Kohn, 1971).

Plasma or serum from aged animals inhibited cell proliferation in tissue culture media. Both a protein and lipid fraction from the serum were inhibitory (Kohn, 1971). It is suggested that toxic factors are present in the blood from aged animals. It is not unlikely that a variety of inhibitory substances that are excreted or metabolized in the young accumulates in the blood of older animals due to less efficient homeostatic mechanisms. There is a decline with age in the function of the major organ systems (heart, lung, kidney, blood vessels) responsible for maintaining homeostasis. In shock, the homeostatic balance is overwhelmed and MDF is produced.

Age-related changes in the structure and function of the thyroid gland have been studied. The thyroxine-binding capacity of serum thyroxine-binding globulin, thyroxine-binding prealbumin, and albumin is decreased with age, despite an increase in quantity of these proteins (Frolkis et al., 1973). This may indicate that the structure of the serum globulins is changing with age.

There is an increase with age in the deiodination processes in heart, muscles, and liver. Frolkis et al. (1973) suggested that the increased deiodination capacity of the myocardium could help explain cardiovascular disorders in

clinical thyrotoxicosis of old people. A similarity between symptoms of hypothyroidism and aging was suggested.

(Frolkis et al., 1973). Although thyroid hormone secretion decreases with increasing age, the rate of thyroxine ( $T_4$ ) disposal decreases, resulting in an unchanged circulating plasma level of  $T_4$  (Finch and Hayflick, 1977). Triiodo-thyronine ( $T_3$ ), a more potent form of thyroid hormone, significantly decreased with age. The significance of this decrease remains to be determined (Finch and Hayflick, 1977). Kohn (1971) concluded that there is no characteristic endocrine gland failure, with respect to the hormones necessary for life, which is associated with aging.

With age, there is a decrease in perfusion of organs and in tissue permeability, an impaired passage of materials between blood vessels and cells, and an increase in peripheral vascular resistance due to a progressive intermolecular cross-linking of collagen. Pancreatic hypoperfusion was also significant in shock and MDF production. Collagen is distributed in and around walls of all blood vessels and around cells; the passage of materials takes place through a collagen-containing matrix. Diffusion of gases, nutrients, metabolites, hormones, and accumulated toxins is hindered by cross-linked structural proteins due to the vessel-connective tissue-cell relationship.

It is suggested that cross-linking of collagen during

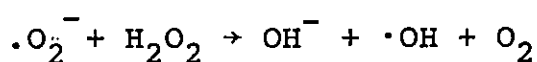
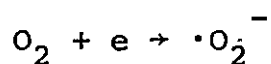
aging results, at least in part, from the oxidation of constituent tyrosine residues to reactive quinoid structures capable of binding covalently to adjacent functional groups (LaBella and Paul, 1965). Amine oxidase plays a role in the oxidative deamination of lysine resulting in cross-linking (Kohn, 1971; Finch and Hayflick, 1977).

Amyloidosis is associated with aging (Finch and Hayflick, 1977). Amyloid is a hyaline eosinophilic material that is mostly in extracellular masses, causing atrophy of adjacent cells. It has different chemical compositions when associated with different diseases. It is suggested that some form of amyloid may be a normal component of connective tissue.

According to Finch and Hayflick (1977), calcium ion concentrations in cardiac muscle of rats decreased as age increased. The increase in collagen content, fibrosis, age pigment, and other morphological changes associated with aging could mechanically interfere with the contractile process.

Free radicals, highly reactive short-lived molecules containing an unpaired electron, increase in the blood with age. Diamine oxidase, an enzyme which increases with age, may produce an excess of superoxide ( $\cdot\text{O}_2^-$ ). Peroxide ( $\text{H}_2\text{O}_2$ ) and oxygen ( $\text{O}_2$ ) are effective in maintaining

autooxidations initiated by active radicals.



The hydroxyl-free radical ( $\cdot\text{OH}$ ) is produced in the above Haber-Weis reaction (Finch and Hayflick, 1977) and plays a role in aging.

Serum copper levels increase with age. Copper serves as an oxidation catalyst for free radical reactions. It is of interest that men with myocardial infarction have significantly higher average serum copper levels (Harman, 1965). A positive correlation of the serum level of copper with coronary artery disease was again shown in Harman and Piette's study in 1966. Ceruloplasmin, a component of the  $\alpha_2$ -globulin fraction of serum, increases with age and is concerned with copper transport, complexing with about 98% of the total serum copper in man (Wilkinson, 1976).

The lipid peroxidation reaction initiating lipofuscin formation is a free radical chain reaction. This reaction causes extensive damage to membrane structure, ATP and  $\alpha$ -tocopherol (Vitamin E) (Finch and Hayflick, 1977). The cross-linking of collagen during aging also results from a free-radical reaction. The most important intermolecular bond, initiated by a reaction of lysyl-oxidase, is catalyzed by copper ions. Oxidative alterations in chromosomal material,

arteriolocapillary fibrosis, and tissue injury are deleterious changes resulting from free radical reactions.

Several substances capable of reacting rapidly with free radicals, such as 2-mercaptoethylamine and cysteine, have been found to significantly prolong the life span of mice (Harman, 1965). It should be remembered that cysteine significantly lowered plasma MDF and cathepsin D activity in shock animals. Perhaps free radicals play a role in shock in addition to aging.

Beneficial effects were produced by free radical reaction inhibitors, and according to Harman (1968) may be due to an inhibiting effect on the rate of amyloid formation.

There is a decrease in serum antioxidants such as ascorbic acid and mercaptans with age (Harman, 1965). Ceruloplasmin is an oxidase and can oxidize ascorbic acid. The decrease in serum levels of readily oxidized substances with advancing age suggests an age-dependent rate of oxidation. Serum mercaptan groups are attached mainly to globulin protein. The possibility exists that newly formed serum protein contains fewer mercaptan groups with increasing age (Harman, 1960).

A major site of formation of extracellular free radicals may be in plasma, since the concentration of molecular oxygen is relatively high, and catalysts for the reaction of

oxygen with lipids, proteins, ascorbic acid, epinephrine are present in small concentrations.

Free radicals appear to be involved with many of the factors that increase in the blood and body with age: diamine oxidase, copper, ceruloplasmin, lipofuscin, cross-linking of collagen, amyloids.

Several investigators have reported age-dependent changes in human cardiac dynamics, such as decreased rates of pressure development, ejection and filling. Contraction rates decreased with increasing age in some papillary muscle studies.

Mechanical properties of muscles reflect the biochemical activity of the contractile proteins within the muscle cells. Heller and Whitehorn (1972) showed that cardiac myosin  $\beta$  extracted from young animals had a significantly higher rate of ATPase activity than that from old animals. Myosin  $\beta$  ATPase activity is the energy-supplying event associated with contraction.

The velocity and extent of shortening of the papillary muscle when lightly preloaded were shown to be significantly age-dependent. Preparations from young animals contracted faster and further. An age-dependent decrease in the velocity of shortening of the contractile element is implied. It is suspected that the series-elastic element is stiffer in the older animal. There was a slight, but

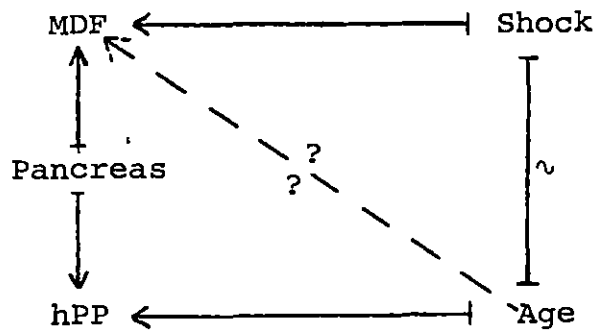
insignificant increase in time to peak tension with age (Heller and Whitehorn, 1972).

The cross-sectional area of the papillary muscle increased significantly with age (Heller and Whitehorn, 1972). When the cross-sectional area increases, mechanical properties can be affected by a hypoxic core (less oxygenation of the inner core of the muscle). The slight decrease in active tension development with increasing age may be due to this hypoxic core effect (Heller and Whitehorn, 1972).

According to Heller and Whitehorn (1972), the rate phenomena of the contracting muscle is most affected by aging, being regulated by the enzymatic activity of the contractile proteins (myosin-ATPase).

Thus, the myocardial contractile properties altered with age were similarly affected in shock. Many of the changes occurring in the blood and body in the aging process can be traced to common elements in the shock picture.

It is this interesting similarity between shock and age that I base my hypothesis. If there really is a shock-induced MDF which I will first confirm, I will attempt to demonstrate its additional presence in the plasma of aged dogs, thus tying together the many similarities between shock and age.



### Mechanics of Myocardial Contraction

It was demonstrated in 1944 that the isolated papillary muscle could be used for mechanical studies of the myocardium (Grimm and Wohlfart, 1974). The papillary muscle provides a sample of parallel fibers of cardiac muscle without the geometric complexities of the heart.

The papillary muscles are attached by chordae tendinae to the leaflets of the atrioventricular valves in vivo. The papillary muscles and the ventricular walls contract to pull the leaflets of the valves toward the ventricular chamber. This prevents the valves from being forced too far backward into the atrial chamber during ventricular contraction. If a chorda tendinea is ruptured or if a papillary muscle is paralyzed, the valve is forced backward, causing it to leak. A severe cardiac incapacity may result.

In vitro, the isolated papillary muscle system can be



used as a bioassay for MDF. Alterations of the mechanical performance of the muscle which are induced by MDF can be demonstrated with force-velocity relations.

Concepts, clarification of the parameters used in experimental procedures, and their relation to in vivo situations are presented.

### A model for muscle

A three-component model devised for skeletal muscle, the Maxwell version of the Hill 1939 model, seems to be the most suitable mechanical model for rat papillary muscle (Minelli et al., 1975). The first component, the contractile element (CE), develops force and shortens when activated, and is extensible at rest. The primary components of the CE are myosin and actin filaments with their cross-bridges. The second component is the series elastic element (SE) which is composed of nonactivatable tissue. In series with the CE, the SE is passively stretched by shortening of the CE. The third component is the parallel elastic element (PE) which is also nonactivatable tissue and is parallel to both the CE and the SE. The PE maintains resting length of the freely extensible CE and supports the SE during resting tension.

In brief, when the CE contracts and shortens, the SE is stretched. When the contractile force stretches the SE

to the point that its elastic tension equals and exceeds the load, the muscle shortens and lifts the load. Thus, the active state of the CE is transformed into external mechanical activity by stretching the SE. The active state represents a capacity of the CE to shorten and develop force. Maximal isometric tension developed by the CE is the greatest tension that can be produced without appreciable shortening of the muscle (Parmley et al., 1972; Grood et al., 1974).

#### Frank-Starling law

The Frank-Starling law of the heart is an underlying concept in cardiac physiology which basically states that cardiac output is a function of venous return. The heart has an intrinsic ability to adapt to changing volumes of inflowing blood. When additional blood enters the heart chambers, cardiac muscle becomes stretched, which alters the initial length of the cardiac muscle fibers. The stretched muscle will normally contract with increased force to pump the extra blood into the arteries.

#### Preload curve

The mechanism of the Frank-Starling law has been demonstrated in vitro with the mechanics of isolated papillary muscle. The dependence of the force of contraction

on initial muscle length (preload) has been depicted by the length-tension curve (preload curve). Preload has been defined as the amount of weight attached to a lever which establishes the resting length and tension in the inactive muscle before a contraction occurs. With the left ventricle as an example, preload is analogous to left ventricular end-diastolic volume in vivo which determines muscle fiber length which in turn is analogous to end-diastolic pressure. Preload determines the degree to which the myocardium is stretched before it contracts.

In the following discussion on preload and afterload it is assumed that the state of contractility is held constant. The ventricle normally functions along the ascending limb of the length-tension curve. The peak of the curve is defined as  $L_{\max}$ , the length of muscle that produces maximal contraction. Sarcomere length is directly related to muscle length. Thus,  $L_{\max}$  is that length determined by a preload which produces the optimal average sarcomere length to give maximal contraction. A preload of a selected percentage of  $L_{\max}$  is a preload which will give that percentage of maximal contraction. When muscle length (sarcomere length) is either shortened or increased from  $L_{\max}$ , developed tension falls.

In isolated papillary muscle, peak developed tension has been shown to occur with a sarcomere length of about

2.2 $\mu$  (Leyton et al., 1971; Detweiler, 1973). The sarcomere is the fundamental contractile unit. The contractile proteins, actin and myosin, are arranged in an interdigitating array within each sarcomere. Contraction involves a movement of the actin filaments towards the center of the sarcomere, sliding between the myosin filaments. A sarcomere length of 2.2 $\mu$  is an optimal overlap of thick and thin (myosin and actin) filaments to produce a maximal contraction. Further stretching causes withdrawal of actin filaments from the interaction with myosin. Lateral projections (cross-bridges) from the thick filaments attach to thin filaments during activation, and are involved with the generation of a force which pulls the thin filaments inward. This is the cross-bridge theory. Thus, optimal overlap between thick and thin filaments allows for potentially more cross-bridge attachments which has the important consequence of the generation of more force.

The length-tension curve is therefore an experimental derivation of the Frank-Starling law of cardiac tissue. A sarcomere length of 2.2 $\mu$ , in addition to corresponding to  $L_{max}$ , occurs at the upper limit of diastolic filling pressure in both the right and left ventricles (Leyton et al., 1971). An increase in diastolic filling changes the length of the individual muscle fibers. This alters the degree of overlap of the filaments, which in turn alters the number of active

contractile sites which are capable of generating force.

### Afterload

The preload and afterload together make up the total load which the muscle contends with when stimulated. In vitro, afterload is the additional weight added after a stop has been fixed onto the arm of a lever. (The stop prevents further stretching of the resting muscle and thus prevents the afterload from acting as a preload). It is an additional load for the muscle when it begins to contract. In vivo, afterload is analogous to the aortic pressure, the resistance against which blood is expelled from the heart.

In summary, the volume of ventricular filling determines the initial length of the muscle fibers (preload). At the time of systole, the fibers contract isometrically until the pressure in the ventricle exceeds that in the arteries and blood is ejected. The ventricular fibers then shorten as contraction proceeds against the pressure in the aorta and pulmonary arteries (afterload).

### Force-velocity relation

When preload, which determines initial muscle length, is kept constant, there is an inverse relationship between force and velocity. The initial velocity of shortening decreases with increasing afterload as demonstrated by the

force-velocity curve (Parmley and Chuck, 1973).

The inverse force-velocity relationship is considered to be associated with the CE and may be explained by the sliding filament and cross-bridge theory. A certain amount of time is required for a cross-bridge to attach to an active site on the thin filament and develop force. The muscle has a slow shortening velocity, because time is consumed by the formation of a large number of cross-bridges which result in a large generation of force. A rapid velocity occurs when less total force is generated by the formation of a fewer number of cross-bridges which require less time to attach to the active sites on actin, as well as to react and develop force (Naylor, 1975).

$P_0$  The two intercepts of the force-velocity curve merit discussion.  $P_0$ , the x-intercept, is the load which just prevents external muscle shortening and represents maximum isometric force.  $P_0$  is proportional to the fraction of active sites capable of producing force (actin-myosin interactions) at zero contractile element velocity. Thus, with a constant or given state of contractility, changes in  $P_0$  are produced by alterations in muscle length.

$\underline{V_{max}}$   $V_{max}$ , the y-intercept on a force-velocity curve, is an extrapolated maximum velocity of shortening of the contractile filaments at zero load.  $V_{max}$  cannot be measured directly because the muscle cannot be fully unloaded. The true  $V_{max}$  occurs when the internal load is zero; this is different from the extrapolated  $V_{max}$  where only the external load is zero.

According to Gulch and Jacob (1975a, 1975b), there are unknown "nonvanishing" internal forces which mechanically hinder the sliding movement of the filaments and influence  $V_{max}$  measurement. Edman and Nilsson (1972) and Grood et al. (1974) also suggested the presence of a substantial intrinsic load acting upon the myofilaments. If muscle fibers are prevented from widening during shortening, a pressure rises, ultimately producing a longitudinal force at each end of the fiber which would act as a load upon the CE.

There is a controversy concerning the independence of  $V_{max}$  on muscle length. This debate is significant since it questions the value of  $V_{max}$  as an index of contractility in cardiac muscle. A constancy of  $V_{max}$  over a range of muscle length is important for its use as such an index, particularly in the intact heart. According to Parmley et al. (1972),  $V_{max}$ -total independence of preload is an ideal requirement for an index of the contractile state.  $V_{max}$

should only be altered by inotropic influences if it is to be used as an index of contractility. Contractility has been described as changes in the mechanical performance of cardiac muscle which are independent of fiber length (Donald et al., 1972). A change in contractile state relates to the rate at which cross-bridges between the myofilaments are formed and broken (Parmley and Chuck, 1973). Thus, an index of cardiac contractility should serve to distinguish altered mechanical responses of muscle due to changes in length from changes in the intensity of the active state due to inotropic interventions.

$V_{\max}$  is determined by the rate at which the actin-activated myosin cross-bridges hydrolyze ATP (myosin ATPase activity), and is independent of the number of active sites.  $V_{\max}$  is increased by positive inotropic agents such as norepinephrine, digitalis, glycosides, calcium.

$V_{\max}$  is unchanged by changes in preload, but altered by changes in contractile state (Parmley et al., 1972; Detweiler, 1973). According to Grood et al. (1974), the only influence of muscle length was to determine the number of participating cross-bridges. There was an increase in the force developed ( $P_0$ ) when preload was increased (Detweiler, 1973; Parmley et al., 1969; Kababgi et al., 1974).



According to Weber and Janicki (1977), shortening velocity was independent of initial muscle length, the initial length serving only as the starting point of the contraction. It has been concluded that the velocity of fiber shortening serves as a useful estimate of the contractile state.

According to Brutsaert et al. (1971, 1973),  $V_{\max}$  remained constant and was thus independent of the initial muscle length from  $L_{\max}$  to 87.5%  $L_{\max}$ . This corresponded to sarcomere lengths of  $2.2\mu$  and  $1.9\mu$  indicating that  $V_{\max}$  was independent of the degree of myofilament overlap.

However, when sarcomere lengths of  $1.8\mu$  or less were reached during shortening,  $V_{\max}$  fell with length. The reason for this decline in  $V_{\max}$  at shorter lengths was and is poorly understood. It is possible that at these short sarcomere lengths, the thin filaments may pass into the opposite half of the sarcomere and interfere with force-generating bonds (Brutsaert et al., 1971; Brutsaert et al., 1973). Internal forces may also come into play at these short lengths.

According to Noble (1974),  $V_{\max}$  exhibited only small length-dependence when muscle lengths were studied from 94%  $L_{\max}$  to 100%  $L_{\max}$ .

Conflicting results have been reported by other investigators. According to Parmley et al. (1972) and Minelli et al. (1975), increasing the muscle length along the ascending limb of the Frank-Starling length-tension curve

resulted in increases in both  $V_{\max}$  of the CE and  $P_0$ . Thus,  $V_{\max}$  was dependent on muscle length.  $V_{\max}$  was significantly dependent on preload (increasing with muscle length) even in the physiological range between 85%  $L_{\max}$  and  $L_{\max}$  (Gulch and Jacob, 1975a).

According to Donald et al. (1972),  $V_{\max}$  was significantly increased with increasing initial muscle length. A linearized form of the Hill equation was used. At the shortest muscle length,  $V_{\max}$  was 76% of its maximum, while the isometric force ( $P_0$ ) was 43% of its maximum. It was concluded that  $V_{\max}$  was less sensitive than isometric force to changes in muscle fiber length in cardiac muscle. It has been proposed that the factors responsible for the drastic fall in isometric force ( $P_0$ ) at muscle lengths below  $L_{\max}$ , would probably have a similar effect on  $V_{\max}$  to the same degree, as is true in skeletal muscle.

The mechanisms which are responsible for the muscle length-dependent change in contractile state have not been determined. One cause may be an increase in available  $Ca^{++}$  to the myofilaments (Parmley and Chuck, 1973).

Loeffler and Sagawa (1975) claimed that use of a three-element muscle model might invalidate the once widespread postulate that  $V_{\max}$  of the CE is independent of initial muscle length.

In spite of these discrepancies concerning the value of

$V_{\max}$  as an index of contractile state, it has been used. Okada et al. (1977) have expressed the depression of myocardial contractility in terms of  $V_{\max}$  by studying sequential changes in  $V_{\max}$  during hemorrhagic shock.

According to Weber and Janicki (1977), an adequate minimum definition of contractile state must include a description of instantaneous force, shortening velocity and fiber length. The most relevant index of myocardial activity may be provided by the force-velocity relation (Edman, 1977).

The Hill equation      The Hill equation should be questioned as to its applicability to cardiac muscle. The true shape of the force-velocity curve in cardiac muscle is still debated. A. V. Hill, in 1938, identified the mathematical relationship between force and velocity as fitting a hyperbolic curve for tetanically stimulated skeletal muscle. The Hill equation is:

$$(P+a)v = b(P_0 - P)$$

$P$  represents force;  $v$  represents velocity;  $P_0$  is isometric force.  $V_{\max}$  is calculated as  $bP_0/a$ . "a" and "b" are mechanical constants; "a" has dimensions of force; "b" has dimensions of velocity. When  $(P_0 - P)/v$  is plotted against  $P$ , a straight line with positive slope  $1/b$  and y-intercept  $a/b$  results

(Brady, 1965).

Since "a" has dimensions of force,  $(P+a)v = \text{force} \times \text{velocity} = \text{energy}$ . The term  $b(P_0 - P)$  increases as the force,  $P$ , decreases. Thus, the energy output of a muscle increases as the load,  $P$ , decreases as defined in the Hill equation (Goll et al., 1977).

The force-velocity relationship was extended to cardiac muscle and found to be significantly nonhyperbolic by many investigators (Loeffler and Sagawa, 1975; Donald et al., 1972; Nayler, 1975; Gulch and Jacob, 1975a; Brady, 1965).

It is rare that cardiac muscle force-velocity curves can be described by the Hill equation (Donald et al., 1972; Nayler, 1975). Cardiac muscle force-velocity curves obtained from afterloaded isotonic contractions are not usually hyperbolic in shape over the entire force domain; they generally become linear or concave downward at the higher forces.

Edman and Nilsson (1972) were only able to obtain a hyperbolic force-velocity relation by an instantaneous quick-release method when they maintained the length of the CE constant. However, the quick-release method has been questioned by those who have claimed that the technique introduces errors (Loeffler and Sagawa, 1975; Noble and Else, 1972).

According to Brady (1965), the data from skeletal muscle

experiments fit the rectangular hyperbola of Hill due to inherent muscle properties which cardiac muscle does not share. There are four basic properties: the onset of contractility is rapid; twitch tensions can be summated by repeated stimulation such that developed tension becomes independent of time; maximum tetanic tension development is not greatly length dependent over a significant range of muscle lengths; and the contribution of resting tension to total tension is negligible over this range of lengths.

Data from rabbit papillary muscle experiments did not fit hyperbolic force-velocity relations. The curves which Brady (1965) developed were not straight lines with positive slopes. It was concluded that the Hill equation for skeletal muscle cannot be applied to cardiac muscle whose force-velocity relation is nonhyperbolic (Brady, 1965). This was explained by proposing that the excitation-contraction coupling in cardiac muscle is different.

## MATERIALS AND METHODS

Surgical Procedure for  
Producing MDF

Pancreatic ischemia was produced by occlusion of the superior and inferior pancreaticoduodenal arteries, and the splenic artery in a young male mongrel dog. Rubber bands were used to occlude the vessels.

A ventral midline abdominal incision was made from the xiphoid process caudally to a point along the linea alba where manipulation of the pancreas would be possible. The superior pancreaticoduodenal artery was ligated caudal to the bifurcation of the gastroduodenal artery (originating from the hepatic artery) into the right gastroepiploic artery and the superior pancreaticoduodenal artery which enters the right pancreatic lobe. The inferior pancreaticoduodenal artery which also enters the right pancreatic lobe was ligated caudal to the superior mesenteric artery bifurcation. The splenic artery which enters the left pancreatic lobe was ligated caudal to the celiac bifurcation. The pancreatic branch of the superior pancreaticoduodenal artery which enters the left lobe and anastomoses with pancreatic branches of the splenic artery was occluded. Small branches from the common hepatic artery entering the left pancreatic lobe were checked for occlusion.

The duration of the occlusion was 130 minutes. The rubber

bands were removed over a 15 minute period. Twenty minutes after removal of the last rubber band, sixty milliliters of blood were withdrawn from the hepatic portal vein for MDF isolation.

#### Blood Collection Procedure

Although blood was withdrawn from the shock animal via the hepatic portal vein, the jugular vein was used to obtain blood from the aged animal.

Blood was collected in 10-ml heparinized vacutainer tubes (Becton-Dickinson) and immediately placed in an ice bath. The blood was centrifuged in a GLC-1 Sorvall centrifuge at 2500 rpm for 20 minutes at 4C. The plasma was removed with a disposable pasteur pipette and placed in 20-ml scintillation vials, bubbled with N<sub>2</sub>, and stored at 0C.

#### Dialysis Procedure

The frozen plasma was thawed, filtered with glass wool to remove the cryoprecipitable proteins, and dialyzed against double distilled, deionized water under a pressure of 200 mm Hg for 48 hours at 4C (Figure 1).

One end of Spectra/Por 6 dialysis tubing with a flat width of 32 mm, a diameter of 20.4 mm, and a molecular weight cutoff of 2000 (Spectrum Medical Industries) was

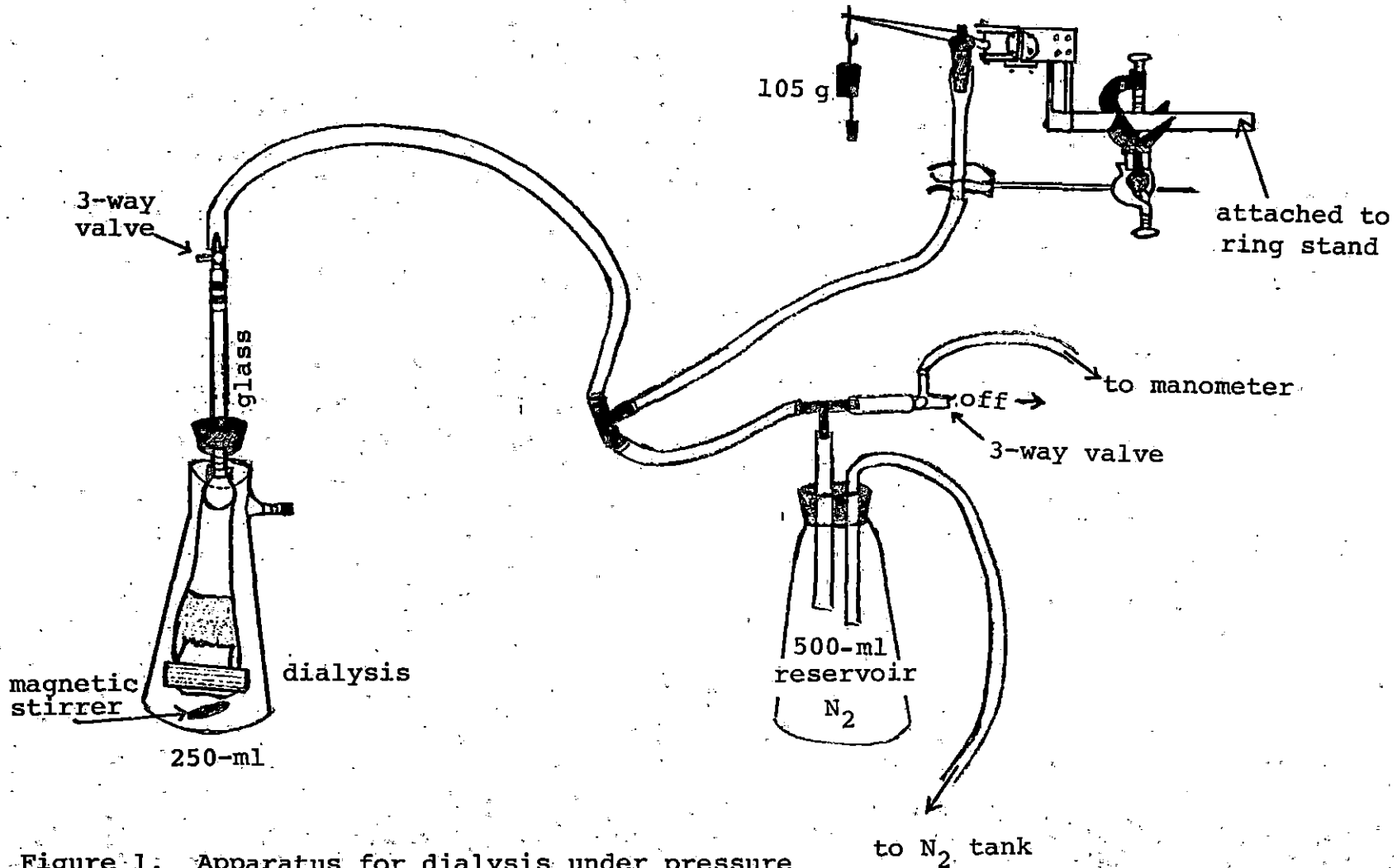


Figure 1. Apparatus for dialysis under pressure



gently fastened onto the half-bulb end of a 1-ml volumetric glass pipette with rubber bands and plastic straps. A spectrapor closure was used to seal off the other end of the dialysis tubing. The dialysis tubing suspended from the pipette was placed into a 250-ml Erlenmeyer flask filled with 250 ml double distilled, deionized water. The membrane was kept moist at all times during the attachment procedure. Approximately twenty ml of filtered plasma was then placed into the dialysis tubing via a three-way valve at the distal end of the pipette.

As the pressure provided by a  $N_2$  tank was slowly increased to 200 mm Hg, which was monitored continuously with a manometer, observations were made for pinhole leaks in the membrane. The dialyzing was periodically checked during the 48 hour period for leaks in the system and a ruptured membrane.

#### Lyophilization Procedure

Ten-milliliter portions of the plasma ultrafiltrate were lyophilized for approximately 7 hours (Labconco freeze dryer-5). The lyophilized sample was either stored under  $N_2$  or reconstituted to 2 ml (20% of the original volume) with double distilled, deionized water and centrifuged at 2250 rpm for 10 minutes at 4C.

## Gel Filtration Chromatography

The supernatant fluid of the centrifuged 2-ml lyophilized plasma ultrafiltrate sample was then layered on a glass barrel Econo-column with a 1.5 cm I.D., 120 cm column length, 190-ml column volume (Bio Rad Laboratories). The column was packed with Bio-Gel P-2, a polyacrylamide gel (200-400 wet mesh). Substances with molecular weights between 200-1600 are separated (Lefer, 1970). This is the exclusion limit for Bio-Gel P-2. A 500-ml Econo-column reservoir was fitted onto the column. Medical grade vinyl tubing (0.082 I.D. x 0.142 O.D.) (Becton-Dickinson) was attached to the Luer outlet of the column and varied in length from 260-330 cm for four columns. The tubing and the height of the column were adjusted so that the pressure head would be sufficient to establish gravity flow rates between 9.2 and 11.4 ml/hr. The eluate was collected in 4.6-5.7 ml fractions (depending on the flow rate) (Buchler Fractometre 200 automatic fraction collector, circular ISCO fraction collector).

### Packing procedure

54.3 g of Bio-Gel P-2 was dissolved in 570 ml of modified Krebs-Henseleit buffer without dextrose and bicarbonate (pH 7.38) in a 1000-ml Erlenmeyer flask with sidearm. The gel was allowed to swell at room temperature for four hours.

After warming the resultant slurry in a 60C water bath for 30 minutes, it was deaerated by vacuum for 15 minutes. The gel was then ready for packing the column.

Deaerated Krebs-Henseleit buffer minus dextrose (pH 7.38) was first poured into the column to fill up approximately 20% of the column volume. The entire slurry was then poured through the reservoir fitted on top of the column. The column settled by gravity flow. After a short while, the column was allowed to flow by removal of a hemostat which was originally placed on the tubing exiting from the column Luer outlet.

The freshly prepared column was then transferred to the cold room (4C) where all additional column work and dialysis were conducted.

#### Layering a sample

Before layering a sample on the column, the optical density of an eluted buffer fraction was read at 230 nm to check for any contamination. A deaerated, modified dextrose-free Krebs-Henseleit buffer (pH 7.38) was used to elute the column.

With a piece of tubing, the buffer was siphoned out of the reservoir and the remainder of the buffer was pipetted out of the column to the level of the bed. The sample was carefully introduced down the sides of the column

with a long pipette without disturbing the bed. After the 2-ml sample was just absorbed, two 2-ml aliquots of buffer were applied in a similar fashion to move the sample down the column.

The first fraction was collected as soon as the sample was applied to the column. After the second 2-ml aliquot of buffer was just absorbed into the bed, fresh buffer was gently pipetted down the sides of the column to fill that portion of the column above the top of the bed. The reservoir was replaced and slowly refilled with fresh buffer. Fractions were collected until the total elution volume reached approximately 300 ml.

#### Maintenance of the column

At the end of each run, the buffer level was drained to the top of the bed. The upper 1.0-1.5 cm layer of the gel bed was stirred up and removed with pasteur pipettes. The entire buffer volume down to the top layer of the bed was removed and replaced with fresh, deaerated buffer on alternate days. Additional fresh buffer was added to the reservoir at all other times. The columns flowed continuously.

#### Calibration of the column

The void volumes of the columns were determined with dextran blue (molecular weight 2,000,000) (Sigma). Twenty mg of dextran blue was dissolved in 1 ml of H<sub>2</sub>O. One drop

of this solution was then placed in 1 ml of buffer and this 1-ml sample was layered on the column. The only modifications were that whenever a 1-ml sample was applied which only occurred for molecular weight markers, 1-ml aliquots of buffer were used instead of 2-ml aliquots to move the sample through the column.

Molecular weight markers Five mg of angiotensin II (1-L-asparaginy1-5-L valyl angiotensin octapeptide) with a molecular weight of 1225 (Ciba Pharmaceutical Company) was dissolved in 1 ml of water (0.0041 M solution) and layered on three columns at separate times. The optical density was read at 280 nm.

Five mg of 5-isoleucine angiotensin II (L-asparaginy1-L-arginyl-L-valyl-L-tyrosyl-L-isoleucyl-L-histidyl-L-prolyl-L-phenylalanine·CH<sub>3</sub>COOH) with a molecular weight of 1106.3 (Sigma) was dissolved in 1 ml of water (0.0045 M solution) and layered on one column. The optical density was read at 280 nm.

Five mg of angiotensin III inhibitor (des-Asp<sup>1</sup>, Ile<sup>8</sup> angiotensin II; H-Arg-Val-Tyr-Ile-His-Pro-Ile-OH) with a molecular weight of 896 (Beckman) was dissolved in 1 ml of 0.1 M acetic acid and layered on one column. The optical density was read at 280 nm.

Fifty mg of hexaglycine white crystals with a molecular

weight of 360.3 (Sigma) was placed in 1 ml of 1N HCl, warmed until dissolution, and then layered on one column. This was repeated using 30 mg of hexaglycine in 1 ml of warm 1N HCl. The optical density was read at 280 nm.

Two ml of a 0.03 M solution of glycylglycine with a molecular weight of 132.1 (ICN Nutritional Biochemicals) was layered on four columns. The optical density was read at 230 nm.

### Detection of Protein

#### Absorption spectrophotometry

Elution chromatograms were derived from optical density readings at 230 nm using quartz cuvettes and a Beckman DB-GT spectrophotometer for the fractions of each column run. Most of the molecular weight markers were detected at 280 nm.

#### Ninhydrin procedure

The presence of amino nitrogen in the eluate was confirmed by the ninhydrin reaction which yields a violet condensation product, diketohydrindylidene-diketohydrindamine. The ninhydrin reagent was prepared according to the method of Kabat (1961): 40 mg  $\text{SnCl}_2 \cdot 2\text{H}_2\text{O}$  dissolved in 25 ml of 0.2 M citrate buffer (pH 5) was added to 0.4 g ninhydrin (1,2,3-indantrione monohydrate) in 12.5 ml of

methyl cellulose (ethylene glycol monomethyl ether).

One tenth-ml samples from each of the peaks eluted from the columns were added to either 5- or 10-ml glass stoppered volumetric flasks with 100-microliter disposable pipettes. One-half ml of ninhydrin reagent was added. All flasks were heated in a boiling water bath for 20 minutes. Samples were colorimetrically tested for the presence or absence of amino nitrogen.

Fractions were pooled within peaks according to their optical densities and ninhydrin reactions.

#### Preparation of Eluted Column Peaks for Papillary Muscle Bioassay

Ten-ml aliquots from peaks that were eluted from the column were lyophilized and reconstituted with double distilled, deionized water to 2 ml.

A modified Krebs-Henseleit buffer was used to elute the column and for the papillary muscle bioassay. The modified Krebs-Henseleit buffer that was used for the papillary muscle bath was modified further for the preparation of the lyophilized test peaks.

The concentration of each of the constituents of the modified Krebs-Henseleit buffer was: NaCl (114.56 mM), KCl (5.00 mM),  $\text{MgCl}_2 \cdot 6\text{H}_2\text{O}$  (1.20 mM),  $\text{NaH}_2\text{PO}_4 \cdot \text{H}_2\text{O}$  (1.26 mM),  $\text{NaHCO}_3$  (25.00 mM), D-glucose (10.99 mM),  $\text{CaCl}_2$  (2.58 mM). The concentration of  $\text{CaCl}_2$  was increased from 2.58 mM

to 3.25 mM when the Krebs-Henseleit buffer was used to prepare the lyophilized test peaks for bioassay.

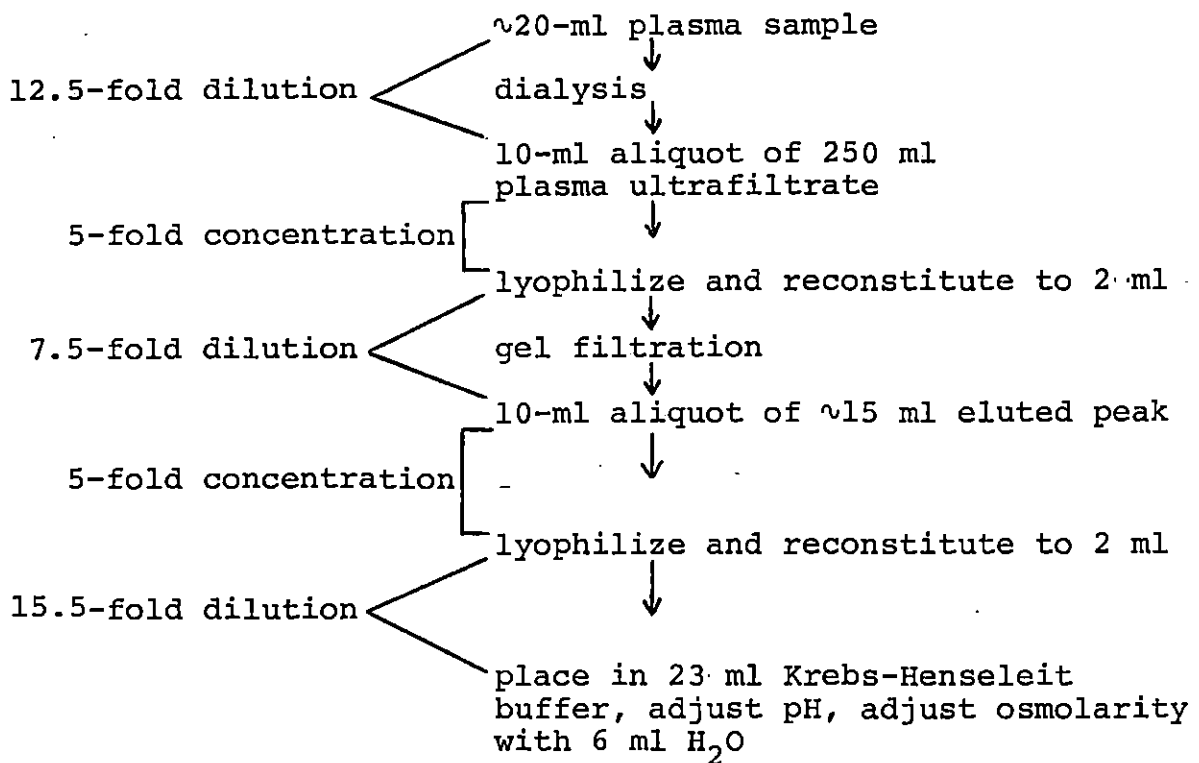
The pH of the Krebs-Henseleit buffer (2.58 mM  $\text{CaCl}_2$ ) was adjusted to 7.38 with 0.4N NaOH and 1N HCl, and the osmolarity which was measured with an osmometer (Advanced Instruments) was between 280 and 285 milliosmols/liter. The buffer prepared in this manner was used in the papillary muscle chamber. The glucose-free buffer used for eluting the column was adjusted for pH only.

Twenty-three ml of the Krebs-Henseleit buffer (3.25 mM  $\text{CaCl}_2$ ) was added to the reconstituted lyophilized test peak. The pH of this 25-ml test sample was adjusted to 7.38. The addition of 6 ml of  $\text{H}_2\text{O}$  was necessary to adjust the osmolarity from 349-356 to 282.

The procedure in brief outline form prior to the papillary muscle bioassay step is diagrammed in Figure 2. A stepwise dilution and concentration scheme for the sample, which was calculated by volume, is indicated.

This procedure was followed for processing shock plasma, and plasma from young and aged dogs. In these experiments, the fourth peak (peak D) of the gel filtration chromatogram was used.





Total: 58.8-fold dilution of original starting material

Figure 2. Procedure prior to the papillary muscle bioassay (A stepwise dilution and concentration of the sample, which was calculated by volume, is indicated. The end result is a 58.8-fold dilution of the original starting material.)

### Experimental Design

Two initial experiments were designed to assay for MDF activity and to confirm the presence of MDF in shock plasma using the papillary muscle system.

In the first experiment, the papillary muscle was subjected to three different muscle baths in the following order: Krebs-Henseleit solution, processed plasma peak D from a young dog, and processed shock plasma peak D. The term "processed" is used to refer to the steps outlined in Figure 2. Thus, a bath consisting of processed plasma is composed of a 2-ml reconstituted-lyophilized plasma ultrafiltrate sample of peak D, 23 ml Krebs-Henseleit buffer, and 6 ml H<sub>2</sub>O.

In the second experiment, the three muscle baths were: Krebs-Henseleit solution, processed shock plasma peak A, and processed shock plasma peak D. Peaks A and D, the first and fourth peaks, respectively, were chosen from the same elution profile.

Ten experiments were then designed to detect differences between plasma from young and aged dogs with respect to the presence of MDF. The three muscle baths in seven of these experiments were: Krebs-Henseleit solution, processed plasma peak D from a young dog, and processed plasma peak D from an aged dog. In the last three experiments,

unprocessed whole plasma was used instead of processed plasma peak D, so that the three muscle baths were: Krebs-Henseleit solution, whole plasma from a young dog, and whole plasma from an aged dog.

The design of all twelve experiments was similar. The first muscle bath was Krebs-Henseleit solution which served as a physiological standard; the second muscle bath was either processed plasma peak D, processed shock plasma peak A, or whole plasma from a young dog and served as a control; the third muscle bath was either processed shock plasma peak D, processed plasma peak D from an aged dog, or whole plasma from an aged dog.

Six young dogs (less than one year of age) were randomly chosen; four dogs were male and two were female. Six old dogs, three male and three female, ranging from 13.5 years to 17 years of age, were selected. Young and old dogs were randomly assigned to an individual muscle experiment as indicated in Table 1.

#### Short medical history of two of the dogs

- 01: mitral valve failure, renal failure, treated for Cushing's syndrome (hyperadrenalcorticism)
- 03: conjunctivitis and vascularization of the cornea which was caused by a bacterium, immunological deficiency in the eye, longstanding Klebsiella infection and epilepsy

Table 1. Assignment of dogs to individual muscle experiments<sup>a</sup>Shock experiments

	<u>Sex</u>	<u>Breed</u>			<u>Sex</u>	<u>Breed</u>
1. DY1	♂	Mongrel	-	DS	♂	Mongrel
2. AS	♂	Mongrel	-	DS	♂	Mongrel

Age experiments

	<u>Sex</u>	<u>Breed</u>			<u>Sex</u>	<u>Breed</u>	<u>Age</u>
1. DY1	♂	Mongrel	-	DO1	♀	Dachshund	15
2. DY2	♂	Mongrel	-	DO2	♂	Beagle	13.5
3. DY3	♂	Shepherd	-	DO3	♂	Weimaraner	14
4. DY3	♂	Shepherd	-	DO4	♂	Collie	16
5. DY4	♀	Shepherd	-	DO5	♀	Beagle	17
6. DY5	♂	Mongrel	-	DO6	♀	Dachshund	15
DY6	♀	Mongrel	-	DO2	♂	Beagle	13.5
7. Plasma Y5	♂	Mongrel	-	Plasma O3	♂	Weimaraner	14
8. Plasma Y4	♀	Shepherd	-	Plasma O2	♂	Beagle	13.5
9. Plasma Y5	♂	Mongrel	-	Plasma O5	♀	Beagle	17

<sup>a</sup>D = processed plasma peak D;

A = processed plasma peak A;

S = shock dog;

Y = young dog;

O = old dog.

Dogs were assigned a number from 1 to 6. "Plasma" precedes a "Y" or an "O" when whole plasma was used instead of a processed plasma peak.

### Papillary Muscle Bioassay

The canine papillary muscle bioassay was used to assay MDF activity.

Six-week old mongrel dogs (1.5-4.5 kg body weight) were anesthetized with sodium pentobarbital (50 mg/kg I.V.). The heart was rapidly excised and immersed in a continuously oxygenated, modified Krebs-Henseleit solution. The right ventricle was opened along the anterior septal margin. Suitable papillary muscles were selected on the basis of length, shape, and geometric configuration. The first papillary muscle adjacent to the interventricular septum was usually the thinnest muscle, and was used if it satisfied the criteria established for suitable muscles.

#### Criteria for judging validity of papillary muscle performance

The ratio of active tension to resting tension in Krebs-Henseleit buffer should exceed 4.5:1. If the ratio was less, but the papillary muscle had a  $P_o$  which was greater than 2 or if the  $P_o$  steadily increased with time, the papillary muscle was acceptable.

Papillary muscles that were too short, stubby, with a thick triangular configuration, or with a cross-sectional area greater than  $2.1 \text{ mm}^2$  were omitted. If the muscle had a cross-sectional area greater than  $2.1 \text{ mm}^2$ , the  $P_o$  had to be large and/or steadily increase with time in order to be

included in the study.

Most importantly, if there was the slightest indication that a papillary muscle was subjected to mechanical damage either by the equipment, a pH or an osmolarity shift, the muscle was not used.

#### Mounting the papillary muscle

The preparation of a stainless steel wire with loop for mounting papillary muscles is diagrammed in Figure 3. A 15-cm stainless steel wire (32 gauge) was threaded through a 3-mm length of aluminum tubing (1.9875 mm I.D.) so that only a very short piece of wire protruded from one end. The long end of the wire was then rethreaded through the same opening of the tubing as in step 1. The wire was pulled taut and then returned through the tubing (indicated by step 3) to form a loop approximately 5 mm long. The other end of the wire was then brought around the side of the tubing as indicated in step 4, threaded through the tubing once more, and pulled taut to secure the loop.

This prepared wire with aluminum tubing and loop at the distal end was then encircled around the chorda tendinea of a selected papillary muscle. The end of the wire was then threaded once more through the aluminum tubing such that the chorda tendinea was also pulled up through the tubing. Care was taken not to pull the muscle up into the

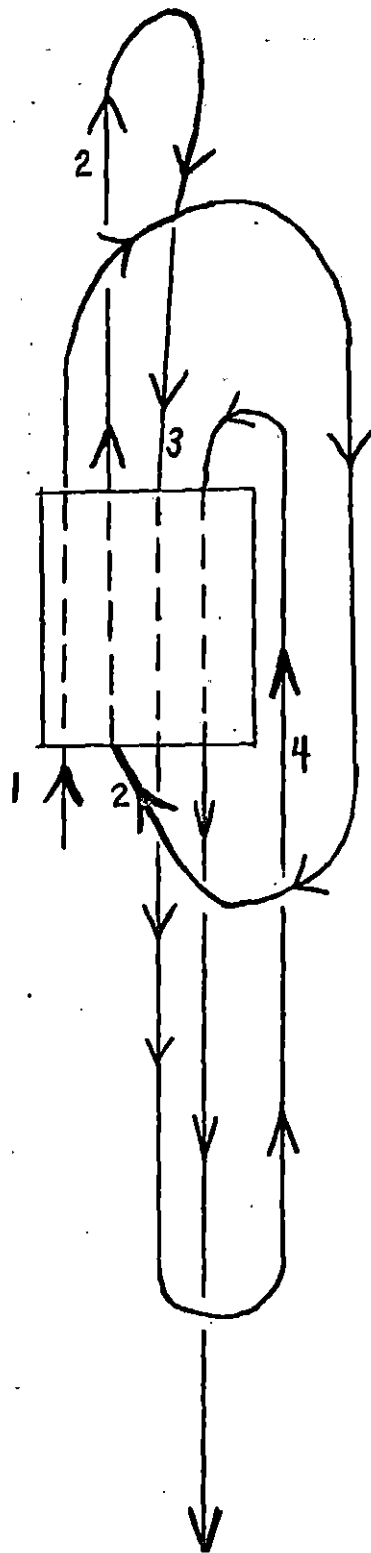


Figure 3. Preparation of stainless steel wire with loop for mounting papillary muscles

tubing. The aluminum tubing was then compressed with a hemostat to fix the chorda tendinea.

The papillary muscle was then dissected free with a small piece of the right ventricular wall adjacent to the muscle base. A lucite clamp was firmly fitted onto this small piece of ventricular wall so that the nontendinous end of the muscle was close to the clamp. The long end of the wire was cut close so that the only wire visible was the loop. This entire procedure was rapidly performed in continuously oxygenated Krebs-Henseleit buffer solution without exposing the muscle to air.

The papillary muscle was then mounted horizontally in a 5-ml inner chamber of a double-chambered constant-temperature bath (27C). The loop of the stainless steel wire was hooked onto the distal end of an aluminum lever mounted on a Brush transducer. The transducer was connected to a 9853 A voltage/pressure input coupler in the pressure/force mode on a R-611 dynograph recorder (Beckman). An isolation transformer which is part of the isotonic muscle transducer (Gould, Inc.) was coupled to the Brush transducer.



### Description of the system

The Krebs-Henseleit solution was continuously gassed with a 95% O<sub>2</sub> and 5% CO<sub>2</sub> mixture. To provide adequate oxygenation and a circulating system for approximately 25 ml of fluid, two additional chambers were made in a lucite plastic block. One tubelike chamber contained a mini-pH probe which took up almost the entire volume of the chamber. The pH was continuously monitored and was maintained within the range of 7.40-7.56. The second tubelike chamber served as a diffusion chamber. A 1.65 m length of silatubing (0.889 mm I.D., 0.51 mm wall thickness) (Silatube, Ronthor Reiss Corp.) was wound symmetrically around an aluminum framework in this 10-ml chamber.

The gas mixture released from the gas pressure tank was directed through a moisturizer to an emergency oxygen roller pump if needed, and the diffusion chamber. The silatubing in the diffusion chamber offered a relatively large outersurface area for diffusion of gas through the wall of the tubing into the circulating chamber fluid.

From the diffusion chamber, the gas mixture was directed to the muscle chamber where silatubing was mounted beside the muscle. Finally, the gas inside the lumen of the silatubing was directed to a bubble chamber where it was released into room air through a short piece of 22 gauge stainless steel tubing.

Circulation of the fluid was accomplished by negative and positive pressure. The chamber fluid was withdrawn by vacuum from the muscle chamber via a 20 gauge stainless steel tube which was mounted on the end of the inner muscle chamber just below the fluid surface. The fluid was directed into the pH-monitoring chamber. A rate controlled roller pump (Cole Parmer) propelled the fluid by positive pressure from the pH-monitoring chamber into the diffusion chamber. The oxygenated fluid was then returned to the muscle chamber via another 20 gauge stainless steel tube which was mounted at the bottom of the inner muscle chamber directly under the muscle.

The papillary muscle was not directly affected when 0.1 N HCl or 0.1 N NaOH was added to adjust pH, because the addition was made into the system through a three-way valve into the tubing and then mixed with the continuously circulating fluid.

During each experiment, the chamber fluid was changed twice. This was accomplished by quickly draining the solution from the pH-monitoring chamber, the diffusion chamber, the muscle chamber and all tubing in the system. The muscle was kept moist during the exchange.

A Grass SD9 stimulator was used to stimulate the papillary muscle constantly at a frequency of 12 stimulations per minute with a duration of 5 msec, and 25-30 volts.

The stimulus pulse passed between one silver electrode placed through the lucite clamp which held the muscle in place, and one platinum electrode fixed into the sidewall of the muscle chamber.

### Measurements

The papillary muscle was allowed to equilibrate while contracting isotonically. After 2 hours of equilibration time, a preload curve was generated in order to determine  $L_{max}$ . The length-tension curve was run backwards beginning with 3.6 g. The muscle was allowed to contract isotonically with this weight for one minute, and then the weight was removed to return the muscle to a zero preload condition for one minute. This was repeated for preloads of decreasing weight. The amplitude (mm) of contraction was measured for each preload. The muscle was prestretched with 3.6 g for 2 contractions prior to each sequential preload of decreasing weight. Care was taken not to overstretch the muscle; smaller muscles were prestretched with a lighter load. The data were immediately analyzed with a model 600 Wang computer which was programmed to calculate the  $L_{max}$ . The selected preload weight was  $\sim 92.5\%$  of the preload weight that would produce a maximal contraction ( $L_{max}$ ). Thus, the resting tension was set at a level just below that which would yield a maximal contraction for the rest of the

experiment.

After the muscle equilibrated with this new constant preload, three afterload curves were generated for each of the three muscle baths with a 30-minute equilibration time after each bath solution was replaced. Afterloading was controlled by a stop on the upper side of the arm of the lever which prevented the afterload from acting as a preload. A micro-drive stepping unit with a multistep and single step adjustment (David Kopf Instruments) was used for raising and lowering the stop in units of microns.

Force-velocity curves were generated backwards by sequentially adding lighter weights after the determination of  $P_0$  (the load that just prevented muscle contraction). Tangents to the contraction curves which were recorded at 25 mm/sec paper speed on a Beckman R-611 dynograph were drawn to determine the velocity of shortening at each afterload. Duplicate determinations were made to verify accuracy. The velocity was calculated by the following equation:

$$\text{Velocity } (\mu/\text{sec}) = \tan \theta \times \text{calibrated difference } (\mu/\text{cm}) \\ \times 1.934 \times 2.5 \text{ cm/sec}$$

The afterload data were fit to either a 2nd, 3rd, or 4th order polynomial by the method of least squares and the  $V_{\max}$  was extrapolated by the model 600 Wang computer.

The latency between the beginning of stimulation and

the beginning of muscle contraction was determined for each afterload. The latency data were also fit to either a 2nd, 3rd, or 4th order polynomial by the computer and plotted against load.

The muscle contraction, stimulus, and time were recorded on a 4-channel R-611 dynograph recorder (Beckman). The osmolarity was monitored every hour throughout the experiment.

A Bausch and Lomb potentiometric recorder was used to measure the length of the papillary muscle. A pinhole light was directed on the muscle while it was mounted in the muscle chamber. As the light which was attached to a rack and pinion device was moved along the length of the muscle, a connected Brush transducer and an isolation transformer converted the signal to a voltage which the potentiometric recorder was able to record.

The cross-sectional area of the muscle was determined from the muscle volume and the muscle length. The muscle volume was estimated with a 10-ml picnometer. The weight of the muscle in air was subtracted from the weight of the muscle and distilled water in the picnometer. This difference was then subtracted from the weight of the picnometer filled with distilled water to give an estimate of the muscle volume. The cross-sectional area was calculated as the quotient of muscle volume ( $\text{mm}^3$ ) and muscle length (mm).

The resting tension was calculated as the quotient of the preload producing  $L_{\max}$  (g) and the cross-sectional area ( $\text{mm}^2$ ).

The active tension of the muscle in each of the three baths was calculated as the quotient of the  $P_0$  (g) and the cross-sectional area ( $\text{mm}^2$ ). The active tension: resting tension ratio was determined for each of the muscles in the Krebs-Henseleit bath.

Equations used in the computerized mathematical derivation of the preload and afterload curves

The preload data were fit to the following two equations by the method of least squares.

$$\text{ascending limb} \quad \hat{Y} = a_1 + b_1 \ln x$$

$$\text{descending limb} \quad \hat{Y} = a_2 e^{b_2 x}$$

"a" and "b" are estimators of the intercepts and the slopes obtained by the method of least squares;  $e$  is an irrational number approximately equal to 2.71828. The data points (load, amplitude of contraction) were entered into the Wang computer up to and including the experimental  $y^{\max}$  to obtain the least squares solution for the ascending limb. To obtain the least squares solution for the descending limb, the experimental  $y^{\max}$  was first reentered into the computer followed by the rest of the data points. If the experimental

$y^{\max}$  appeared to be between two points, then both points were used in both the ascending and descending curve calculation. The preload producing  $L_{\max}$  was the intersection of the two least squares solutions.

The afterload (force-velocity) and latency data were each fit to both a polynomial equation and an exponential equation by the method of least squares.

$$\hat{Y} = b_0 + b_1x + b_2x^2 + b_3x^3 + \dots + b_nx^n$$

There are  $m$  data points of the form  $(X_1, Y_1), (X_2, Y_2), \dots (X_m, Y_m)$ ;  $m > n+1$ . The  $b$ 's are estimators (obtained by the method of least squares) of the measurements of the model.

$$\hat{Y} = ae^{bx}$$

"a" and "b" are estimators of the intercept and the slope obtained by the method of least squares;  $e \approx 2.71828$ . The resultant equations were solved for  $\hat{Y}$  values at chosen  $x$  points.

### Statistical Analysis

The first six processed plasma peak D age experiments and the three whole plasma age experiments (Table 1) were subjected to a 3-way analysis of variance where the third factor is nested within the first treatment. The two shock experiments were analyzed separately using a t-test. Five

parameters were studied: the slope of the latency curve,  $P_o$ ,  $V_{max}$ ,  $V_{max}$  per unit of cross-sectional area, and active tension.

The papillary muscle is the primary experimental unit and is assigned to a main treatment (method 1 or 2). Six muscles were subjected to plasma that was prepared according to method 1. Three muscles were subjected to plasma that was prepared according to method 2. Each muscle is a block for the subtreatment, age. Each muscle nested within a main treatment received three age treatments. Since each muscle served as its own control, muscle to muscle differences were removed. Two randomizations were made: the assignment of muscles to a main treatment, and the assignment of the subtreatment (K-H, plasma from young and old dogs) to the muscle.

#### Statistical objectives

1. To determine if there are main treatment (method) effects.
2. To determine if there are subtreatment (age) effects.
3. To determine if the age effect, if present, is the same for methods 1 and 2 (age by method interaction).
4. To study a comparison of the means:  
To determine if age treatment #2 (young) is different from age treatment #3 (old).

To determine if age treatment #1 (K-H) is different from the mean of age treatments #2 and #3 (young and old).



Age

	<u>Muscle</u>	<u>K-H</u>	<u>Y</u>	<u>O</u>
<u>Method</u> <u>1</u>	1	#1	DY1	DO1
	2	#2	DY2	DO2
	3	#3	DY3	DO3
	4	#4	DY3	DO4
	5	#5	DY4	DO5
	6	#6	DY5	DO6
<u>Method</u> <u>2</u>	1	#7	Plasma Y5	Plasma O3
	2	#8	Plasma Y4	Plasma O2
	3	#9	Plasma Y5	Plasma O5

Method 1 = processed plasma peak D

Method 2 = unprocessed whole plasma

Age = three muscle baths: Krebs-Henseleit (K-H) buffer,  
plasma from young dog, plasma from old dog

<u>Source</u> <sup>1</sup>		<u>d.f.</u>
Methods	$m-1$	1
Muscles (Methods)	$m_1(u-1)$	5
	$m_2(u-1)$	2
		> error (a)
Age	$a-1$	2
Methods x Age	$(m-1)(a-1)$	2
Muscles (Methods) x Age	$m_1(u-1)(a-1)$	10
	$m_2(u-1)(a-1)$	4
		> error (b)
TOTAL		26

<sup>1</sup>  
m = Methods,  
u = Muscles,  
a = Age.

Figure 4. Diagram of statistical design

If an age effect is present, a comparison of the means will determine where the difference lies.

5. To analyze individual muscle experiments with the pooled variance from the analysis of variance for differences between young and old (shock).

## RESULTS

Column elution patterns of plasma from all dogs (shock, young, old) are first presented, followed by a composite elution pattern of molecular weight markers used to calibrate the columns. Using peak D from the chromatogram of each dog, and whole plasma from five of these dogs, force-velocity and load-latency curves were generated for papillary muscle.

Various composites of the force-velocity curves for Krebs-Henseleit buffer, processed plasma peak D from young dogs, processed plasma peak D from old dogs, whole plasma from young dogs and whole plasma from old dogs, where papillary muscles were normalized with respect to force and velocity per unit of cross-sectional area, are presented.

Tables with ninhydrin tests, estimated molecular weights for the six peaks of Bio-Gel P-2 chromatograms, characteristics of the individual papillary muscles, and numerical responses elicited by each of the test peaks or plasmas are included within the section. A concluding, detailed statistical analysis is also presented.

Figure 5. Bio-Gel P-2 column elution pattern of processed shock plasma ultrafiltrate obtained from a young male mongrel dog with experimental pancreatic vessel ischemia

The peaks are designated A through F in order of decreasing molecular weight. Peak D was bio-assayed and contained significant MDF activity. The column flow rate was 10.4 ml/hr (5.2-ml fractions). Fractions 1 through 10 had optical density readings less than 0.02.

<u>Peaks</u>	<u>Elution volume (ml)</u>	<u>Location of peak height (ml)</u>
A	62.0-82.8	67.2
B	88.0-98.4	93.2
C	103.6-119.2	108.8
D	124.4-140.0	129.6
E	171.2-192.0	176.4
F	192.0-212.8	197.2

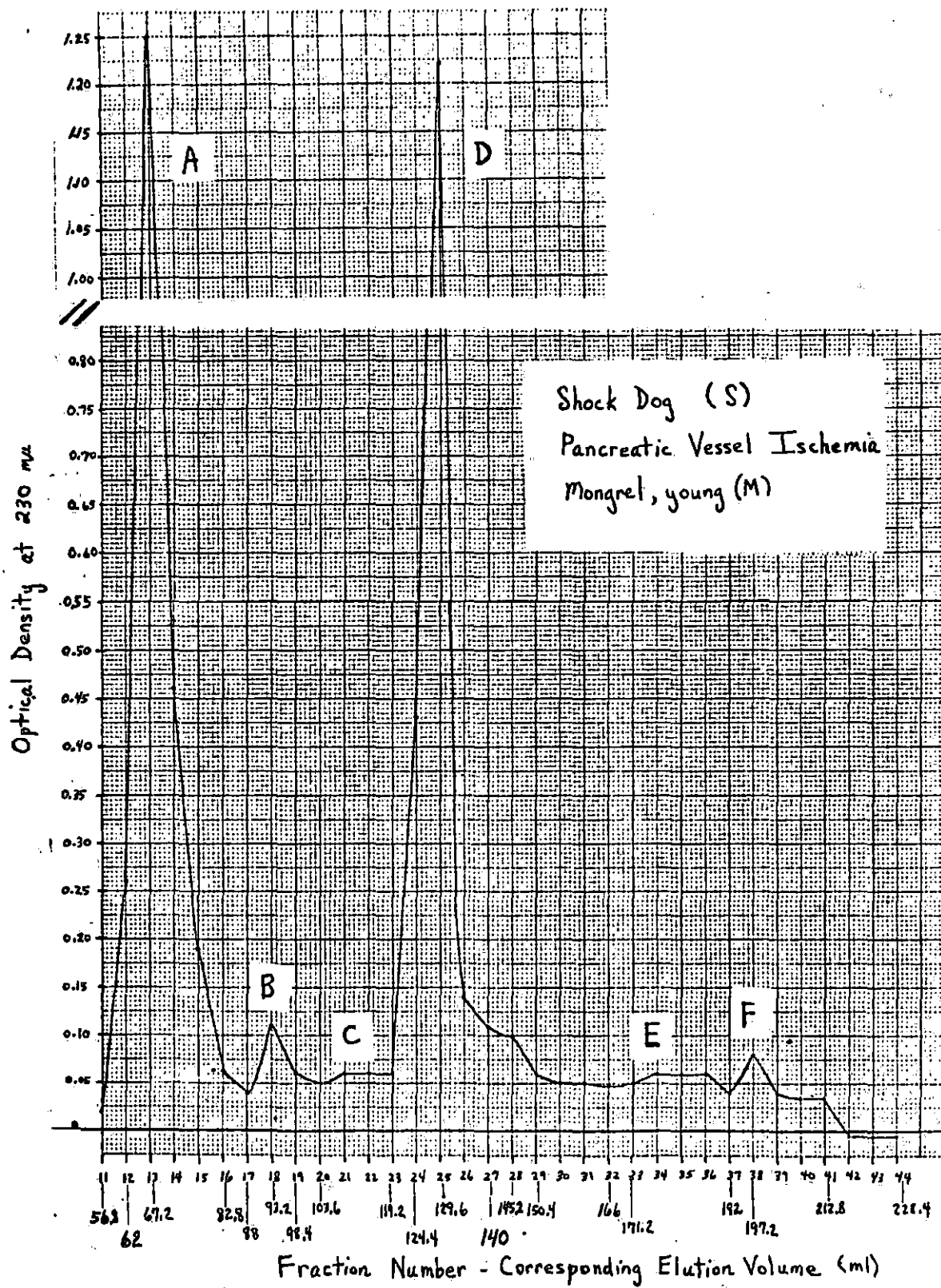


Figure 6. Bio-Gel P-2 column elution pattern of processed shock plasma ultrafiltrate obtained from a young male mongrel dog with experimental pancreatic vessel ischemia

The peaks are designated A through F in order of decreasing molecular weight. Peaks A and D were bioassayed to differentiate between the two large peaks and to confirm the presence of MDF in peak D. The column flow rate was 7.6 ml/hr (3.8-ml fractions). Fractions 1 through 14 had optical density readings less than 0.018.

<u>Peaks</u>	<u>Elution volume (ml)</u>	<u>Location of peak height (ml)</u>
A	64.4-83.4	68.2
B	87.2-102.4	91.0
C	106.2-125.2	113.3
D	129.0-144.2	136.6
E	163.2-208.8	163.2
F	216.4-243.0	227.8

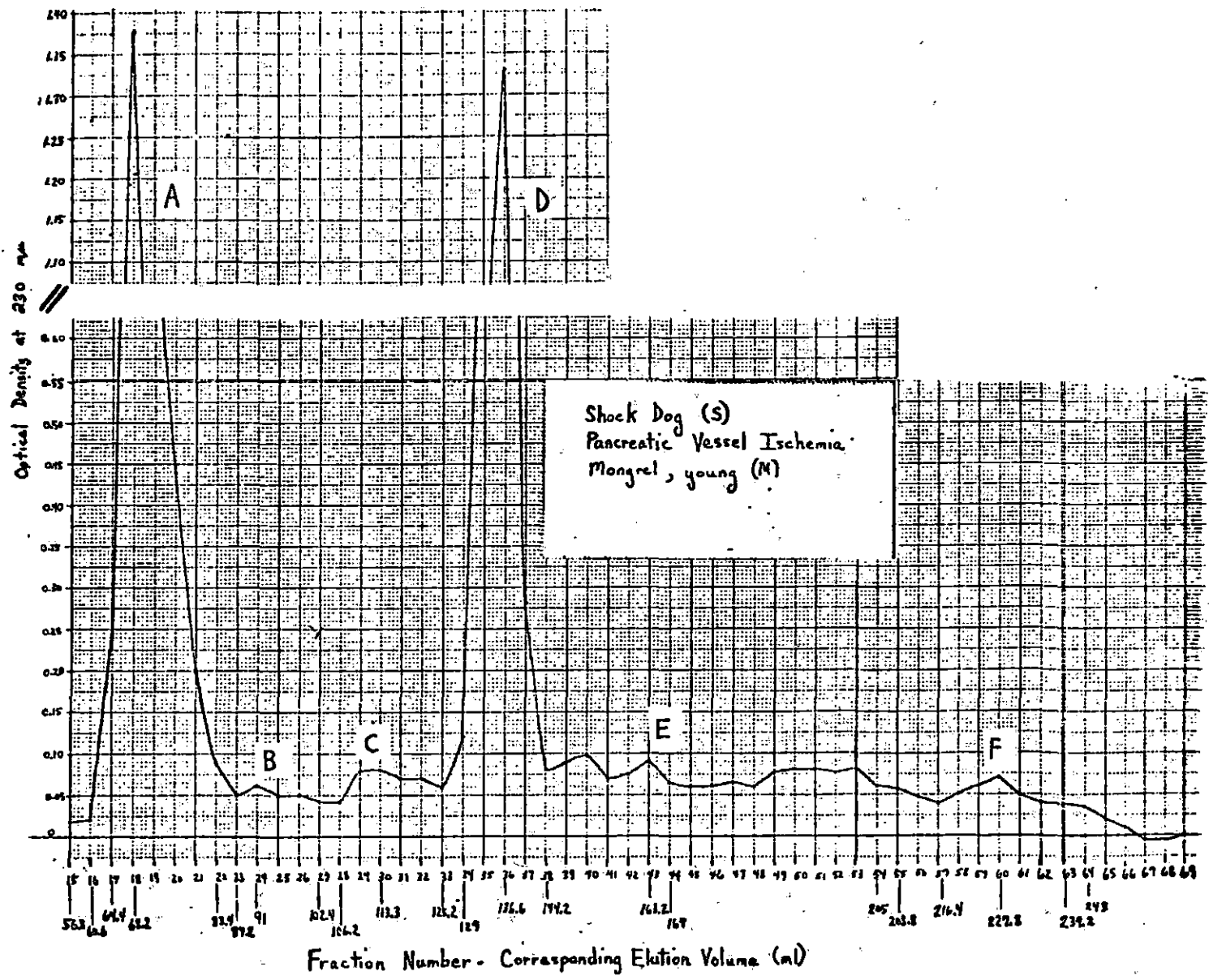


Figure 7. Bio-Gel P-2 column elution pattern of processed plasma ultrafiltrate obtained from a young male mongrel dog (Y1)

The peaks are designated A through F in order of decreasing molecular weight. The column flow rate was 10.4 ml/hr (5.2-ml fractions). Fractions 1 through 10 had optical density readings less than zero.

<u>Peaks</u>	<u>Elution volume (ml)</u>	<u>Location of peak height (ml)</u>
A	64.4-95.6	74.8
B	116.4-126.8	121.6
C	126.8-147.6	137.2
D	147.6-168.4	152.8
E	178.8-210.0	194.4
F	225.6-236.0	230.8



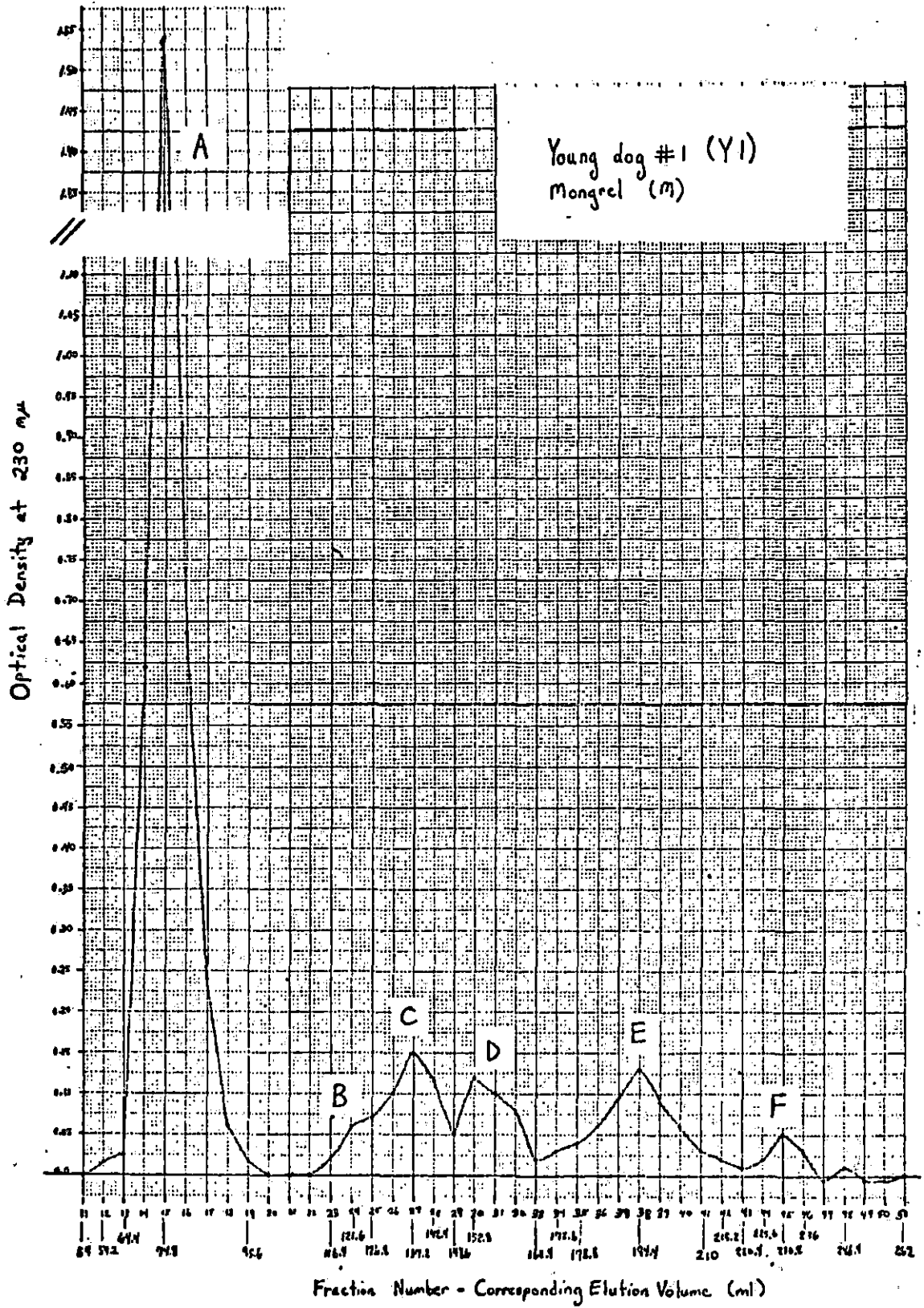


Figure 8. Bio-Gel P-2 column elution pattern of processed plasma ultrafiltrate obtained from a young male mongrel dog (Y2)

The peaks are designated A through F in order of decreasing molecular weight. The column flow rate was 10.8 ml/hr (5.4-ml fractions). Fractions 1 through 10 had optical density readings of 0.04.

<u>Peaks</u>	<u>Elution volume (ml)</u>	<u>Location of peak height (ml)</u>
A	63.3-90.3	68.7
B	106.5-122.7	117.3
C	122.7-138.9	133.5
D	138.9-155.1	144.3
E	165.9-198.3	165.9
F	214.5-263.1	246.9

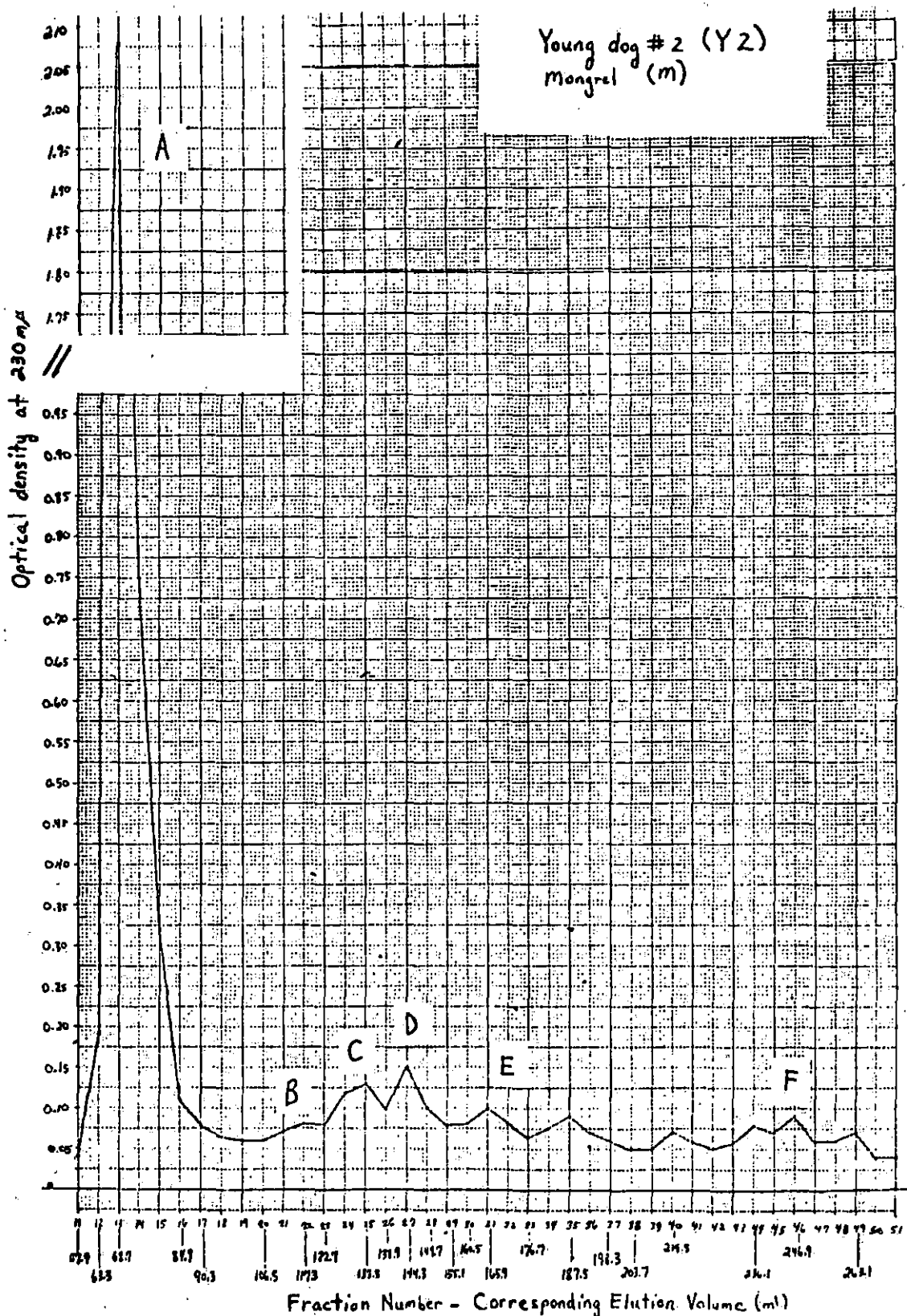
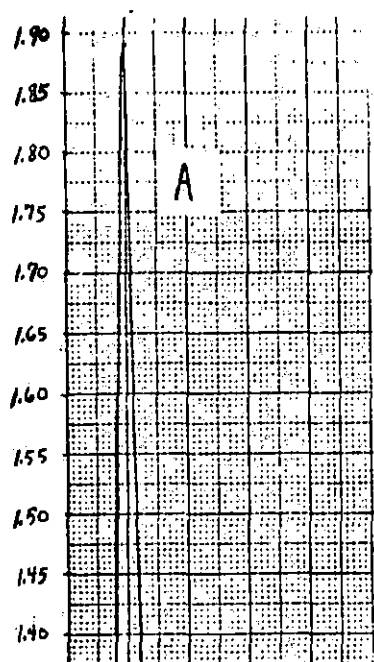


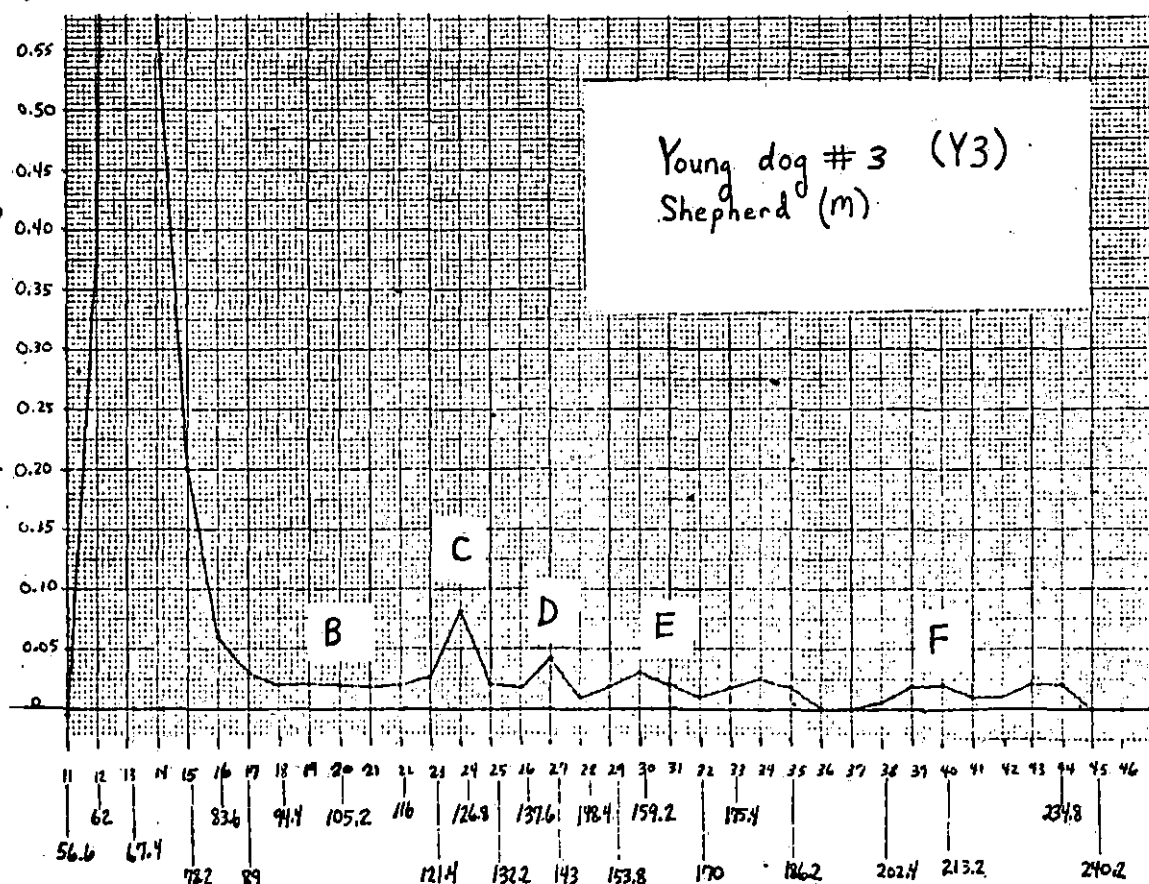
Figure 9. Bio-Gel P-2 column elution pattern of processed plasma ultrafiltrate obtained from a young male shepherd (Y3)

The peaks are designated A through F in order of decreasing molecular weight. The column flow rate was 10.8 ml/hr (5.4-ml fractions). Fractions 1 through 10 had optical density readings less than zero.

<u>Peaks</u>	<u>Elution volume (ml)</u>	<u>Location of peak height (ml)</u>
A	62.0-83.6	67.4
B	94.4-116.0	105.2
C	121.4-132.2	126.8
D	137.6-148.4	143.0
E	153.8-186.2	159.2
F	202.4-240.2	213.2



Optical Density at 230 mμ



Fraction Number - Corresponding Elution Volume (ml)

Figure 10. Bio-Gel P-2 column elution pattern of processed plasma ultrafiltrate obtained from a young male shepherd (Y3)

The peaks are designated A through F in order of decreasing molecular weight. The column flow rate was 10.8 ml/hr (5.4-ml fractions). Fractions 1 through 10 had optical density readings less than or equal to 0.01.

<u>Peaks</u>	<u>Elution volume (ml)</u>	<u>Location of peak height (ml)</u>
A	60.9-82.5	66.3
B	98.7-114.9	109.5
C	114.9-131.1	120.3
D	131.1-141.9	136.5
E	152.7-185.1	158.1
F	195.9-228.3	222.9

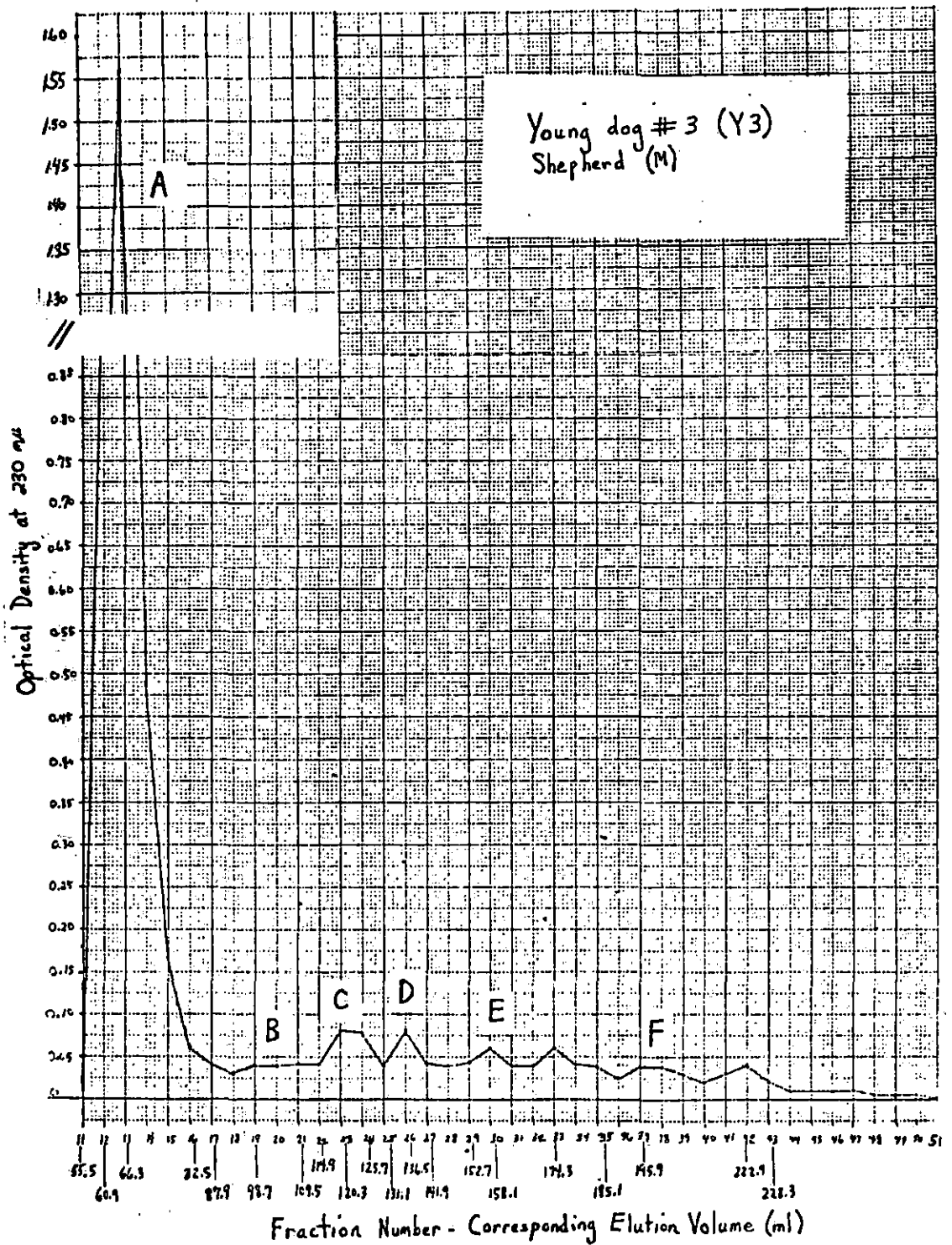




Figure 11. Bio-Gel P-2 column elution pattern of processed plasma ultrafiltrate obtained from a young female shepherd (Y4)

The peaks are designated A through F in order of decreasing molecular weight. The column flow rate was 11.2 ml/hr (5.6-ml fractions). Fractions 1 through 10 had optical density readings of 0.039.

<u>Peaks</u>	<u>Elution volume (ml)</u>	<u>Location of peak height (ml)</u>
A	59.6-93.2	70.8
B	104.4-121.2	121.2
C	126.8-138.0	132.4
D	138.0-154.8	149.2
E	160.4-194.0	188.4
F	205.2-255.6	222.0



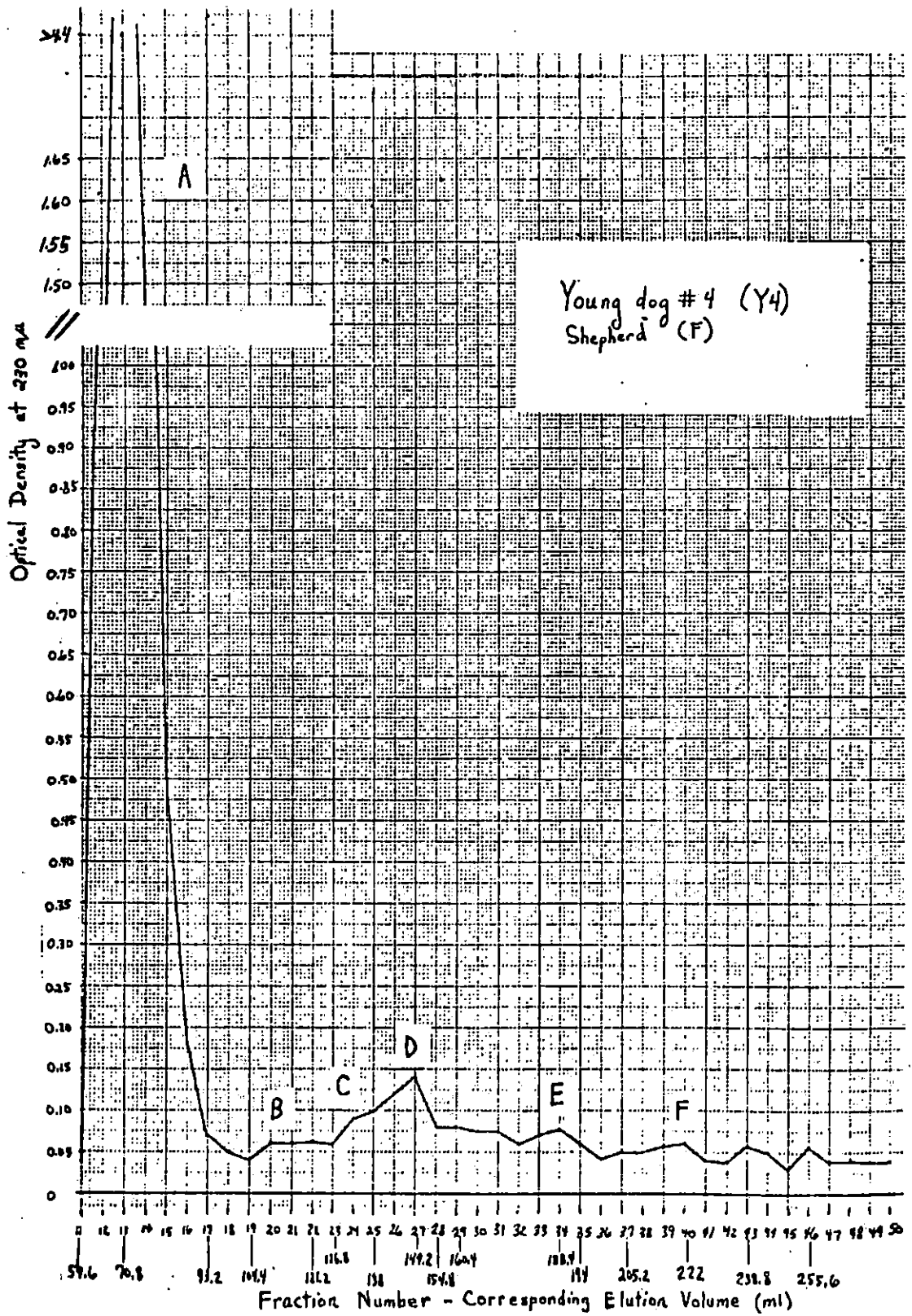


Figure 12. Bio-Gel P-2 column elution pattern of processed plasma ultrafiltrate obtained from a young male mongrel dog (Y5)

The peaks are designated A through F in order of decreasing molecular weight. The column flow rate was 9.2 ml/hr (4.6-ml fractions). Fractions 1 through 14 had optical density readings of 0.039.

<u>Peaks</u>	<u>Elution volume (ml)</u>	<u>Location of peak height (ml)</u>
A	67.9-95.5	77.1
B	100.1-118.5	100.1
C	123.1-141.5	136.9
D	141.5-155.3	150.7
E	159.9-173.7	164.5
F	178.3-238.1	178.3

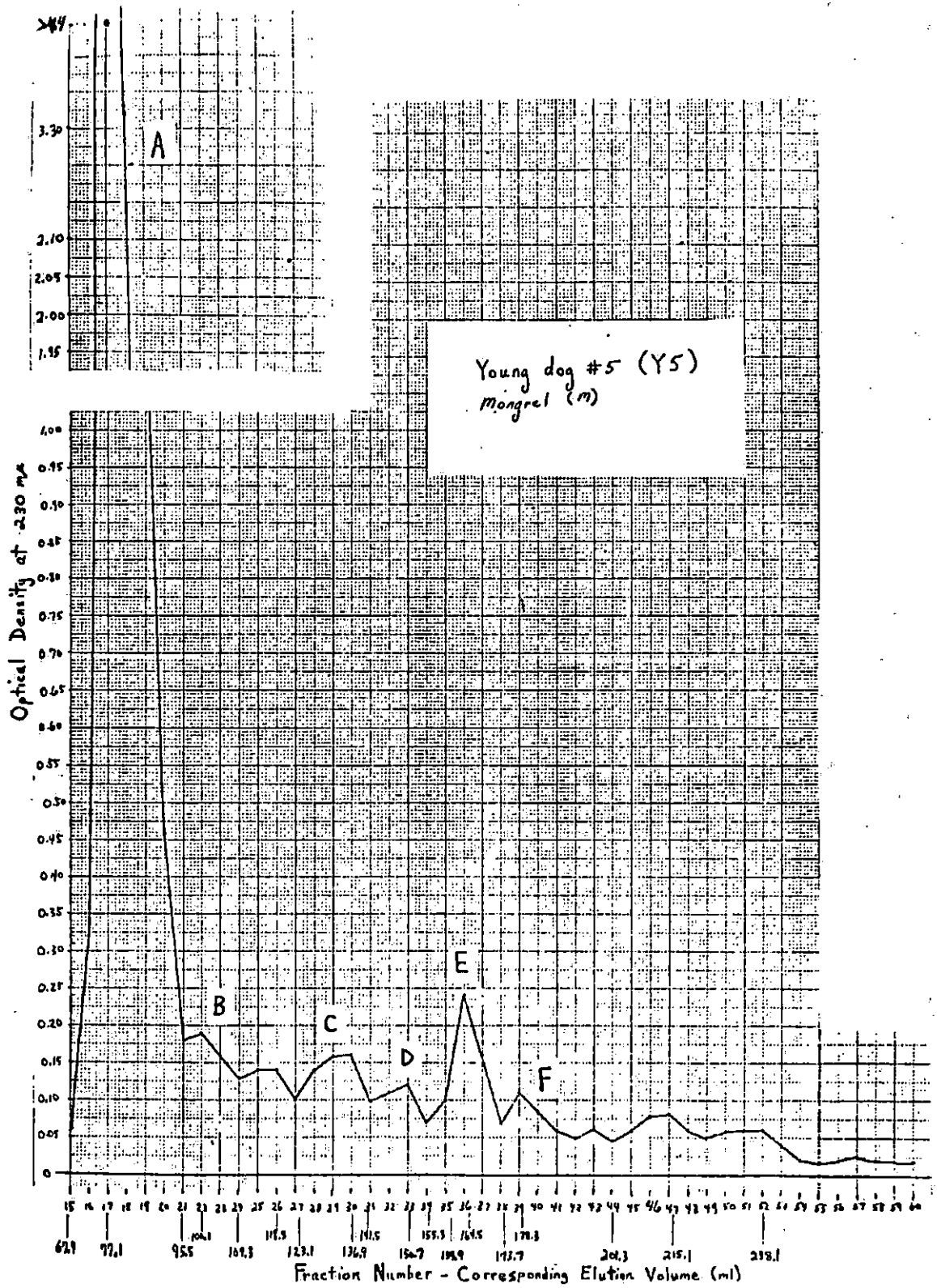


Figure 13. Bio-Gel P-2 column elution pattern of processed plasma ultrafiltrate obtained from a young female mongrel dog (Y6)

The peaks are designated A through F in order of decreasing molecular weight. The column flow rate was 10.8 ml/hr (5.4-ml fractions). Fractions 1 through 8 had optical density readings of 0.005.

<u>Peaks</u>	<u>Elution volume (ml)</u>	<u>Location of peak height (ml)</u>
A	55.4-82.4	66.2
B	104.0-114.8	109.4
C	114.8-131.0	125.6
D	131.0-141.8	136.4
E	147.2-168.8	158.0
F	168.8-201.2	174.0

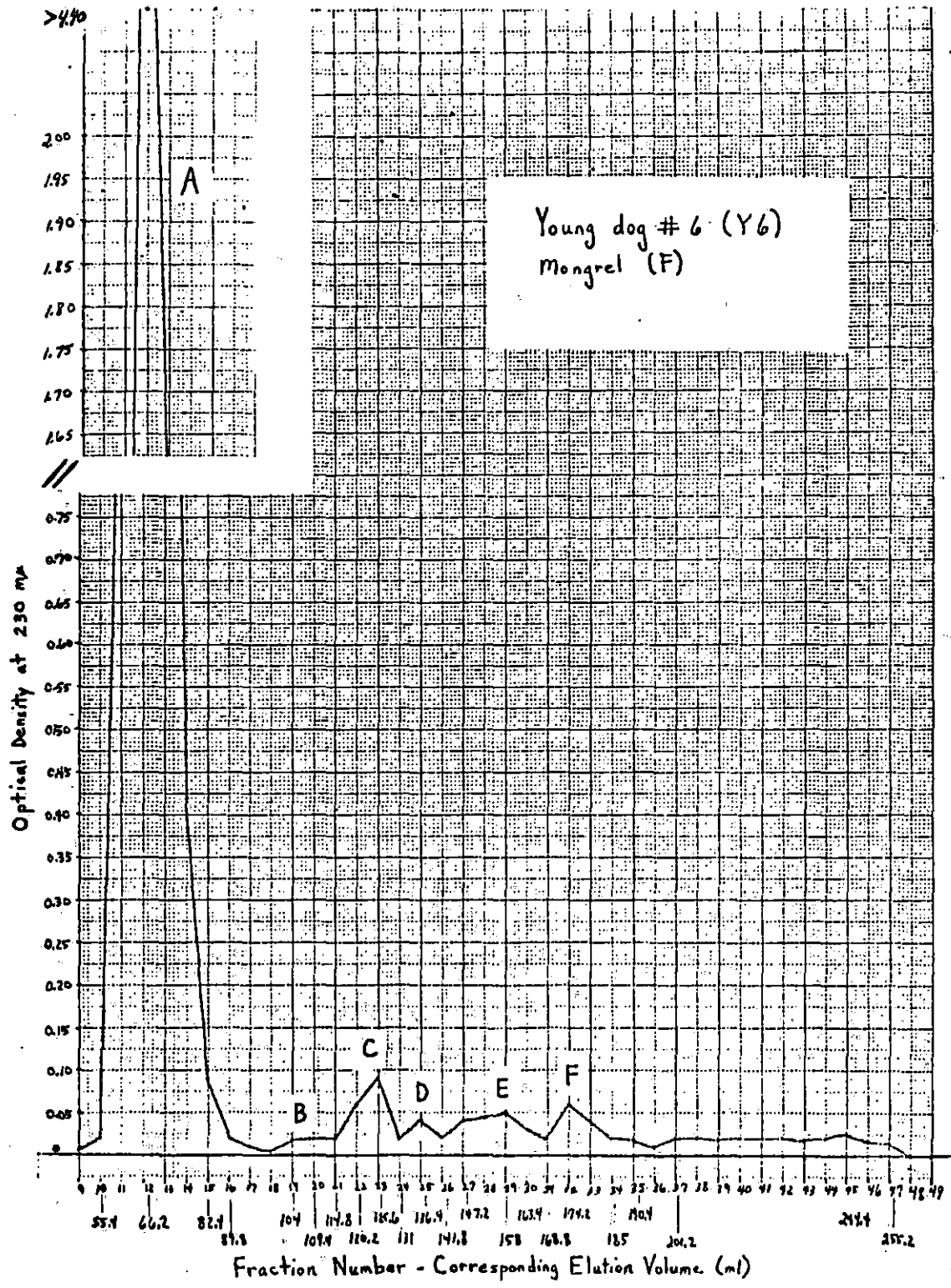


Figure 14. Bio-Gel P-2 column elution pattern of processed plasma ultrafiltrate obtained from an aged female dachshund (15 years) (O1)

The peaks are designated A through F in order of decreasing molecular weight. The column flow rate was 11.2 ml/hr (5.6-ml fractions). Fractions 1 through 10 had optical density readings of zero.

<u>Peaks</u>	<u>Elution volume (ml)</u>	<u>Location of peak height (ml)</u>
A	65.2-87.6	70.8
B	104.4-121.2	110.0
C	126.8-143.6	138.0
D	143.6-160.4	149.2
E	166.0-194.0	177.2
F	216.4-255.6	250.0

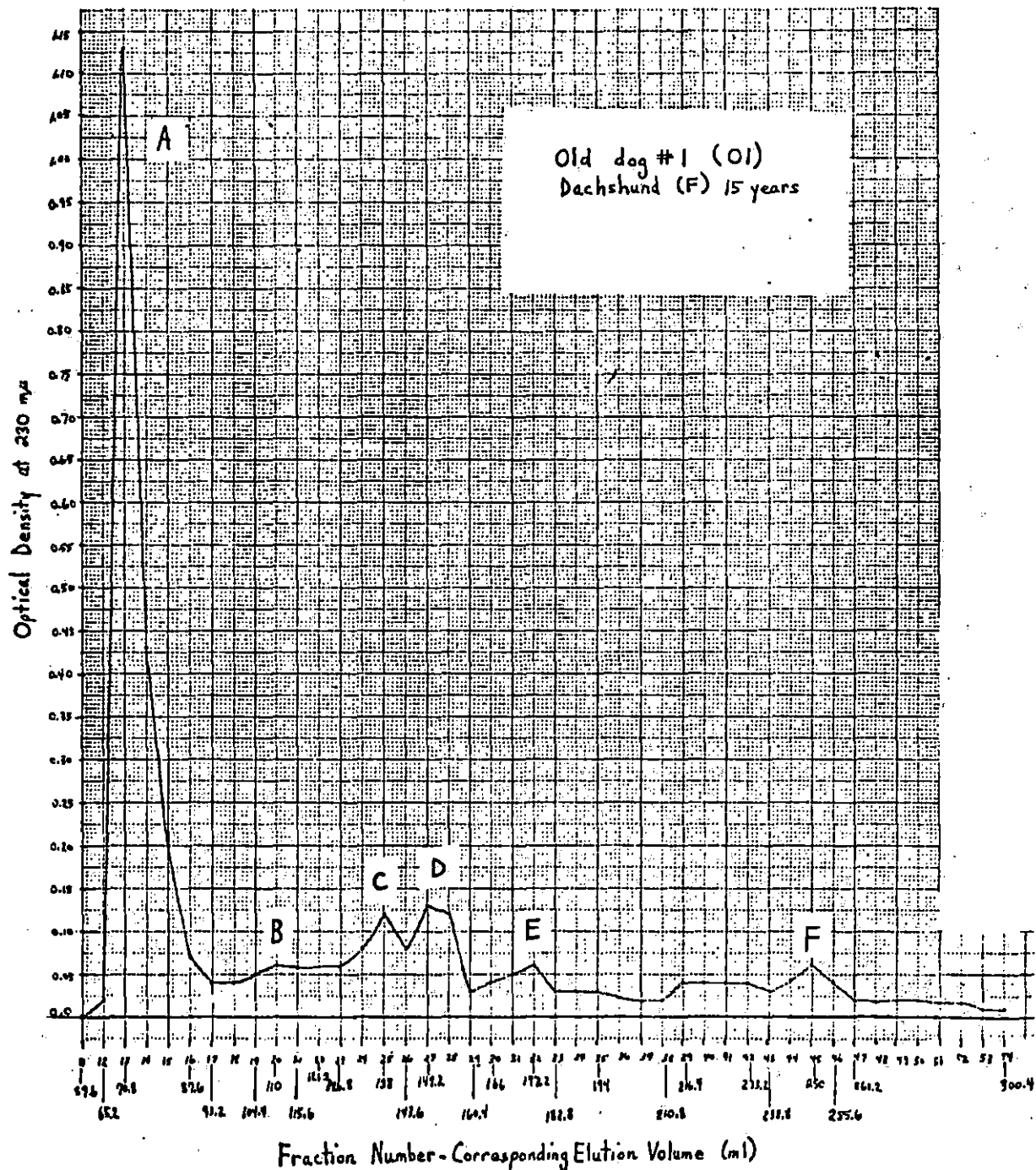




Figure 15. Bio-Gel P-2 column elution pattern of processed plasma ultrafiltrate obtained from an aged male beagle (13.5 years) (O2)

The peaks are designated A through F in order of decreasing molecular weight. The column flow rate was 11.2 ml/hr (5.6-ml fractions). Fractions 1 through 9 had optical density readings less than or equal to 0.02.

<u>Peaks</u>	<u>Elution volume (ml)</u>	<u>Location of peak height (ml)</u>
A	64.7-87.1	70.3
B	98.3-120.7	109.5
C	126.3-137.5	131.9
D	143.1-154.3	148.7
E	165.5-199.1	171.1
F	210.3-249.5	221.5



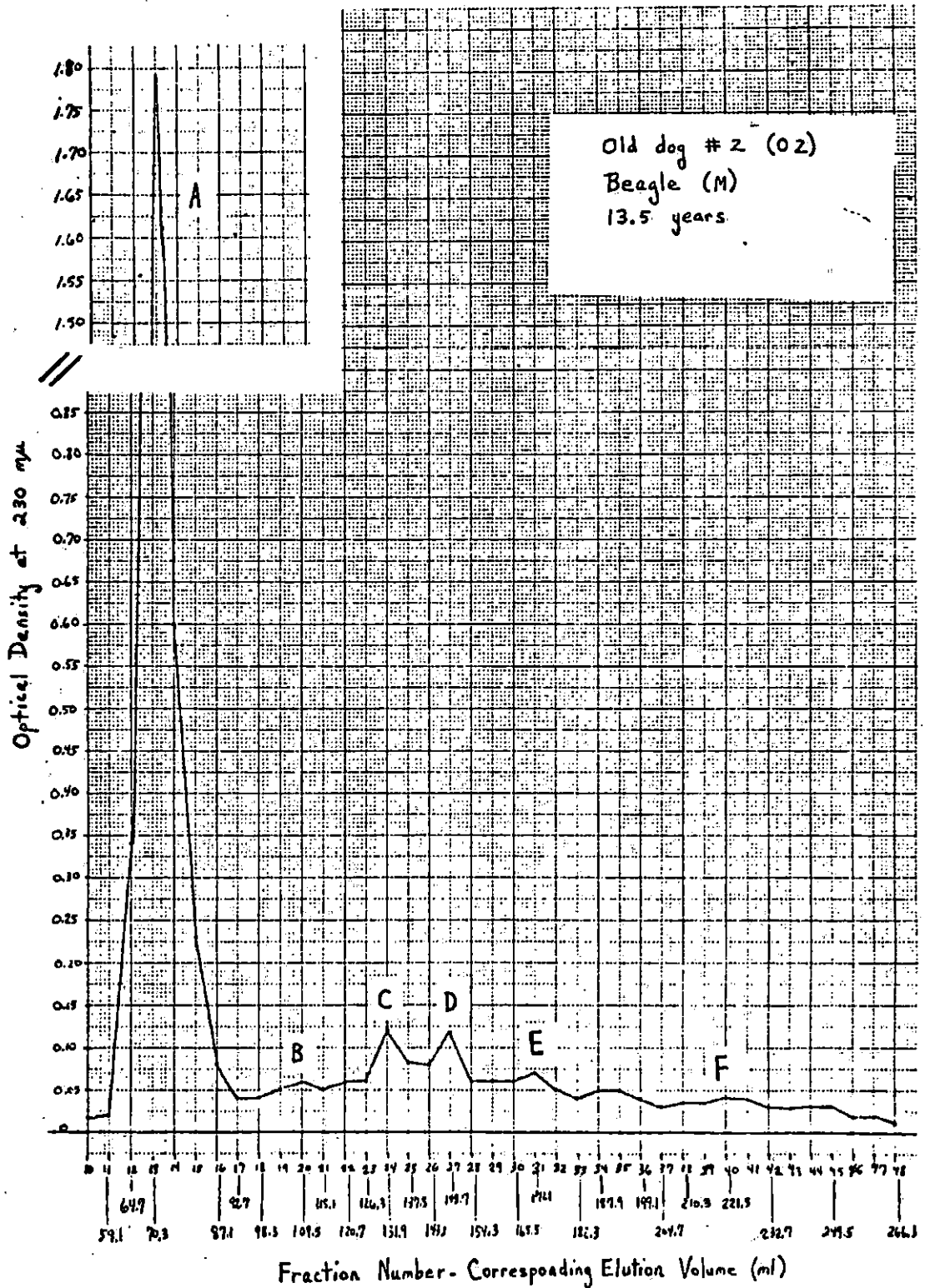


Figure 16. Bio-Gel P-2 column elution pattern of processed plasma ultrafiltrate obtained from an aged male Weimaraner (14 years) (O3)

The peaks are designated A through F in order of decreasing molecular weight. The column flow rate was 11 ml/hr (5.5-ml fractions). Fractions 1 through 10 had optical density readings less than or equal to 0.02.

<u>Peaks</u>	<u>Elution volume (ml)</u>	<u>Location of peak height (ml)</u>
A	64.4-86.4	69.9
B	91.9-113.9	91.9
C	119.4-135.9	130.4
D	135.9-152.4	141.4
E	157.9-185.4	163.4
F	196.4-267.9	245.9

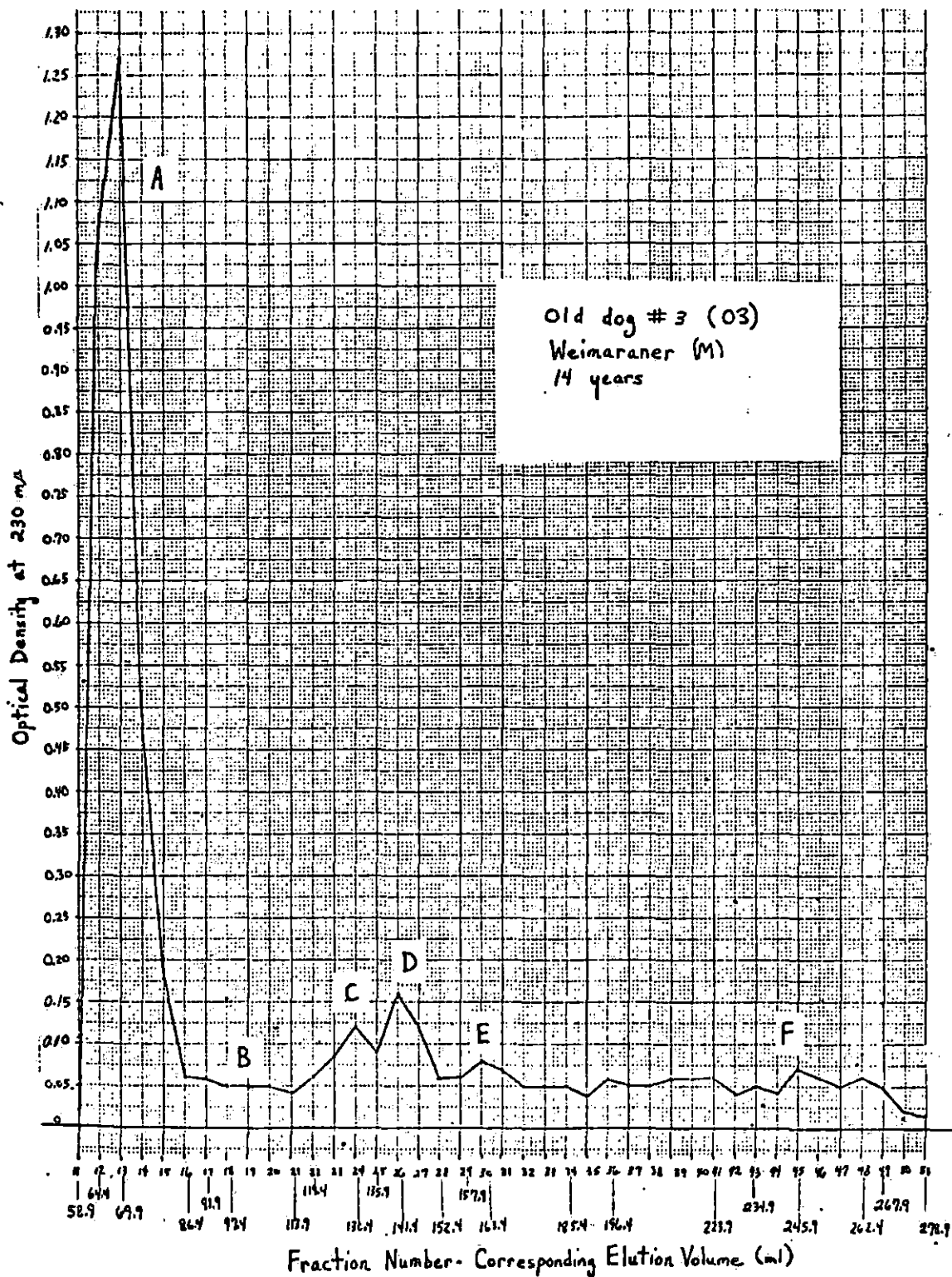


Figure 17. Bio-Gel P-2 column elution pattern of processed plasma ultrafiltrate obtained from an aged male collie (16 years) (O4)

The peaks are designated A through F in order of decreasing molecular weight. The column flow rate was 9.2 ml/hr (4.6-ml fractions). Fractions 1 through 13 had optical density readings of zero.

<u>Peaks</u>	<u>Elution volume (ml)</u>	<u>Location of peak height (ml)</u>
A	73.1-96.1	77.7
B	100.7-114.5	100.7
C	119.1-142.1	132.9
D	142.1-160.5	155.9
E	160.5-174.3	165.1
F	188.1-215.7	192.7

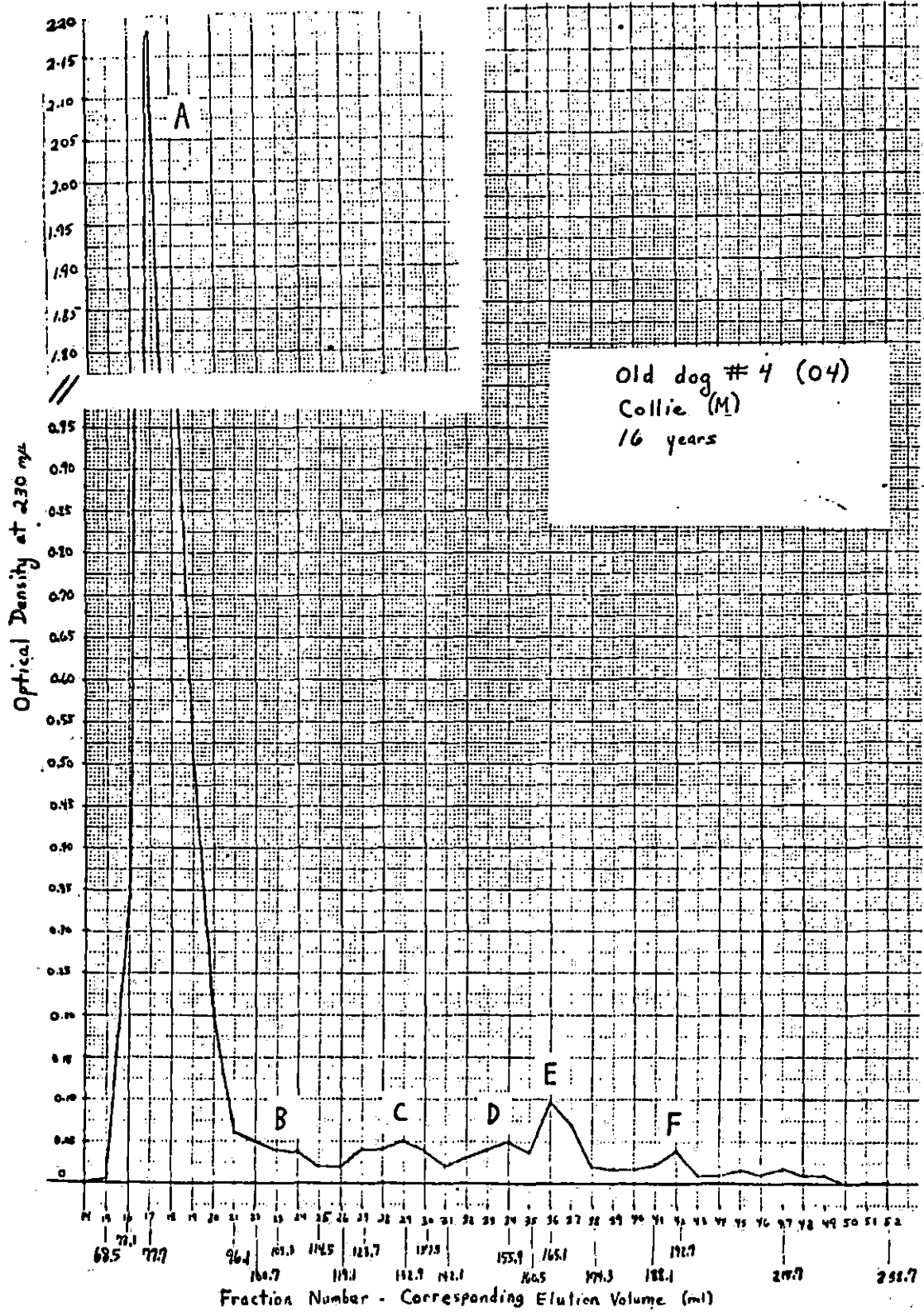


Figure 18. Bio-Gel P-2 column elution pattern of processed plasma ultrafiltrate obtained from an aged female beagle (17 years) (05)

The peaks are designated A through F in order of decreasing molecular weight. The column flow rate was 11.4 ml/hr (5.7-ml fractions). Fractions 1 through 10 had optical density readings less than or equal to 0.03.

<u>Peaks</u>	<u>Elution volume (ml)</u>	<u>Location of peak height (ml)</u>
A	60.2-83.0	65.9
B	105.8-122.9	117.2
C	128.6-140.0	134.3
D	140.0-157.1	145.7
E	162.8-197.0	168.5
F	208.4-265.4	219.8

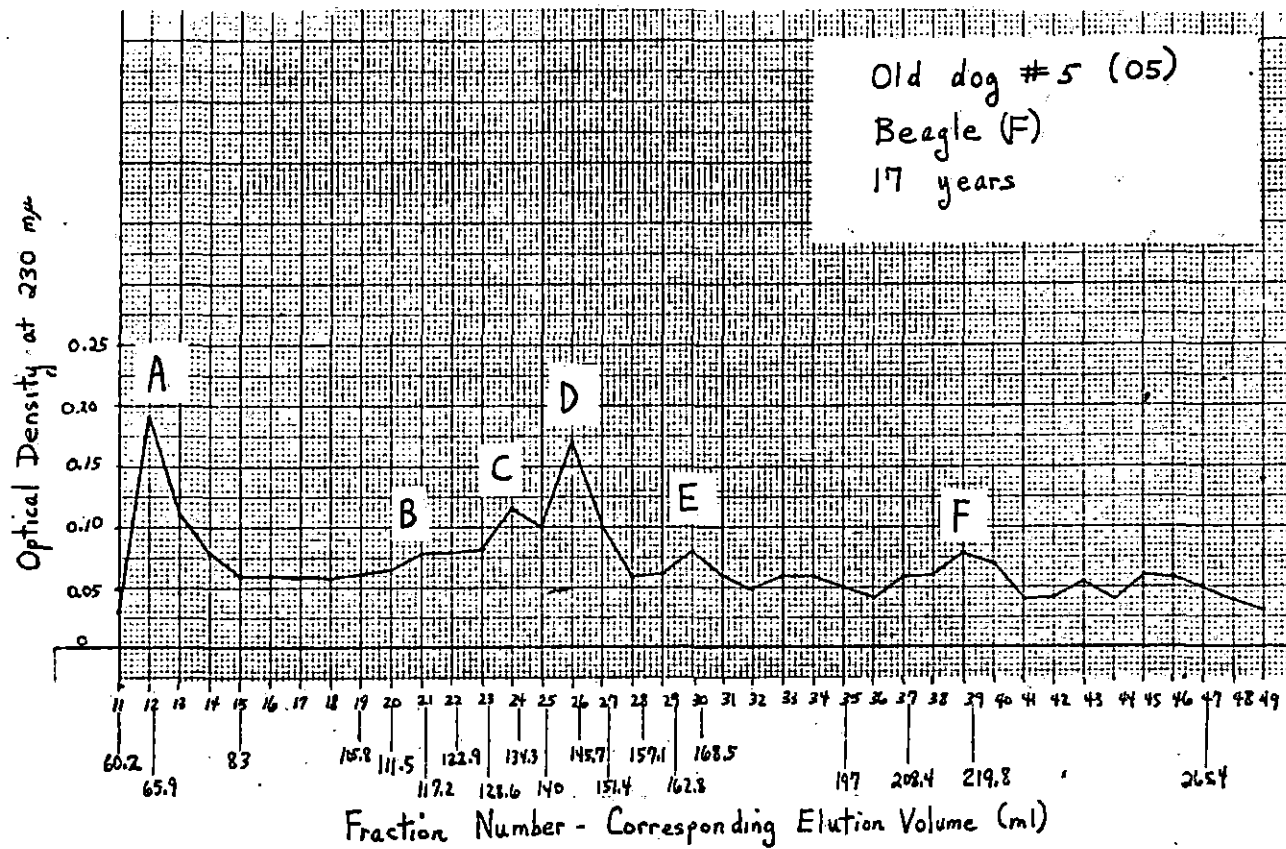


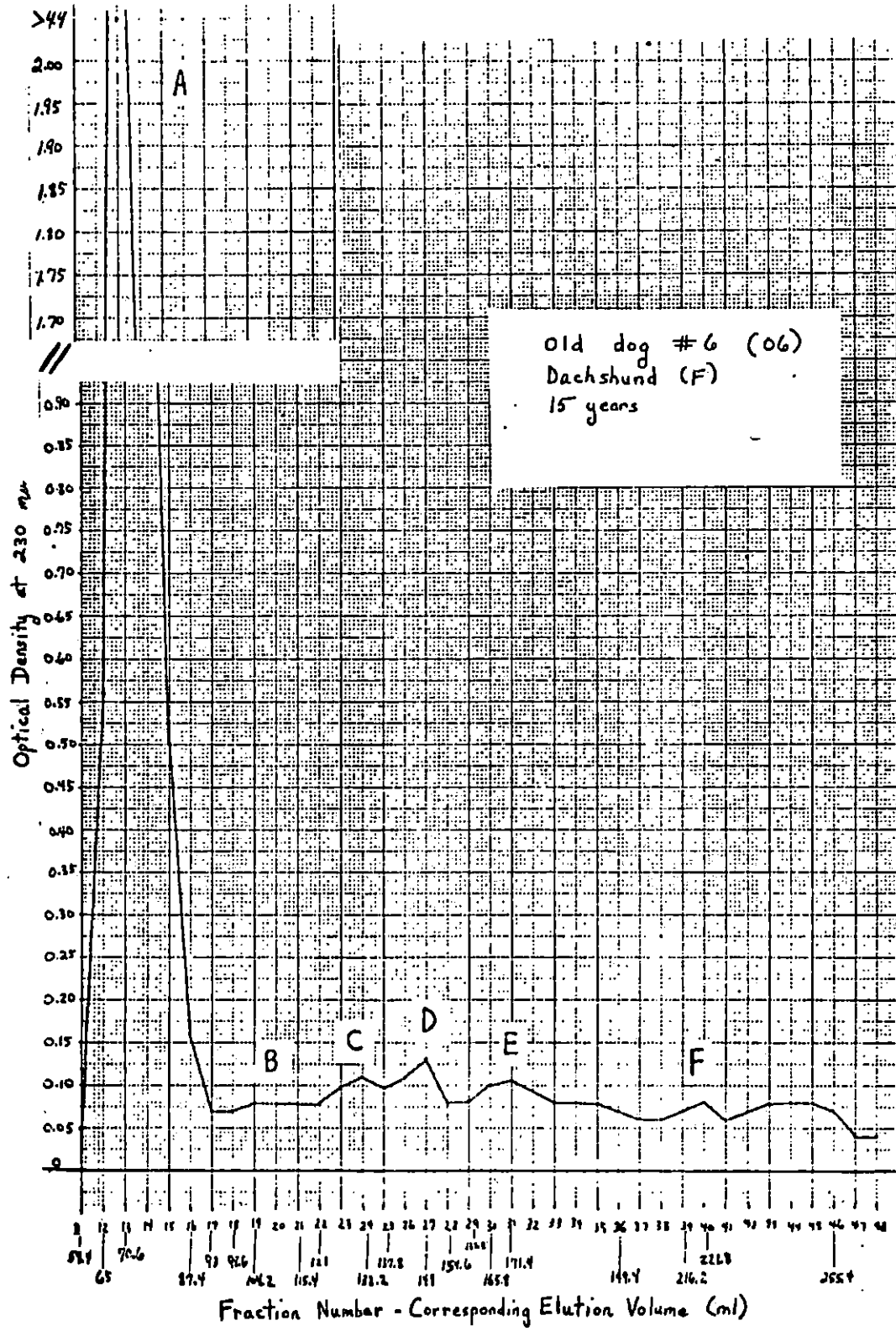


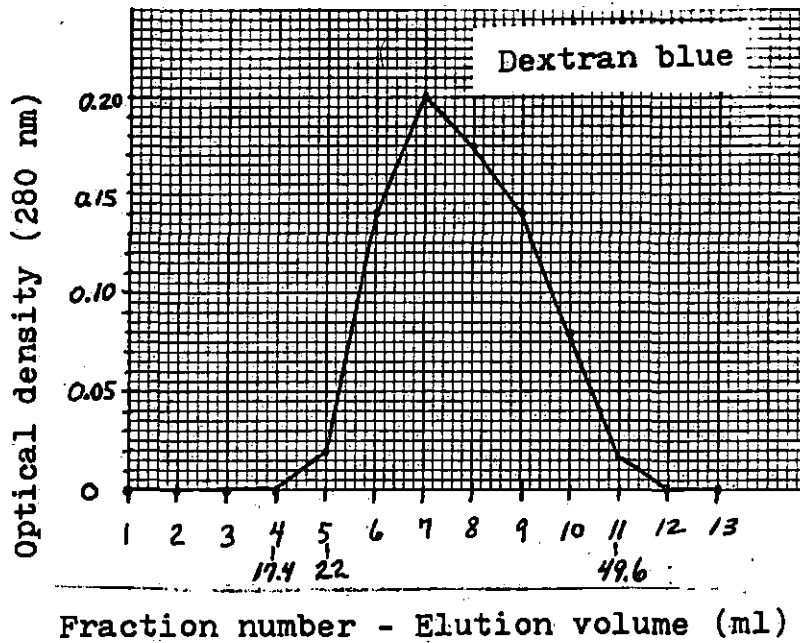
Figure 19. Bio-Gel P-2 column elution pattern of processed plasma ultrafiltrate obtained from an aged female dachshund (15 years) (O6)

The peaks are designated A through F in order of decreasing molecular weight. The column flow rate was 11.2 ml/hr (5.6-ml fractions). Fractions 1 through 10 had optical density readings less than or equal to 0.039.

<u>Peaks</u>	<u>Elution volume (ml)</u>	<u>Location of peak height (ml)</u>
A	65.0-93.0	70.6
B	98.6-115.4	104.2
C	121.0-137.8	132.2
D	137.8-154.6	149.0
E	160.2-199.4	171.4
F	216.2-255.4	221.8







Average void volume was 51 ml.

Figure 20. Bio-Gel P-2 column elution pattern of dextran blue (molecular weight 2,000,000)

Figure 21. Composite Bio-Gel P-2 column elution pattern of molecular weight markers

— — — — —	Angiotensin II (1225 daltons)	11.2 ml/hr flow rate
	99.8-122.2 ml	location of peak height 111 ml
-----	Angiotensin II (1225 daltons)	9.2 ml/hr flow rate
	108.2-135.8 ml	location of peak height 122 ml
— — — — —	Angiotensin II (1225 daltons)	9.2 ml/hr flow rate
	110.2-137.8 ml	location of peak height 124 ml
— — — — —	Angiotensin II (1106.3 daltons)	10.6 ml/hr flow rate
	100.9-127.4 ml	location of peak height 111.5 ml
—————	Angiotensin III Inhibitor (896 daltons)	11.2 ml/hr flow rate
	92.0-117.8 ml	location of peak height 101 ml
— — — — —	MDF-peak D shock (?)	10.4 ml/hr flow rate
	122-140 ml	location of peak height 129.6 ml
- - - - -	MDF-peak D shock (?)	7.6 ml/hr flow rate
	129.0-144.2 ml	location of peak height 136.6 ml
— □ — □ — □ —	Hexaglycine (360.3 daltons)	10.8 ml/hr flow rate (50 mg)
	155.4-214.8 ml	location of peak height 177 ml
— ▲ — ▲ — ▲ —	Hexaglycine (360.3 daltons)	9.2 ml/hr flow rate (30 mg)
	168.9-187.3 ml	location of peak height 173.5 ml

The average elution volumes of peak D from young dogs and old dogs were 138.0-152.2 ml and 140.4-156.6 ml, respectively.

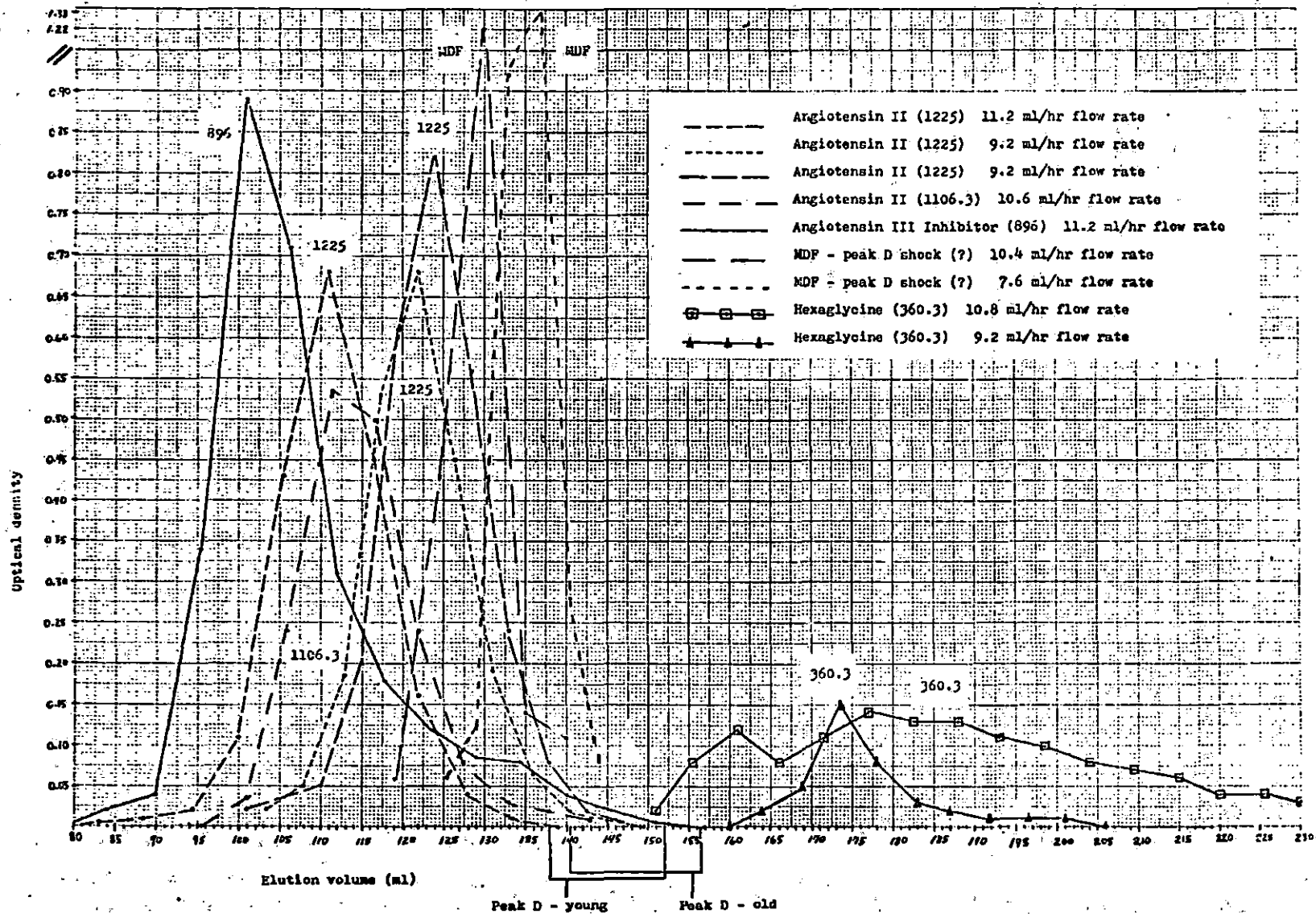
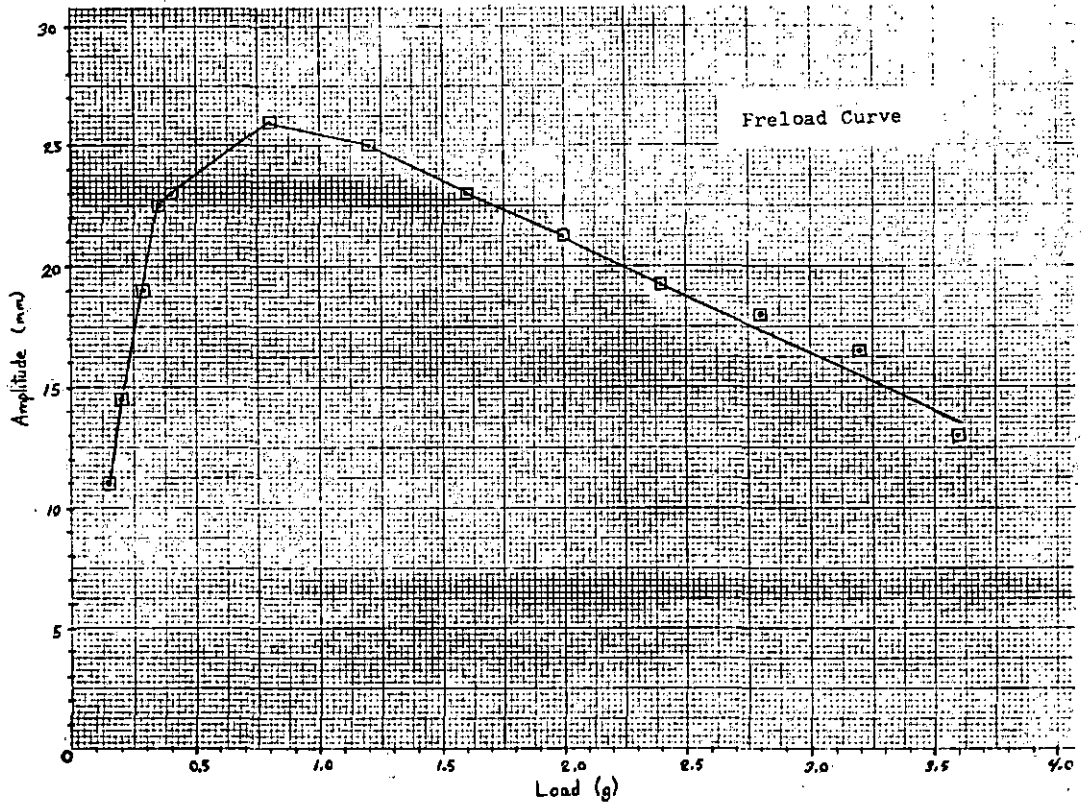


Table 2. Ninhydrin test and average elution volumes of the six peaks of Bio-Gel P-2 chromatograms with an estimate of molecular weight<sup>a</sup>

	Ninhydrin Test	Average Elution Volume (ml)	Estimated Molecular Weight
Peak A - young (n=7)	+	061.93-089.01	>1225
old (n=6)	+	065.43-088.87	
Peak B - young (n=7)	+	103.50-119.27	~1100
old (n=6)	+	099.95-118.10	
Peak C - young (n=7)	+	121.50-137.19	700-850
old (n=6)	+	123.53-139.48	
Peak D - shock (n=2)	+	126.70-142.10	700-850 600-700
young (n=7)	+	137.96-152.24	
old (n=6)	+	140.42-156.55	
Peak E - young (n=7)	+	159.81-188.01	~360
old (n=6)	+	162.15-191.53	
Peak F - young (n=7)	+	198.67-237.50	<350
old (n=6)	+	205.97-251.58	

<sup>a</sup>Note that the column separation of plasma from young and old dogs is virtually identical, and that the elution volume for MDF (found in peak D of shock plasma) is similar to the elution volume for peak C of plasma from young and old dogs.



Length (amplitude) is plotted against tension (load). Note that the experimental  $L_{\max}$  is at a preload of 0.8 g. The  $L_{\max}$  computed from the ascending and descending limbs of the preload curve was at a preload of 0.761 g.

Figure 22. Typical preload curve

Table 3. Cross-sectional area, muscle length,  $L_{\max}$  preload, resting tension, and active tension to resting tension ratio values for papillary muscles in the shock and age experiments<sup>a</sup>

<u>Shock experiments</u>					
	Cross-sectional area (mm <sup>2</sup> )	Muscle length (mm)	$L_{\max}$ preload (g)	Resting tension (g/mm <sup>2</sup> )	Active tension: resting tension ratio
1.	1.263	2.93	0.620	0.491	7.90
2.	0.571	4.73	0.675	1.181	2.15
<u>Age experiments</u>					
1.	3.289	2.25	0.761	0.231	2.15
2.	5.206	1.94	1.076	0.207	1.15
3.	3.077	3.64	1.383	0.449	2.90
4.	0.437	4.35	1.006	2.302	4.79
5.	0.347	4.61	0.582	1.677	7.11
6.	0.969	3.20	0.773	0.798	6.74
7.	2.063	2.71	0.485	0.235	4.78
8.	1.048	2.10	0.818	0.781	3.26
9.	0.955	3.77	1.001	1.048	7.39
$\bar{X}$ (n=11):	1.748	3.29	0.835	0.855	4.57

<sup>a</sup>Note that the papillary muscle subjected to DY6 and D02 treatments (Table 1) was omitted.

Table 4. Latency (slope),  $P_o$ ,  $V_{max}$ ,  $V_{max}$  per unit of cross-sectional area, and active tension values for all muscle experiments<sup>a</sup>

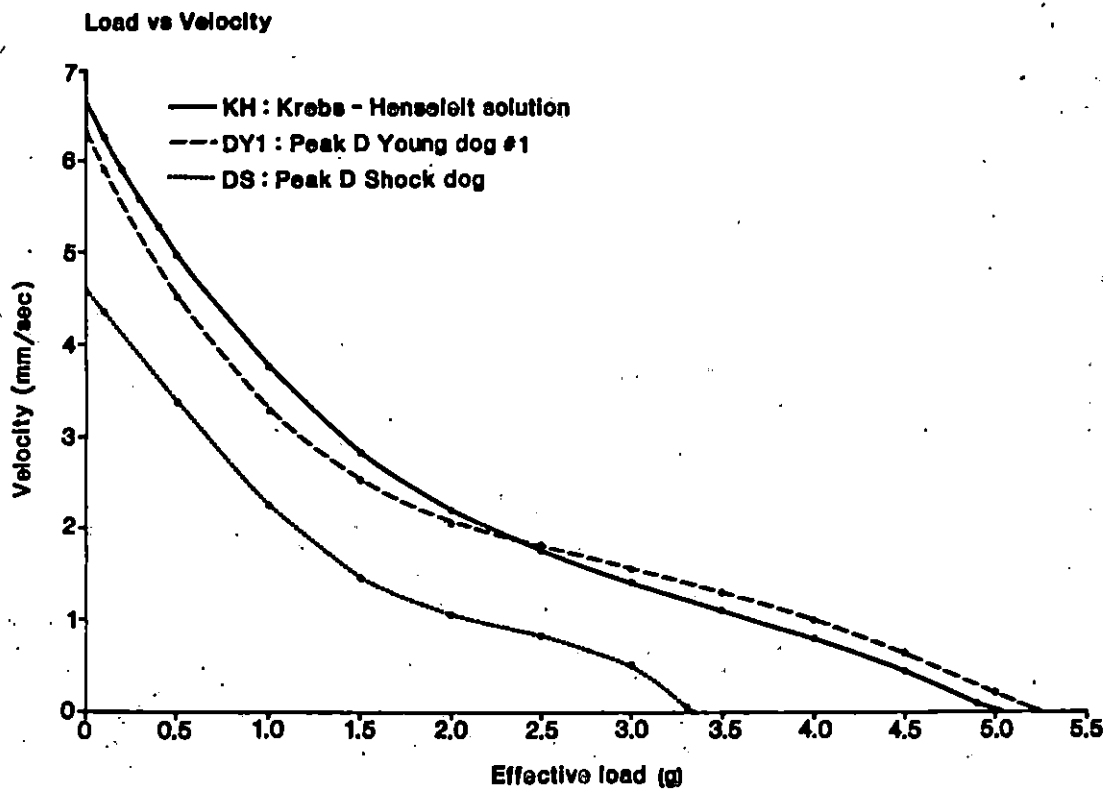
		Latency slope (msec/g)	$P_o$ (g)	$V_{max}$ (mm/sec)	$V_{max}$ /cross- sectional area (mm·sec) <sup>-1</sup>	Active tension (g/mm <sup>2</sup> )
<u>Shock</u>						
1.	KH	062.398	4.902	6.647		03.881
	DY1	045.905	5.274	6.369		04.176
	DS	094.039	3.247	4.590		02.571
2.	KH	228.192	1.448	2.792		02.534
	AS	157.963	1.510	2.818		02.643
	DS	218.570	1.055	2.861		01.846
<u>Age</u>						
1.	KH #1	214.600	1.634	5.057	01.554	00.497
	DY1	126.200	1.903	5.852	01.781	00.579
	DO1	088.510	1.903	7.156	02.177	00.579
2.	KH #2	403.460	1.241	2.060	00.396	00.238
	DY2	306.115	1.282	2.344	00.451	00.246
	DO2	327.090	1.324	3.036	00.581	00.254
3.	KH #3	337.445	4.012	2.583	00.839	01.304
	DY3	347.255	4.095	2.824	00.917	01.331
	DO3	294.915	4.137	2.572	00.835	01.344
4.	KH #4	095.071	4.819	6.028	13.823	11.027
	DY3	091.521	4.984	5.399	12.393	11.405
	DO4	104.109	4.716	5.602	12.826	10.792
5.	KH #5	051.084	4.137	8.467	24.401	11.922
	DY4	045.984	4.054	7.123	20.538	11.683
	DO5	068.563	3.557	6.415	18.353	10.251

<sup>a</sup>The linear portion of the load-latency curve (2nd, 3rd, or 4th order polynomial) was fit by linear regression to a straight line from which the slope was calculated.  $P_o$  values are experimental.  $V_{max}$ /cross-sectional area values were extrapolated from force-velocity curves where velocity per unit of cross-sectional area was plotted against  $P/P_o$ . Explanation of symbols (DY1, DO1, AS, DS, Plasma Y5, etc.) is found in Table 1.



Table 4 (Continued)

			Latency slope (msec/g)	P <sub>o</sub> (g)	V <sub>max</sub> (mm/sec)	V <sub>max</sub> /cross- sectional area (mm·sec) <sup>-1</sup>	Active tension (g/mm <sup>2</sup> )
<u>Age</u>	6.	KH #6	048.591	5.212	6.482	06.687	05.379
		DY5	060.461	4.633	5.959	06.147	04.781
		DO6	094.554	3.909	6.248	06.445	04.034
		KH	251.116	1.324	2.966		00.197
		DY6	420.799	0.724	2.114		00.108
		DO2	364.943	0.786	2.106		00.117
	7.	KH #7	121.166	2.316	3.221	01.559	01.123
		Plasma Y5	154.814	1.923	2.763	01.343	00.932
		Plasma O3	259.384	1.324	1.166	00.565	00.642
	8.	KH #8	136.175	2.668	1.924	01.836	02.546
		Plasma Y4	153.740	2.627	1.752	01.672	02.507
		Plasma O2	130.970	2.523	1.725	01.646	02.407
	9.	KH #9	047.759	7.394	6.853	07.171	07.742
		Plasma Y5	155.670	5.440	6.144	06.433	05.696
		Plasma O5	130.425	5.584	5.900	06.181	05.847



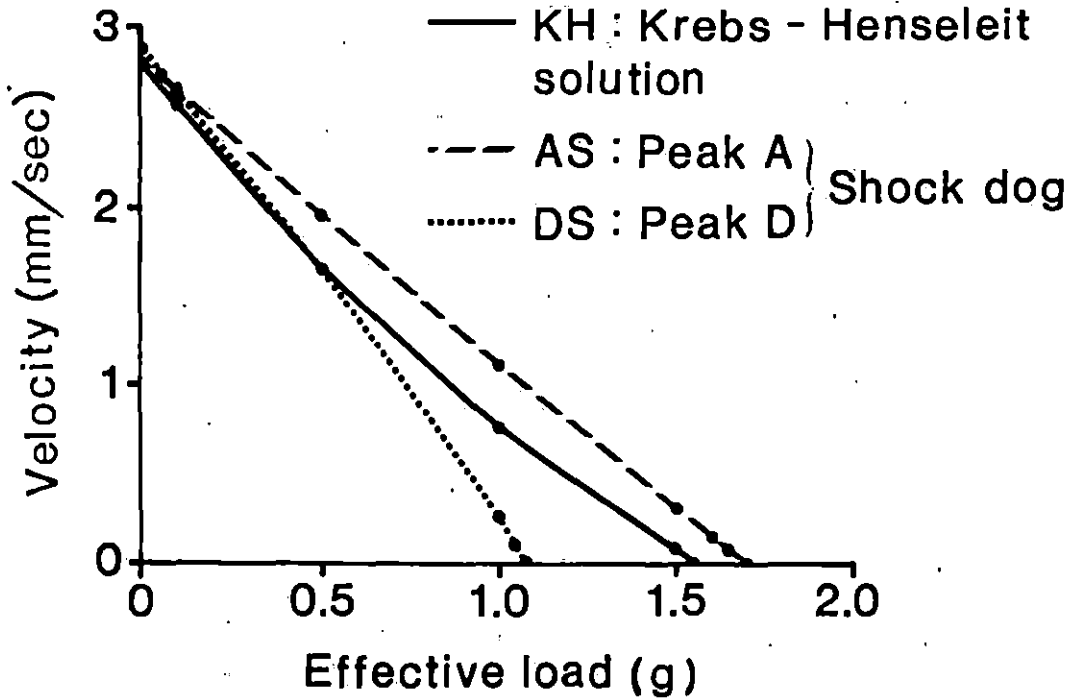
— KH: Krebs-Henseleit solution  
 - - - DY1: Peak D, Young dog #1, mongrel (M)  
 ..... DS: Peak D, Shock dog, mongrel (M)

Fourth power equation curve.

Significant MDF activity was present in peak D of shock plasma indicated by the depressed  $P_o$  and  $V_{max}$  values.  $P_o$ ,  $V_{max}$ , and active tension were significantly different ( $\alpha = 0.0025, 0.05, 0.025$ , respectively) for papillary muscle subjected to peak D of shock plasma and peak D of plasma from a young dog.

Figure 23. Force-velocity curve

## Load vs Velocity



— KH: Krebs-Henseleit solution  
 - - - AS: Peak A } Shock dog, mongrel (M)  
 ..... DS: Peak D }

Second power equation curve.  
 MDF activity was present in peak D of shock plasma indicated by the depressed  $P_0$  value. Peak A of shock plasma caused the initial increase in  $P_0$  beyond the K-H  $P_0$  value.

Figure 24. Force-velocity curve

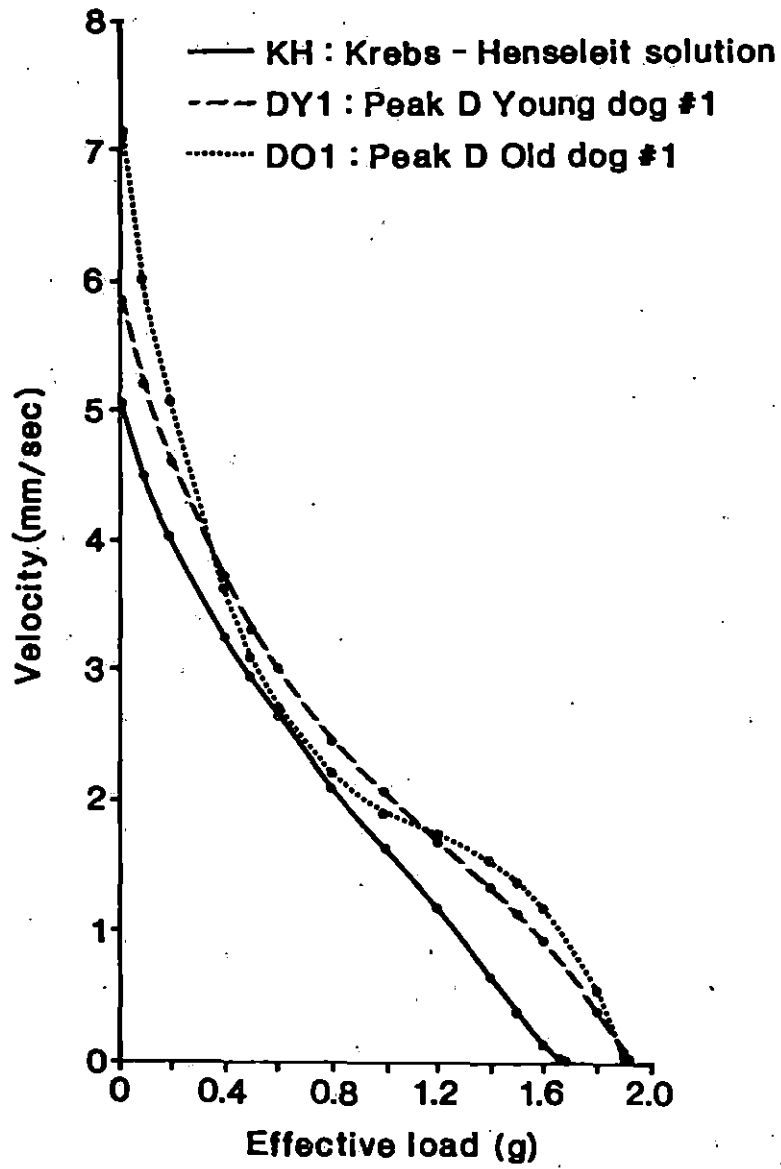
Figure 25. Force-velocity curve

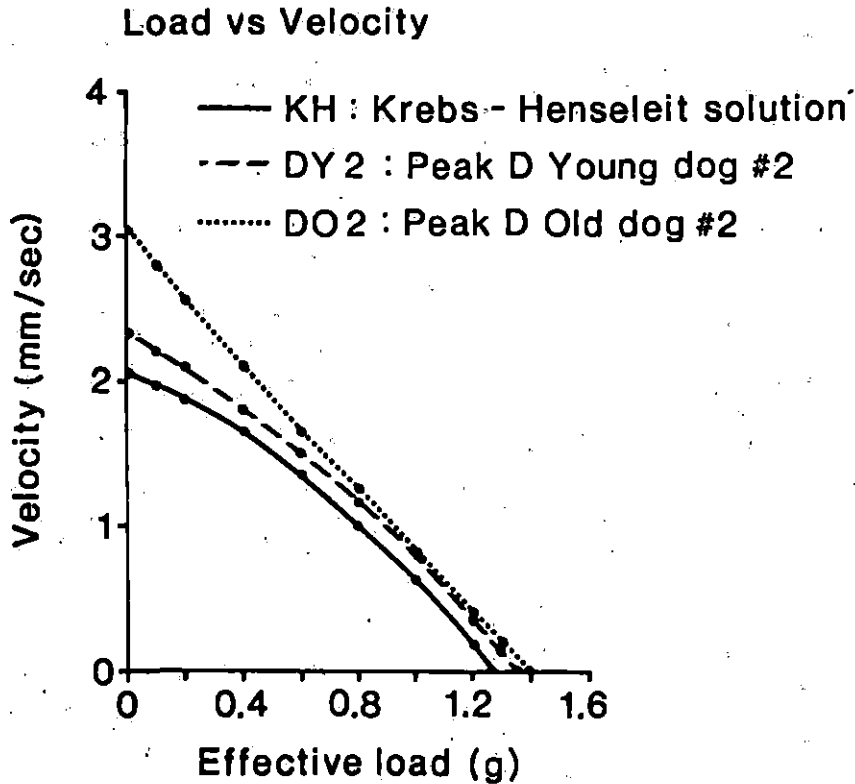
—— KH: Krebs-Henseleit solution  
- - - DY1: Peak D, Young dog #1, mongrel (M)  
..... DO1: Peak D, Old dog #1, dachshund (F),  
15 years

Third power equation curve.

Note that the  $P_o$  value of the muscle was the same for peak D of plasma from both the young and old dog. The  $V_{max}$  value of the muscle when subjected to peak D of plasma from the old dog was greater than the value when the muscle was subjected to peak D of plasma from the young dog or K-H. The difference between peak D of plasma from the young dog and peak D of plasma from the old dog was not significant.

## Load vs Velocity



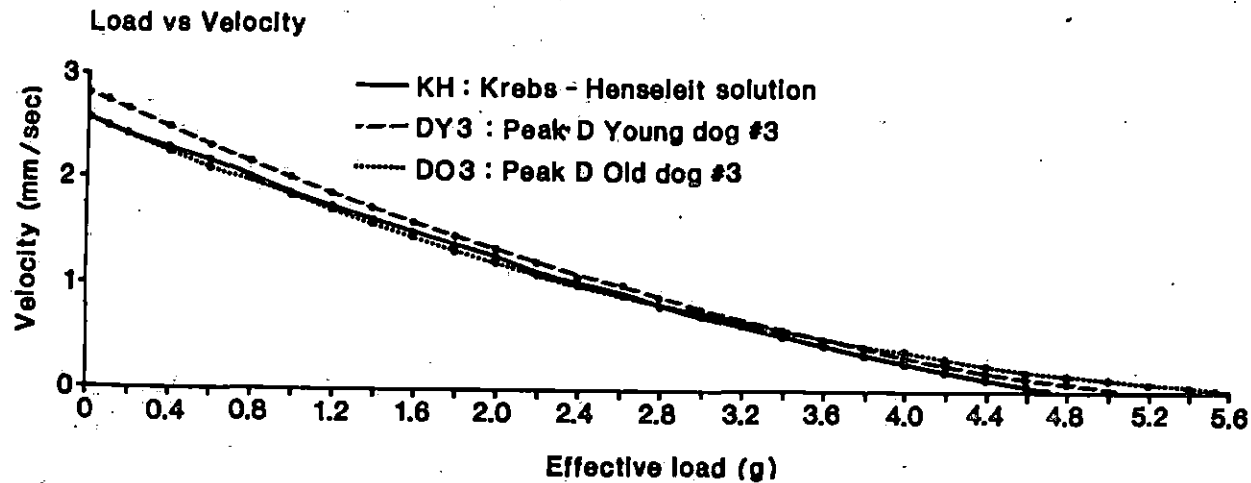


— KH: Krebs-Henseleit solution  
 - - - DY2: Peak D, Young dog #2, mongrel (M)  
 ..... DO2: Peak D, Old dog #2, beagle (M), 13.5 years

Second power equation curve.

Note that there was an improvement in muscle performance with peak D from the old dog. The difference between peak D of plasma from the young dog and peak D of plasma from the old dog was not significant.

Figure 26. Force-velocity curve

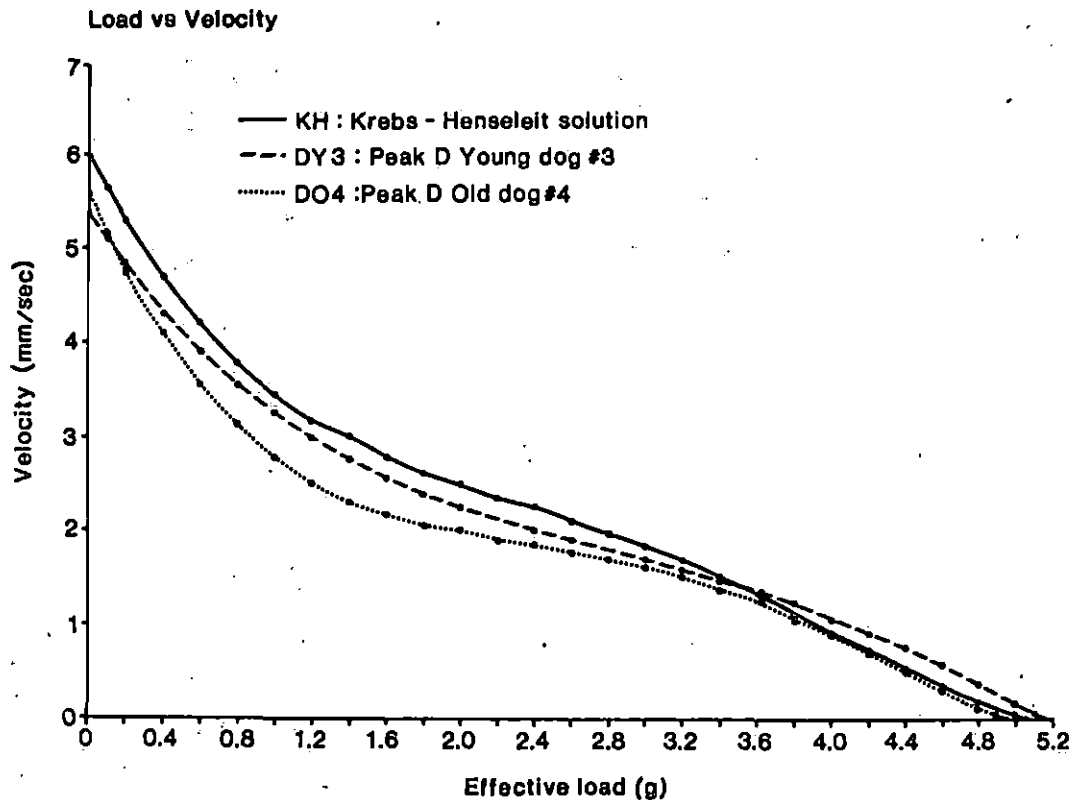


— KH: Krebs-Henseleit solution  
 - - - DY3: Peak D, Young dog #3, shepherd (M)  
 ..... DO3: Peak D, Old dog #3, Weimaraner (M), 14 years

Second power equation curve.

Note that all three curves are very similar. The  $P_0$  value of the muscle subjected to peak D of plasma from the old dog was greatest, and the  $V_{max}$  value of the muscle subjected to peak D of plasma from the old dog was identical to the  $V_{max}$  value of the muscle subjected to K-H. The difference between peak D of plasma from the young dog and peak D of plasma from the old dog was not significant.

Figure 27. Force-velocity curve



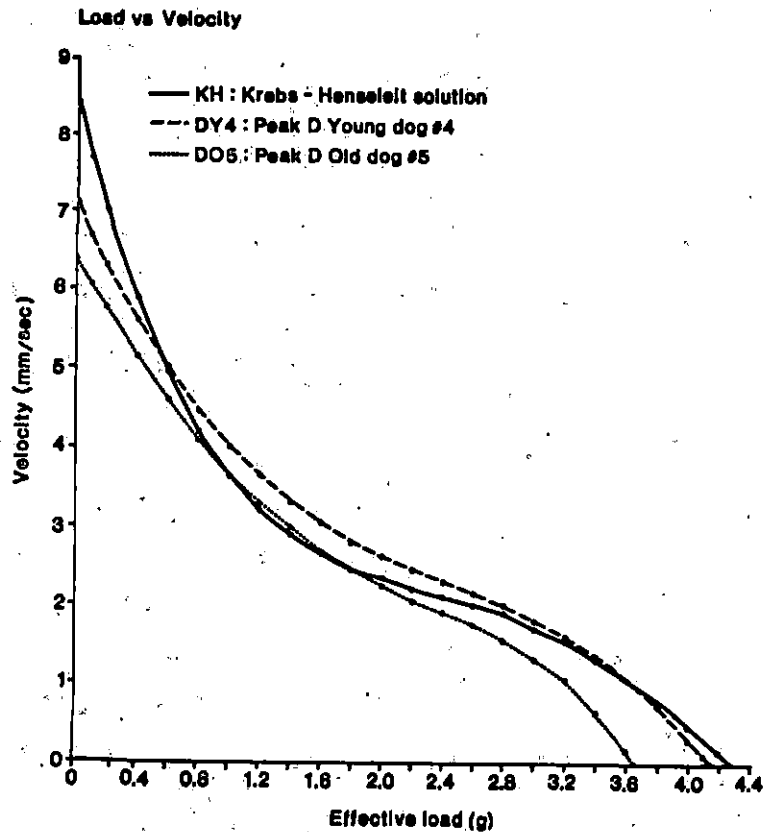
— KH: Krebs-Henseleit solution  
 - - - DY3: Peak D, Young dog #3, shepherd (M)  
 ..... DO4: Peak D, Old dog #4, collie (M), 16 years

Fourth power equation curve.

Note that the  $P_0$  value of the muscle subjected to peak D of plasma from the old dog was close to the value for K-H, and that the  $V_{max}$  value of the muscle subjected to peak D of plasma from the old dog was actually higher than the value when the muscle was subjected to peak D of plasma from the young dog. The difference between peak D of plasma from the young dog and peak D of plasma from the old dog was not significant.

Figure 28. Force-velocity curve

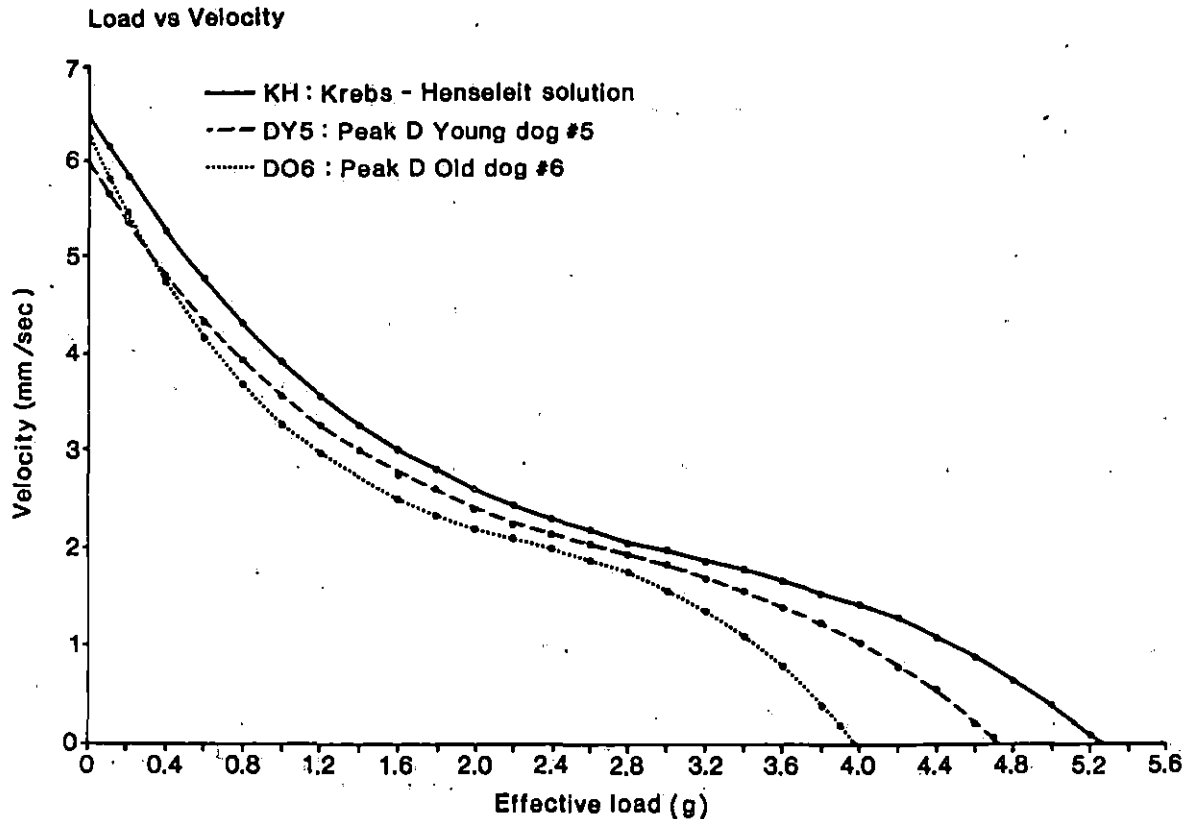




— KH: Krebs-Henseleit solution  
 - - - DY4: Peak D, Young dog #4, shepherd (F)  
 ..... DO5: Peak D, Old dog #5, beagle (F), 17 years

Fourth power equation curve. Although there was a decrease in  $P_0$  and  $V_{max}$  values of the muscle when subjected to peak D of plasma from the old dog, the difference between peak D of plasma from the young dog and peak D of plasma from the old dog was not significant.

Figure 29. Force-velocity curve



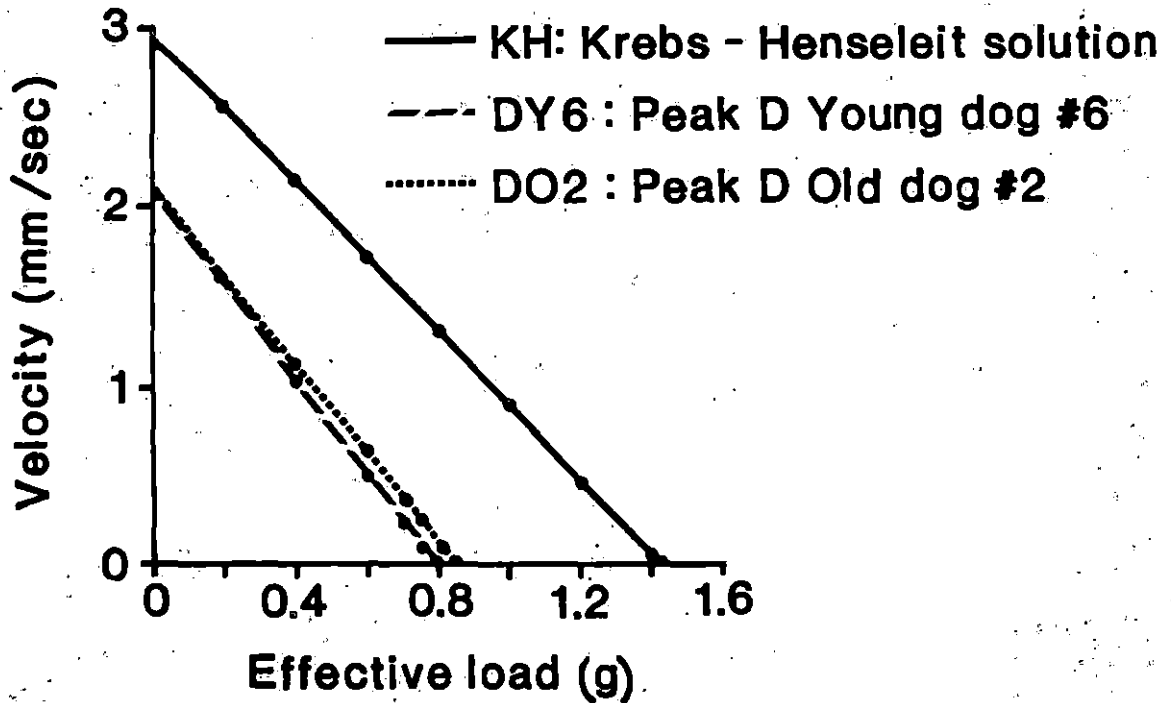
— KH: Krebs-Henseleit solution  
 - - - DY5: Peak D, Young dog #5, mongrel (M)  
 ..... DO6: Peak D, Old dog #6, dachshund (F), 15 years

Third power equation curve.

Although there was a decrease in the  $P_0$  value, the difference between peak D of plasma from the young dog and peak D of plasma from the old dog was not significant. Note that the velocity of the muscle subjected to peak D of plasma from the old dog approaches and exceeds the velocity of the muscle when subjected to peak D of plasma from the young dog.

Figure 30. Force-velocity curve

## Load vs Velocity



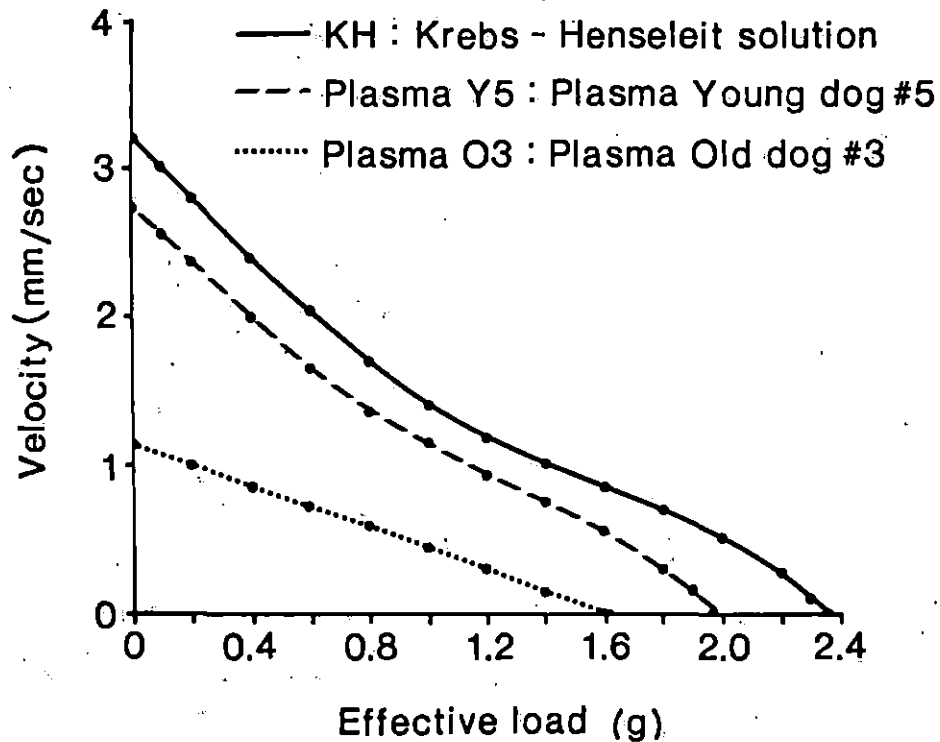
— KH: Krebs-Henseleit solution  
 - - - DY6: Peak D, Young dog #6, mongrel (F)  
 ..... DO2: Peak D, Old dog #2, beagle (M), 13.5 years

Linear equation curve.

Note that the curves for peak D of plasma from the young dog and peak D of plasma from the old dog are virtually identical. The  $P_0$  value was only slightly larger when the muscle was subjected to peak D of plasma from the old dog. Because of the unexpected large depression in muscle performance after the buffer was replaced with peak D from young dog #6, this muscle was omitted and DO2 was repeated (Figure 26).

Figure 31. Force-velocity curve

## Load vs Velocity



— KH: Krebs-Henseleit solution  
 - - - Plasma Y5: Plasma, Young dog #5, mongrel (M)  
 ..... Plasma O3: Plasma, Old dog #3, Weimaraner (M),  
 14 years

Fourth power equation curve: KH, Plasma Y5.

Linear equation curve: Plasma O3.

Although there was a depression in  $P_o$  and  $V_{max}$

values of the muscle when subjected to whole plasma from the old dog, the difference in  $P_o$  between whole plasma from the young dog and whole plasma from the old dog was not significant and only approached significance for  $V_{max}$ . Note that

the response elicited by peak D03 was very different (Figure 27).

Figure 32. Force-velocity curve

Figure 33. Force-velocity curve

—— KH: Krebs-Henseleit solution  
----- Plasma Y4: Plasma, Young dog #4, shepherd (F)  
..... Plasma O2: Plasma, Old dog #2, beagle (M), 13.5 years

Second power equation curve.

Note that the three curves are very similar. There was no significant difference between whole plasma from the young dog and whole plasma from the old dog. Note that there was a slight improvement in muscle performance when peak DO<sub>2</sub> was used (Figures 26, 31) instead of whole plasma.

### Load vs Velocity

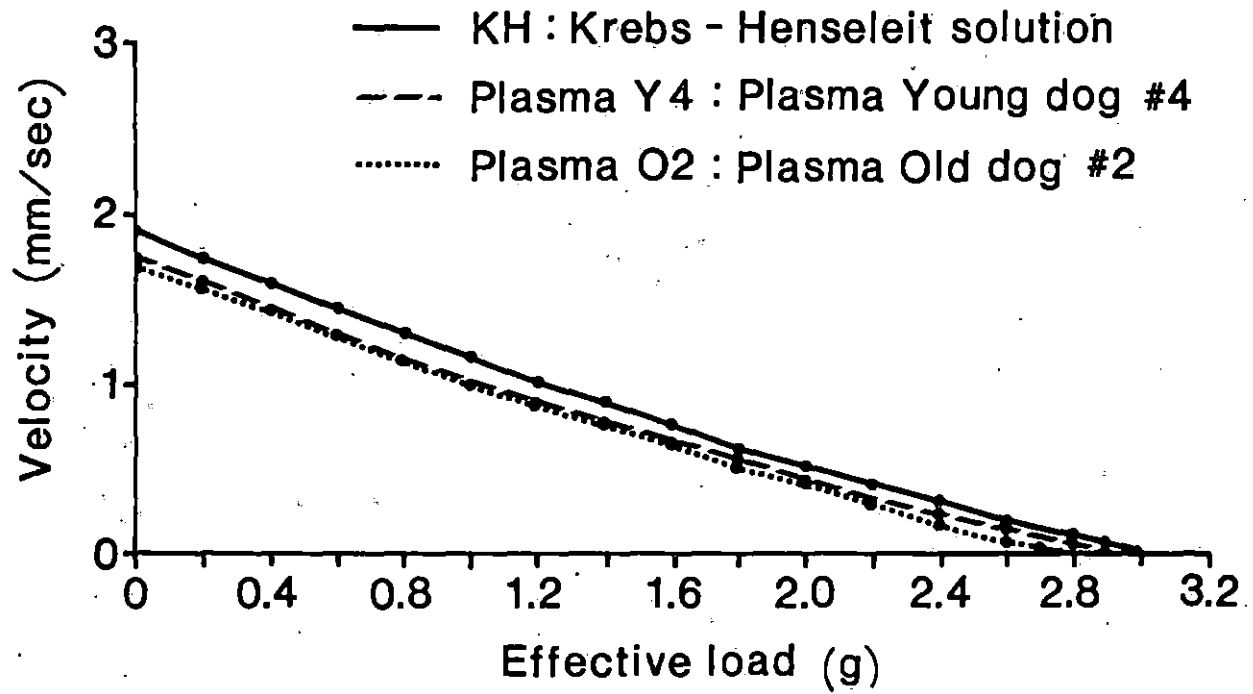


Figure 34. Force-velocity curve

\_\_\_\_\_ KH: Krebs-Henseleit solution  
----- Plasma Y5: Plasma, Young dog #5, mongrel (M)  
..... Plasma O5: Plasma, Old dog #5, beagle (F), 17 years

Third power equation curve.

Note that the  $P_0$  value of the muscle when subjected to whole plasma from the old dog was slightly greater than the value when whole plasma from the young dog was used. The difference between whole plasma from the young dog and whole plasma from the old dog was not significant. The curves for peak D from a young dog and peak DO5 (Figure 29) are similar to the curves for whole plasma except that there was a decrease in  $P_0$  when peak D from the old dog was used.

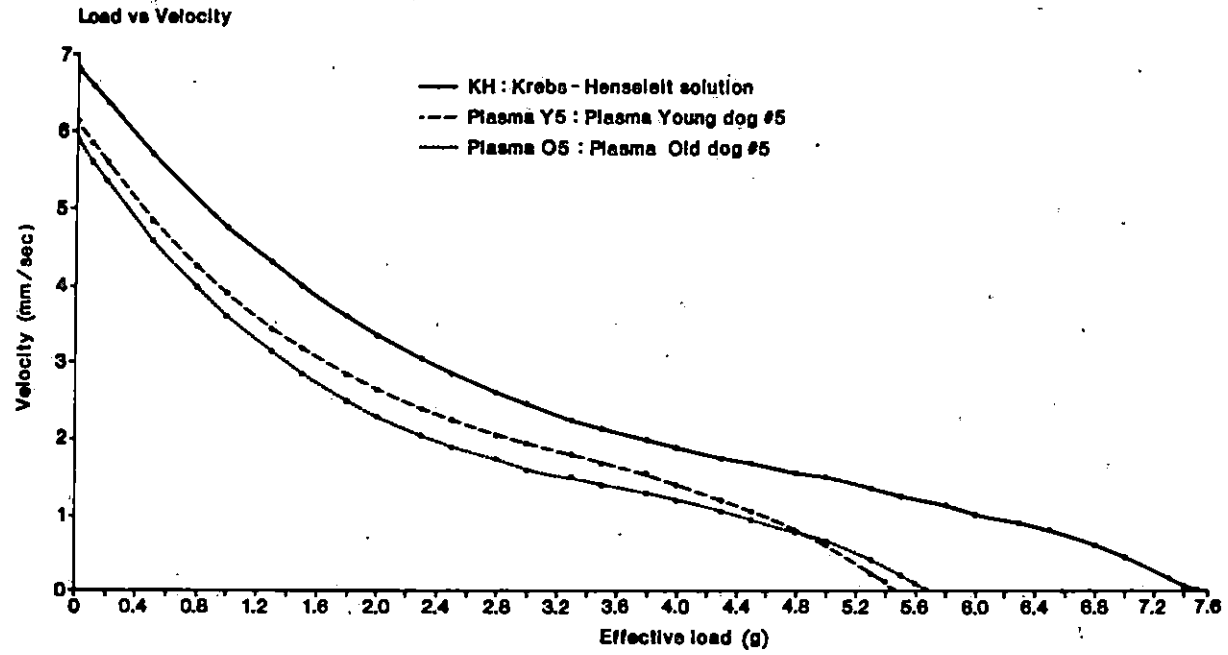
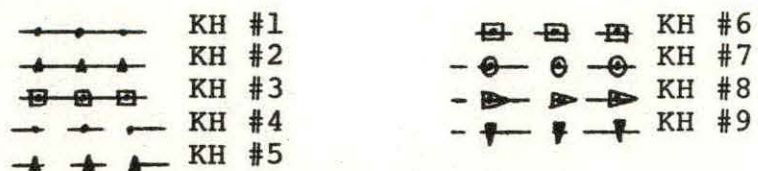




Figure 35. Composite of Krebs-Henseleit force-velocity curves where velocity is plotted against  $P/P_0$



The number following KH indicates the buffer that preceded a certain peak DY (peak D of plasma from a young dog) or plasma Y (whole plasma from a young dog) bath and thus refers to a certain muscle experiment (Table 4).

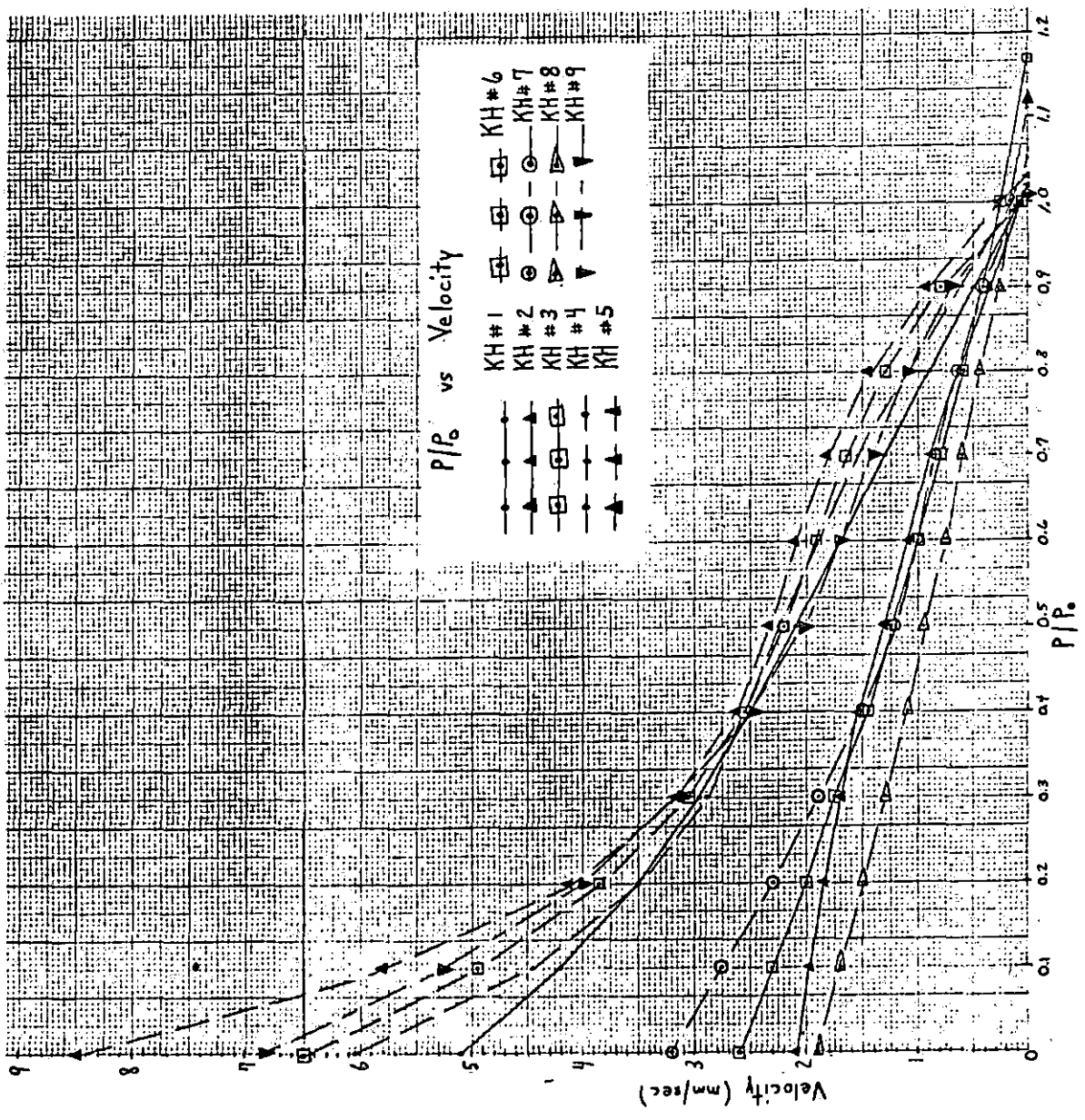


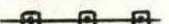





Figure 36. Composite of processed plasma peak D-young force-velocity curves where velocity is plotted against  $P/P_0$

	DY1 #1: Peak D, Young dog #1
	DY2 #2: Peak D, Young dog #2
	DY3 #3: Peak D, Young dog #3
	DY3 #4: Peak D, Young dog #3
	DY4 #5: Peak D, Young dog #4
	DY5 #6: Peak D, Young dog #5

DY3 #3 and DY3 #4 were preceded by KH #3 and KH #4, respectively (Table 4).

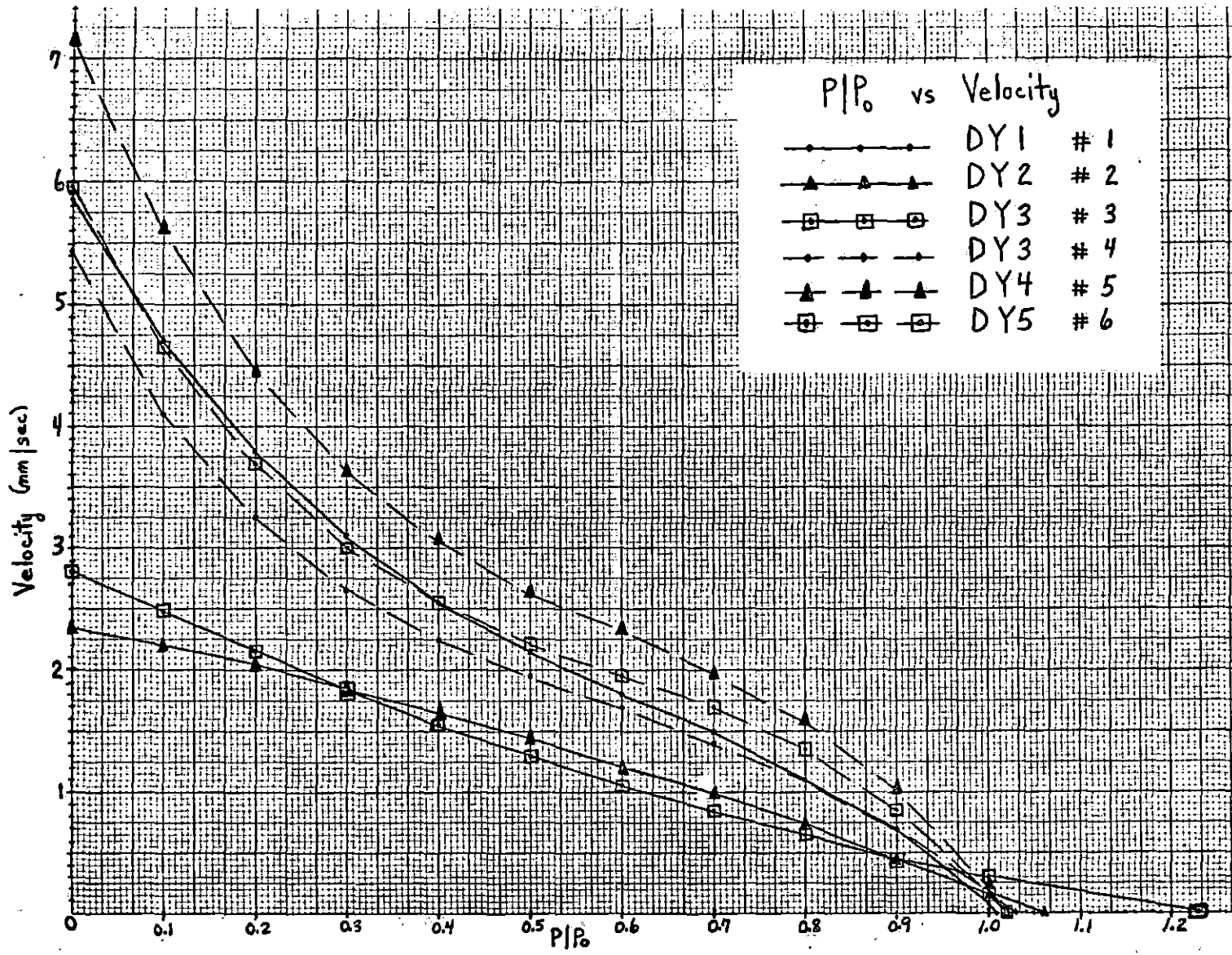
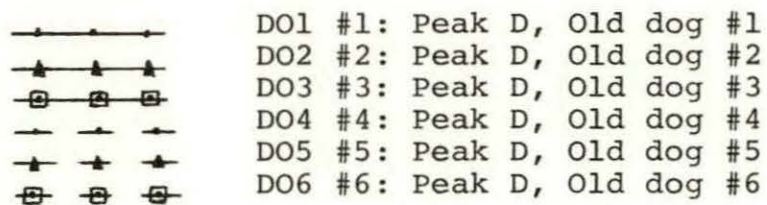
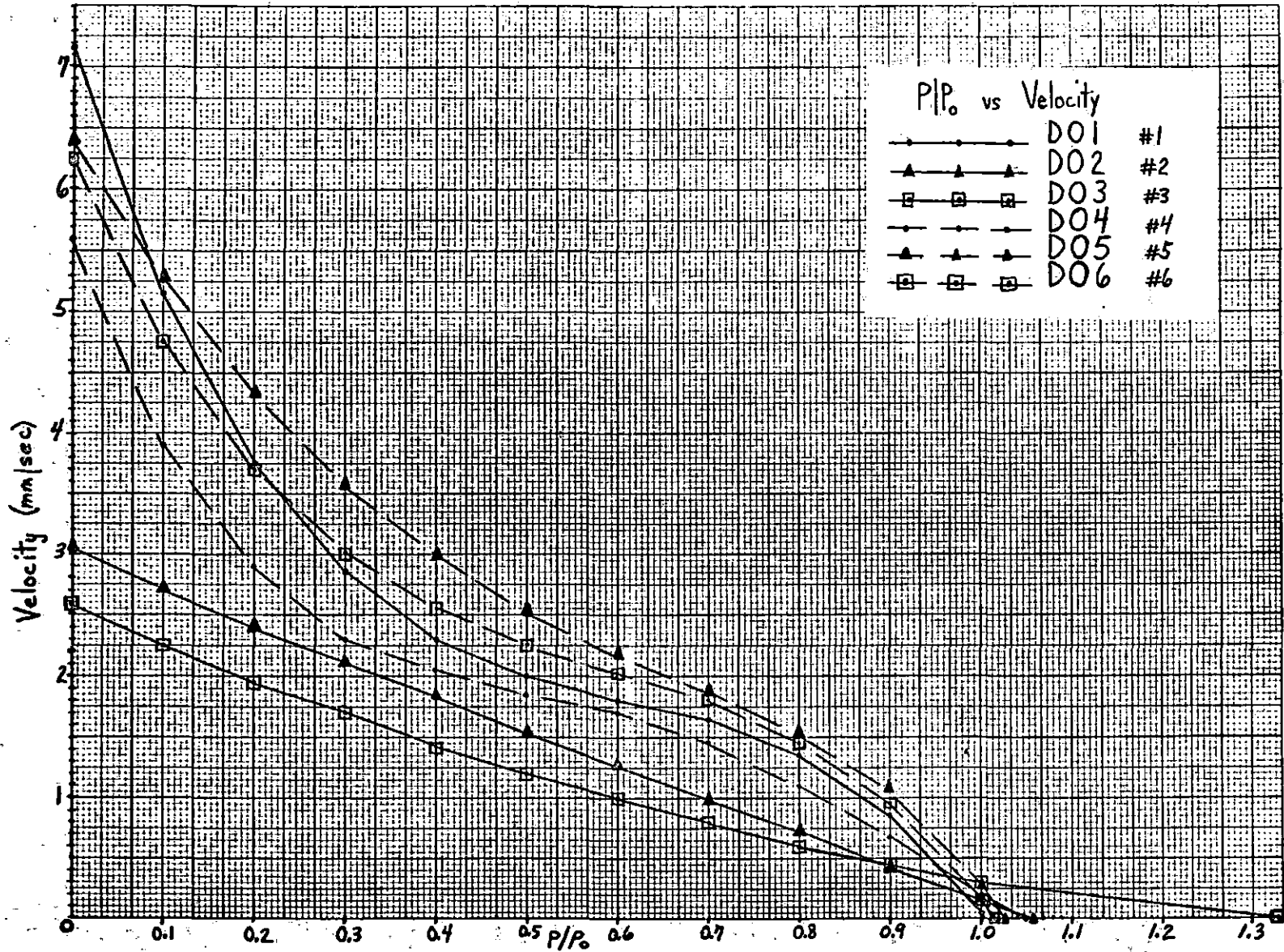
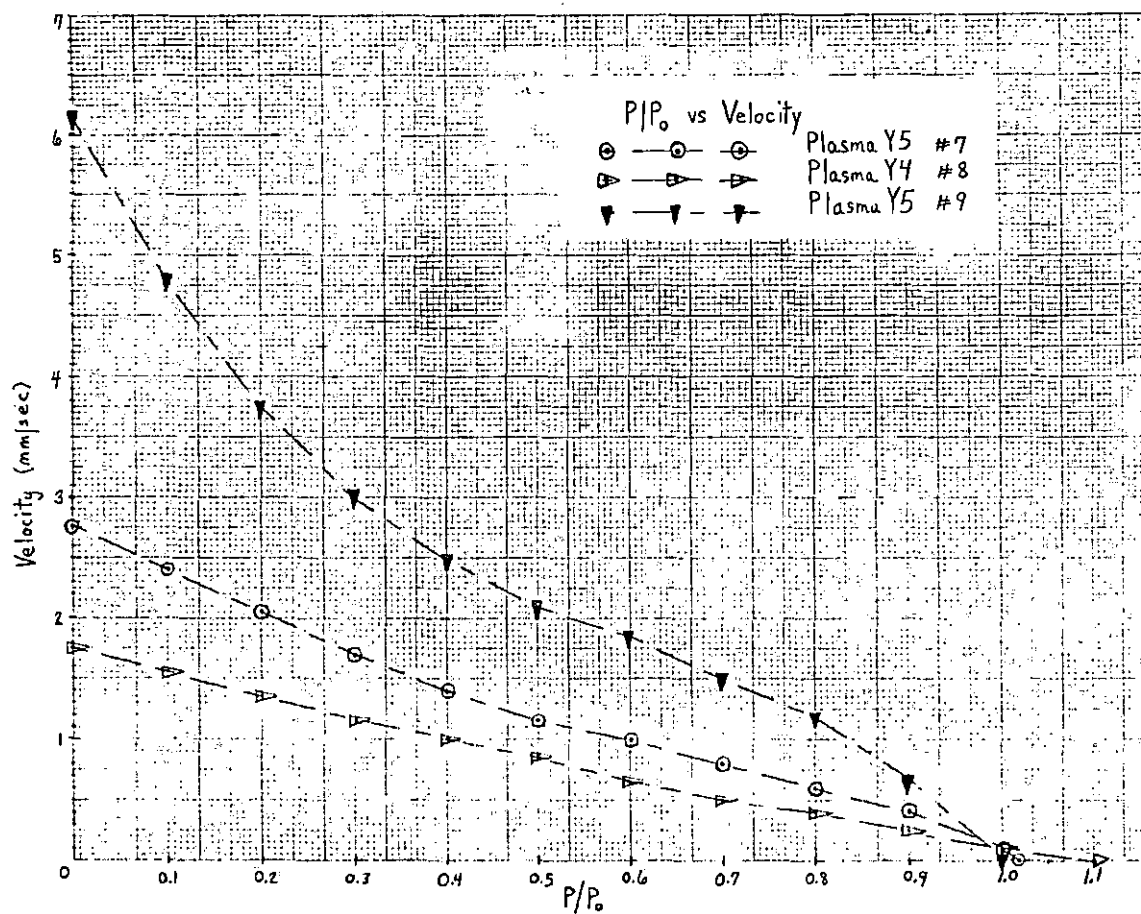


Figure 37. Composite of processed plasma peak D-old force-velocity curves where velocity is plotted against  $P/P_0$







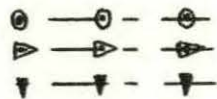
⊙ — ⊙ — ⊙ Plasma Y5 #7: Whole plasma, Young dog #5  
 ▼ — ▼ — ▼ Plasma Y4 #8: Whole plasma, Young dog #4  
 ▲ — ▲ — ▲ Plasma Y5 #9: Whole plasma, Young dog #5

Plasma Y5 #7 and Plasma Y5 #9 were preceded by KH #7 and KH #9, respectively (Table 4).

Figure 38. Composite of whole plasma-young force-velocity curves where velocity is plotted against  $P/P_0$ .



Figure 39. Composite of whole plasma-old force-velocity curves where velocity is plotted against  $P/P_0$



Plasma 03 #7: Whole plasma, Old dog #3  
Plasma 02 #8: Whole plasma, Old dog #2  
Plasma 05 #9: Whole plasma, Old dog #5



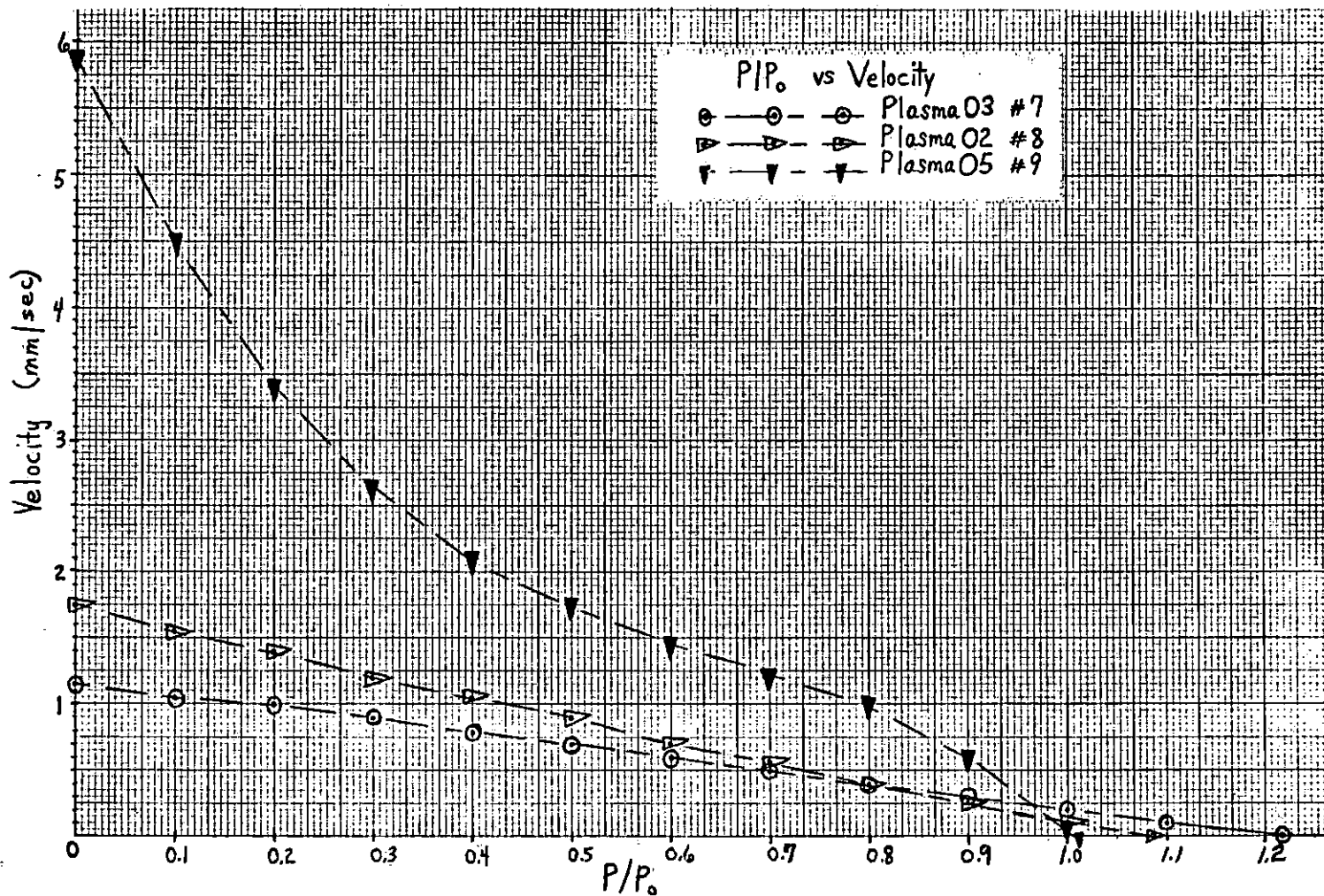
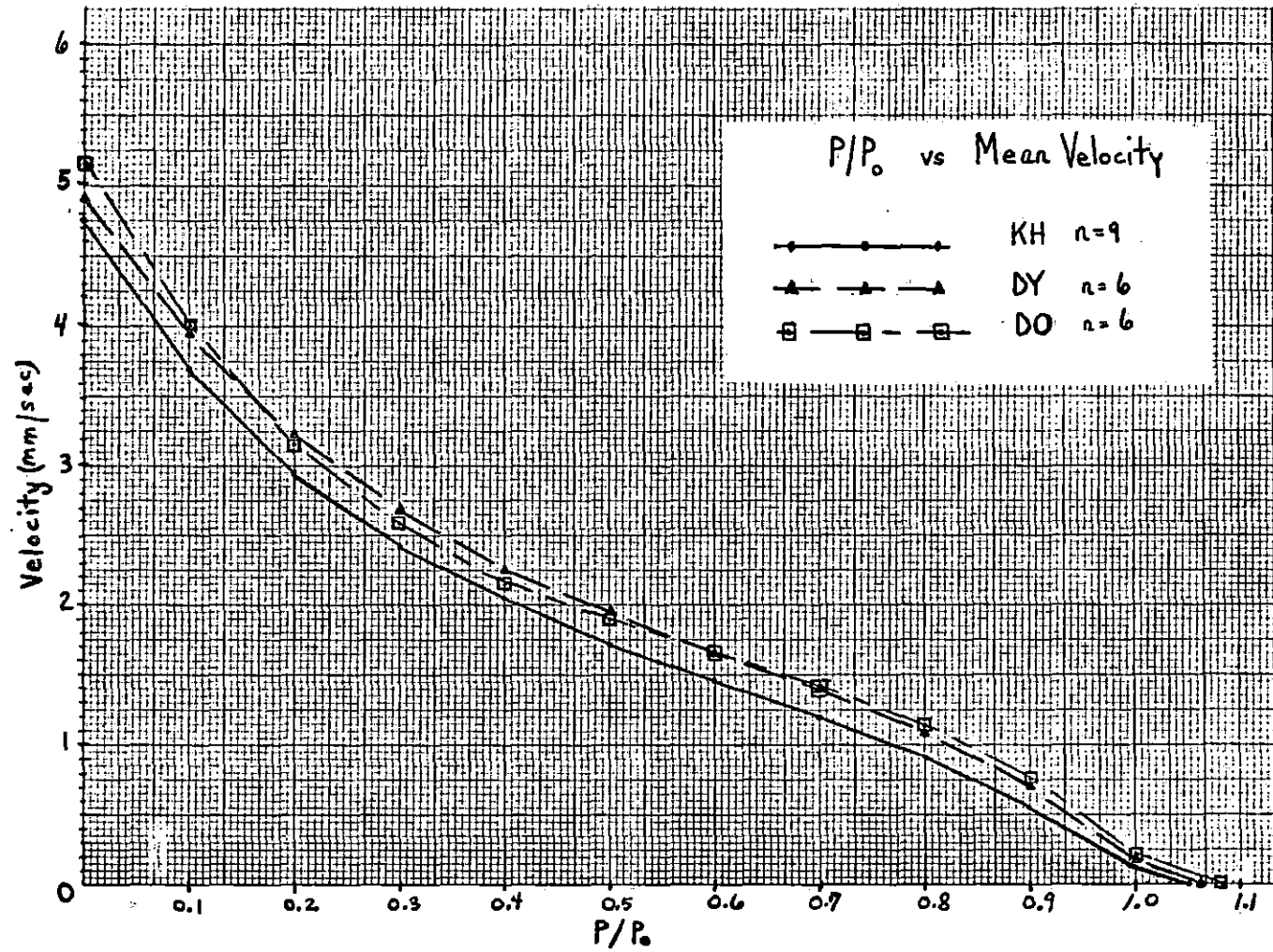
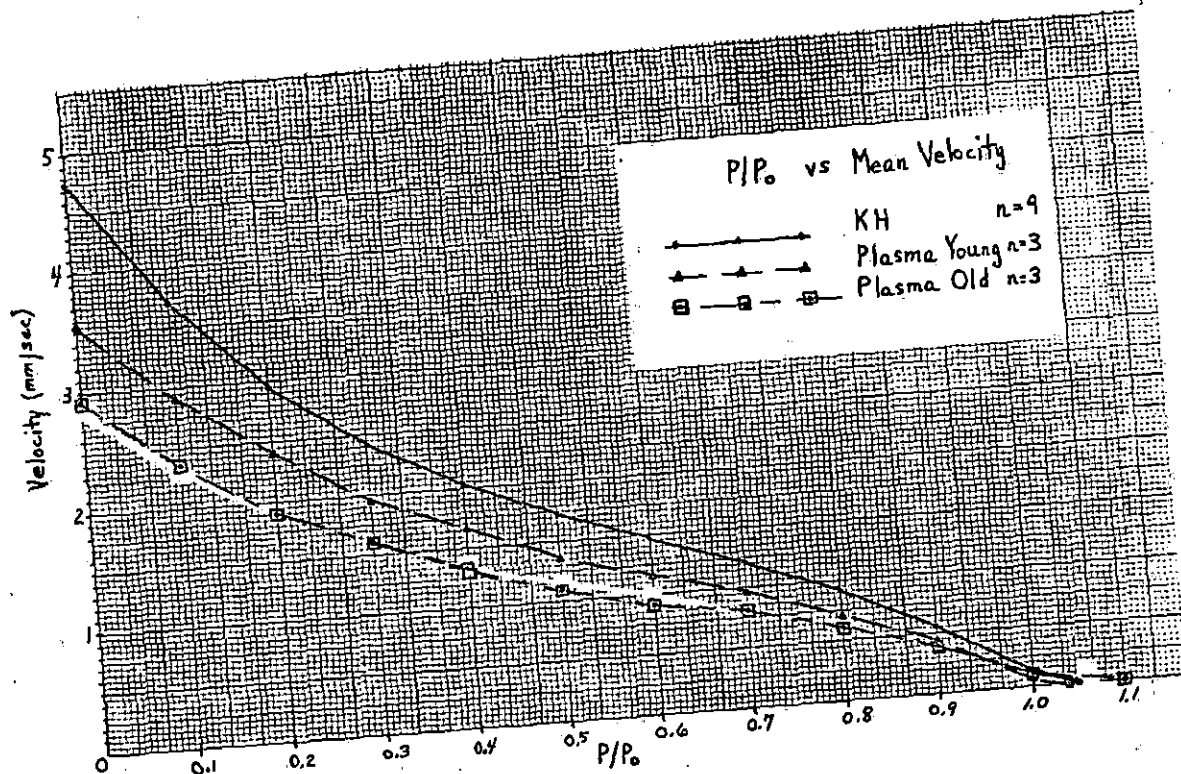


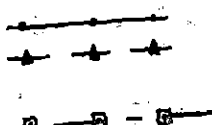
Figure 40. Composite Krebs-Henseleit, peak D-young and peak D-old force-velocity curves from age muscle experiments where mean velocity is plotted against  $P/P_0$

—•—•—•— KH n=9: Krebs-Henseleit solution  
—▲—▲—▲— DY n=6: Peak D of plasma from young dogs  
—■—■—■— DO n=6: Peak D of plasma from old dogs

The velocities for the Krebs-Henseleit curve are the means of the velocities for the nine K-H curves (Figure 35) from the nine age muscle experiments. The velocities for the peak D-young and -old curves are the means of the velocities for the six DY and DO curves (Figures 36, 37) from the corresponding six age muscle experiments. The three points along the x-axis (zero velocity) are means of similar points from the composites of K-H, DY, and DO. Note that the curves for DY and DO are very similar, and that the  $V_{\max}$  value for DO is greater than that for DY or K-H.









  
 KH n=9: Krebs-Henseleit solution  
 Plasma Young n=3: Whole plasma from young dogs  
 Plasma Old n=3: Whole plasma from old dogs

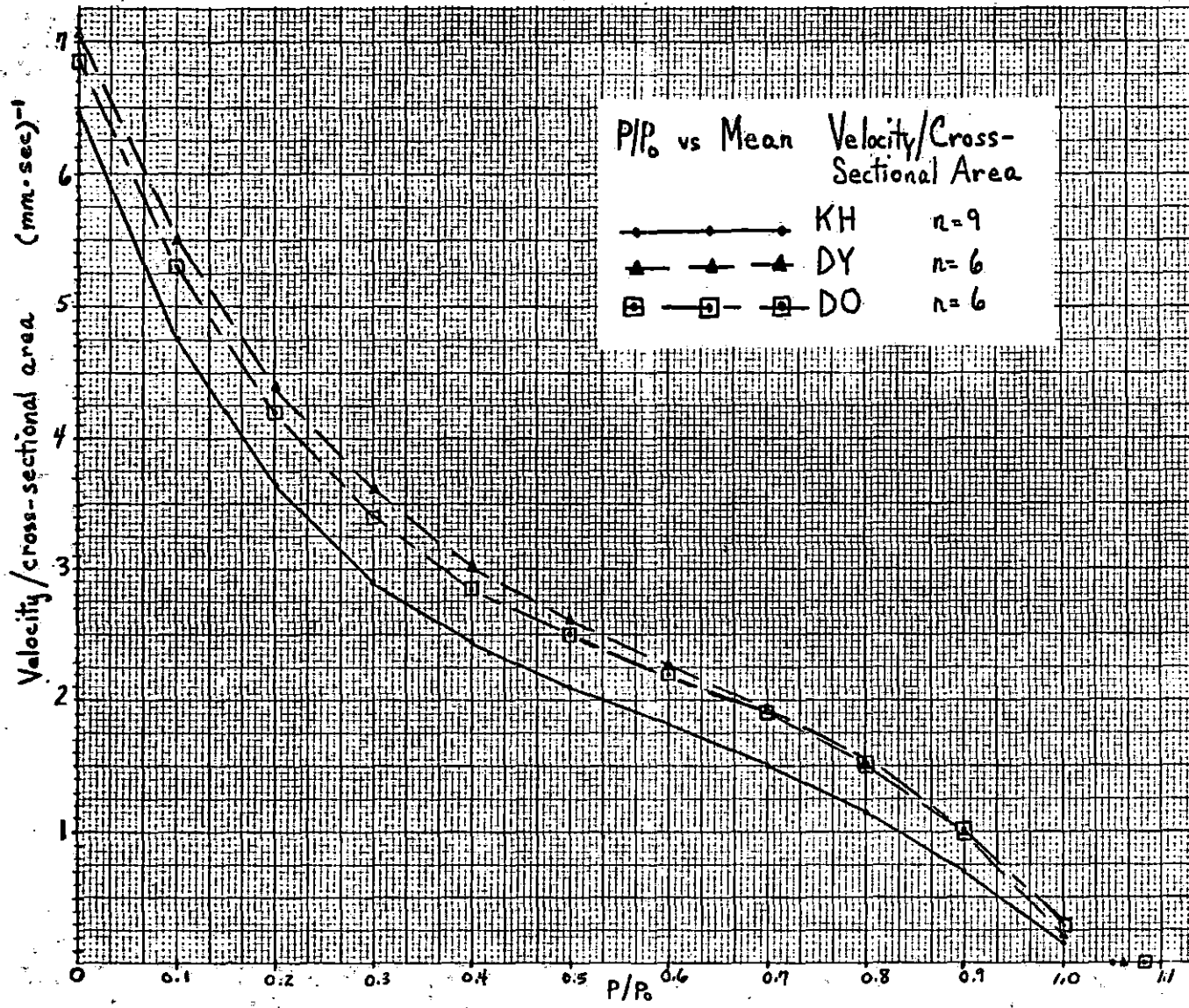
The velocities for the K-H curve are the means of the velocities for the nine K-H curves (Figure 35). The velocities for plasma-young and plasma-old are the means of the velocities for the three plasma-young and plasma-old curves (Figures 38, 39). The three points along the x-axis (zero velocity) are means of similar points from the composites of K-H, plasma-young, and plasma-old.

Figure 41. Composite Krebs-Henseleit, plasma-young and plasma-old force-velocity curves from age muscle experiments where mean velocity is plotted against P/P<sub>0</sub>.

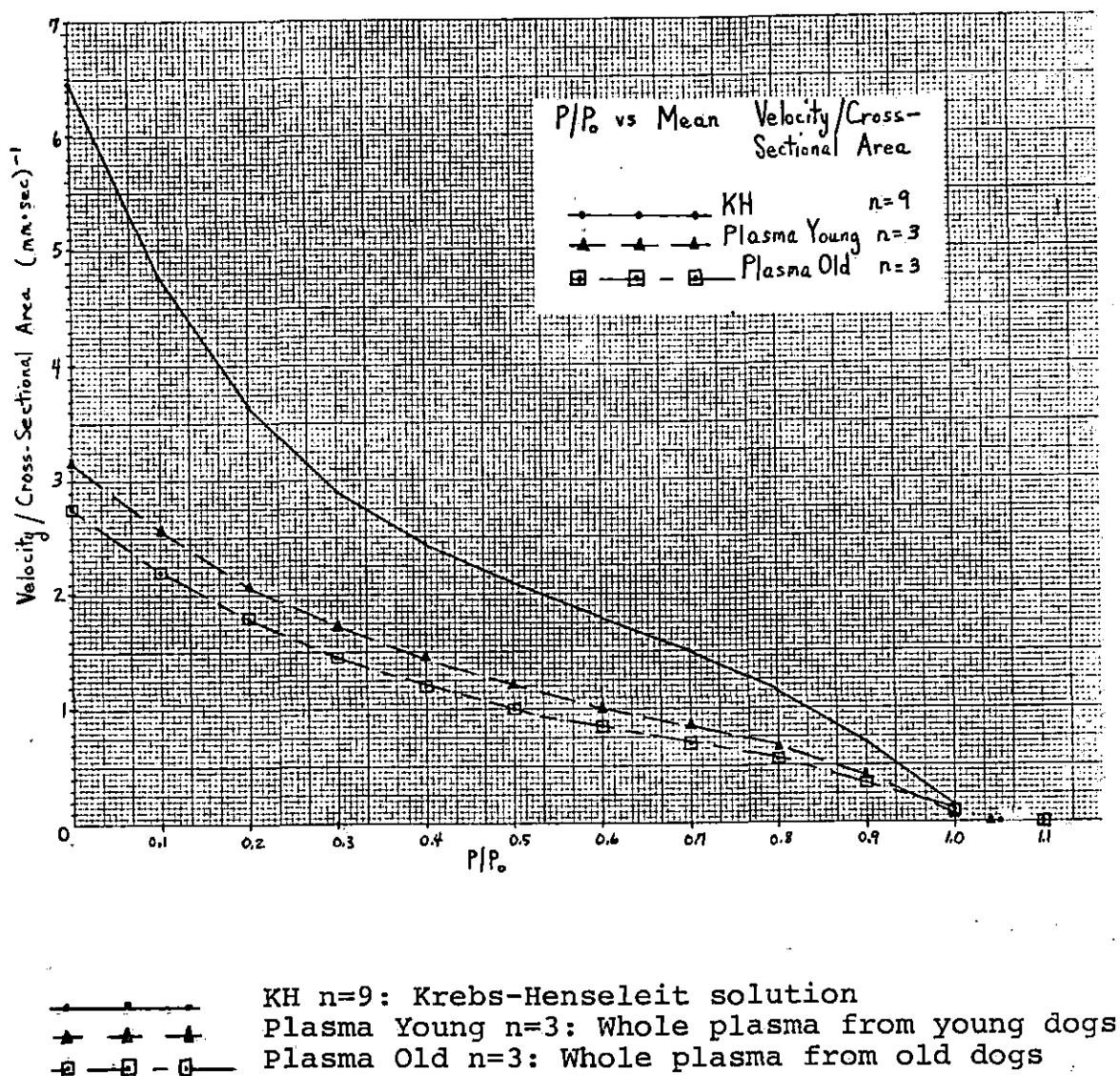
Figure 42. Composite Krebs-Henseleit, peak D-young and peak D-old force-velocity curves from age muscle experiments where the mean of velocity per unit of cross-sectional area is plotted against  $P/P_0$

	KH n=9: Krebs-Henseleit solution
	DY n=6: Peak D of plasma from young dogs
	DO n=6: Peak D of plasma from old dogs

Note the similarity in the curves for DY and DO.

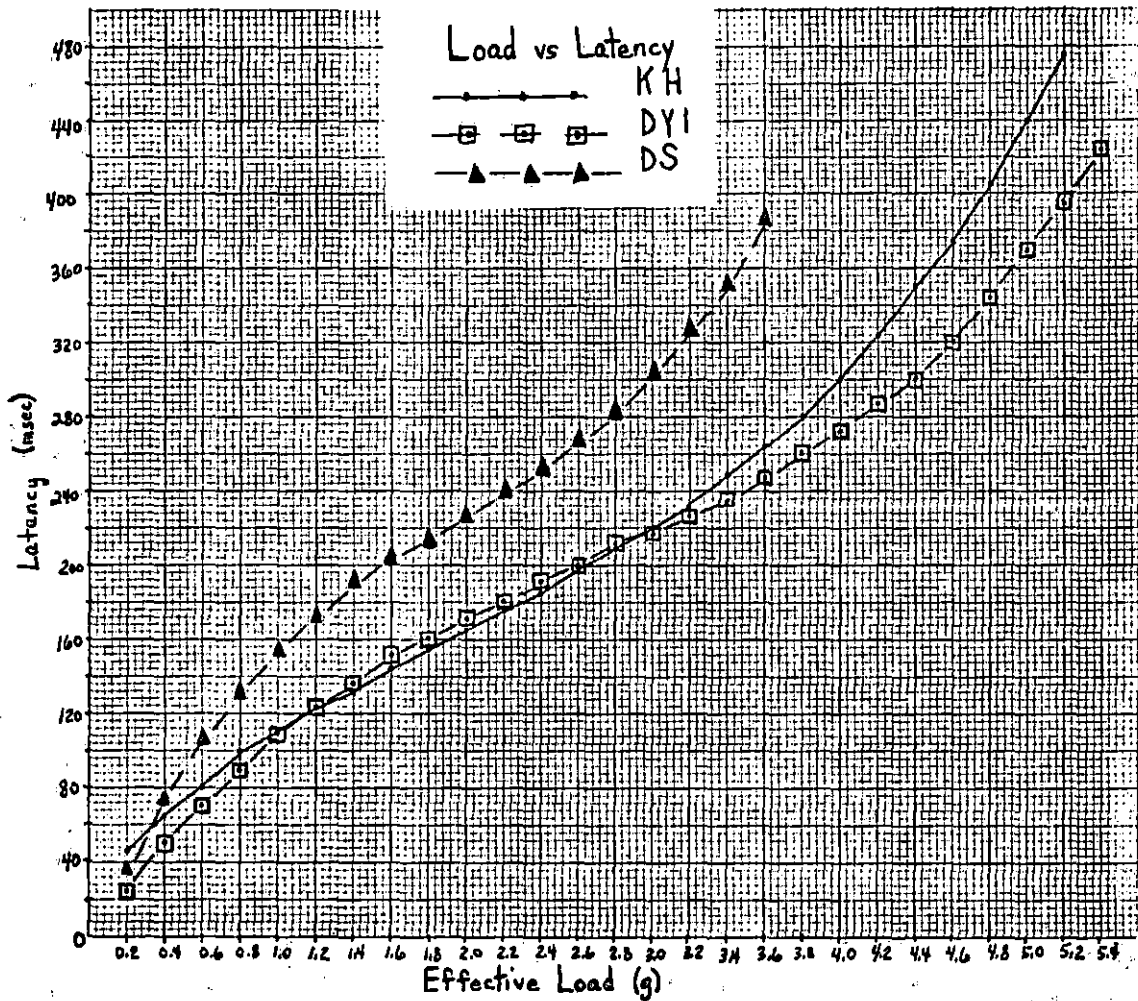






Note the similarity in the curves for whole plasma from young dogs and whole plasma from old dogs.

Figure 43. Composite Krebs-Henseleit, plasma-young and plasma-old force-velocity curves from age muscle experiments where the mean of velocity per unit of cross-sectional area is plotted against  $P/P_0$ .



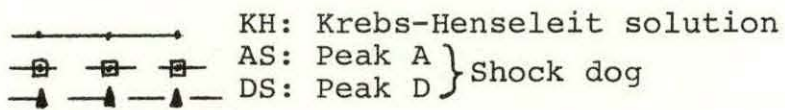
—●— KH: Krebs-Henseleit solution  
 —□— DY1: Peak D, Young dog #1  
 —▲— DS: Peak D, Shock dog

Third power equation curve.  
 Although the slope of the shock curve was  
 greater than that of the K-H or young curve,  
 it was not significantly different.

Figure 44. Load-latency curve



Figure 45. Load-latency curve



Second power equation curve.

Note that the slope decreased with shock plasma peak A and then increased with shock plasma peak D. The difference in slope was not significant.

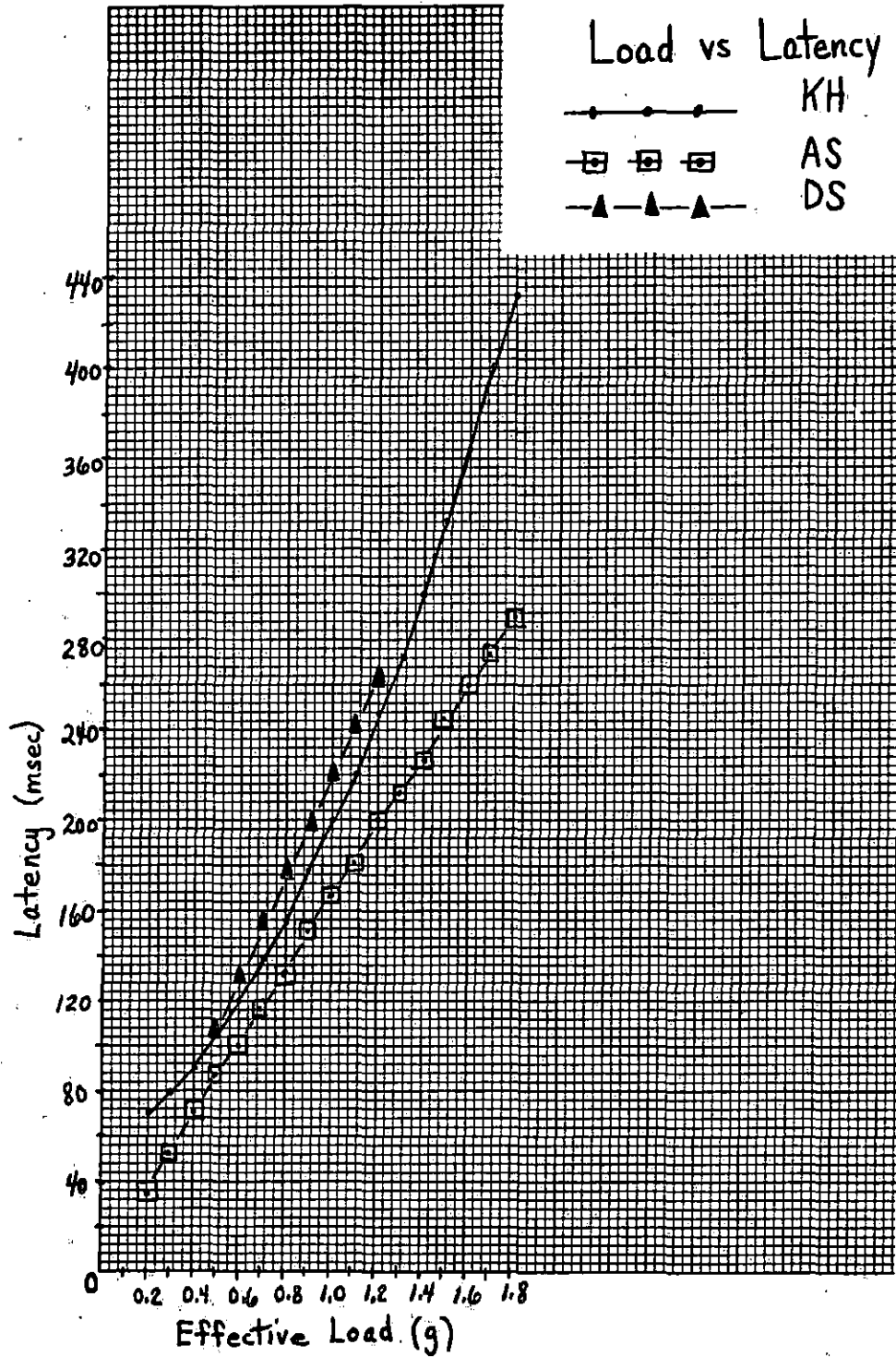
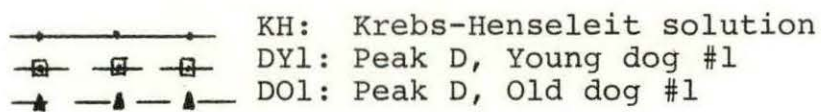


Figure 46. Load-latency curve



Third power equation curve.

The slope continually decreased as Krebs-Henseleit was replaced with peak D of plasma from a young dog and then with peak D of plasma from an old dog. There was no significant difference between peak D of plasma from the young dog and peak D of plasma from the old dog.

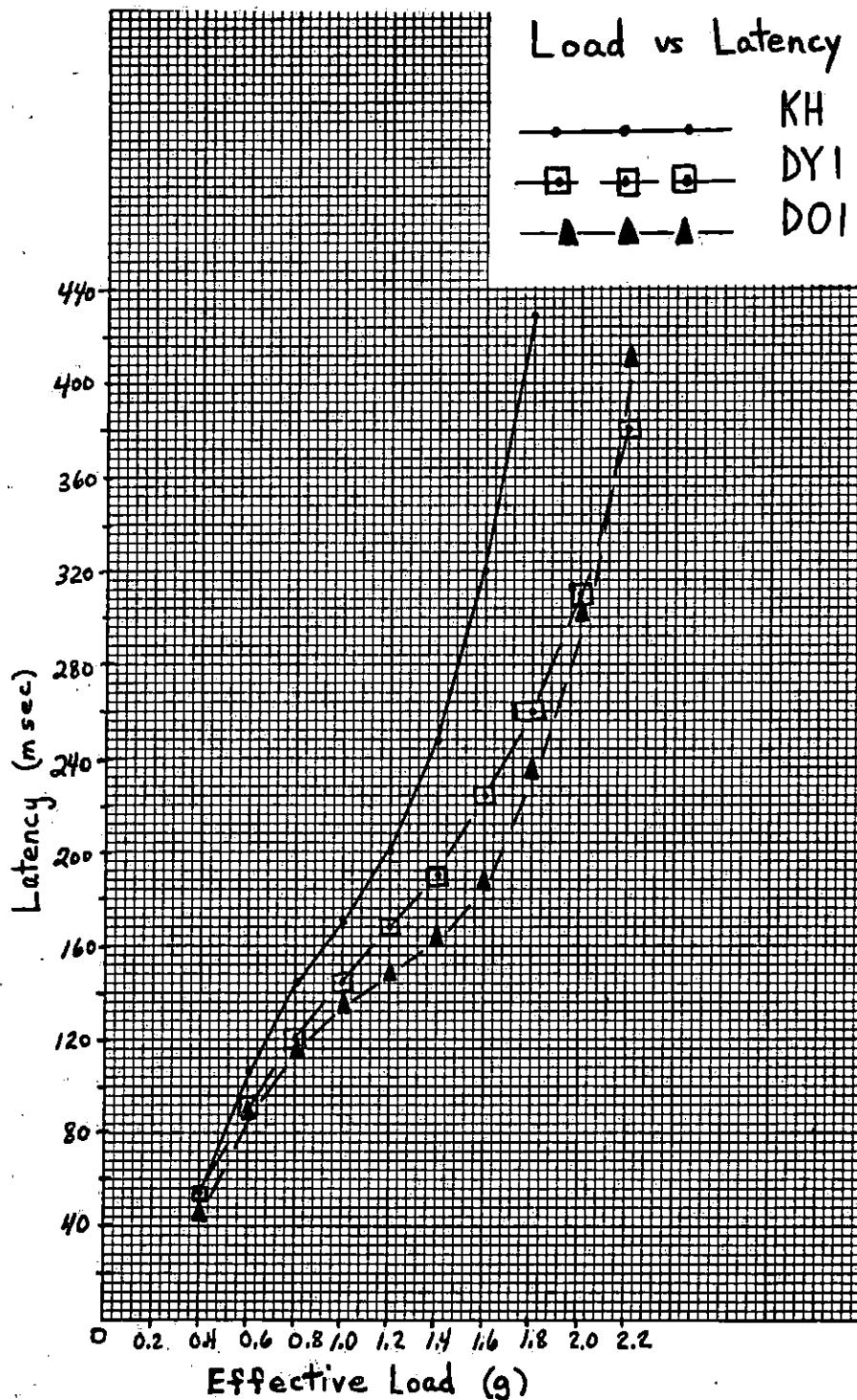


Figure 47. Load-latency curve

—•—•—•— KH: Krebs-Henseleit solution  
—□—□—□— DY2: Peak D, Young dog #2  
—▲—▲—▲— DO2: Peak D, Old dog #2

Second power equation curve.

There was no significant difference between peak D of plasma from a young dog and peak D of plasma from an old dog.

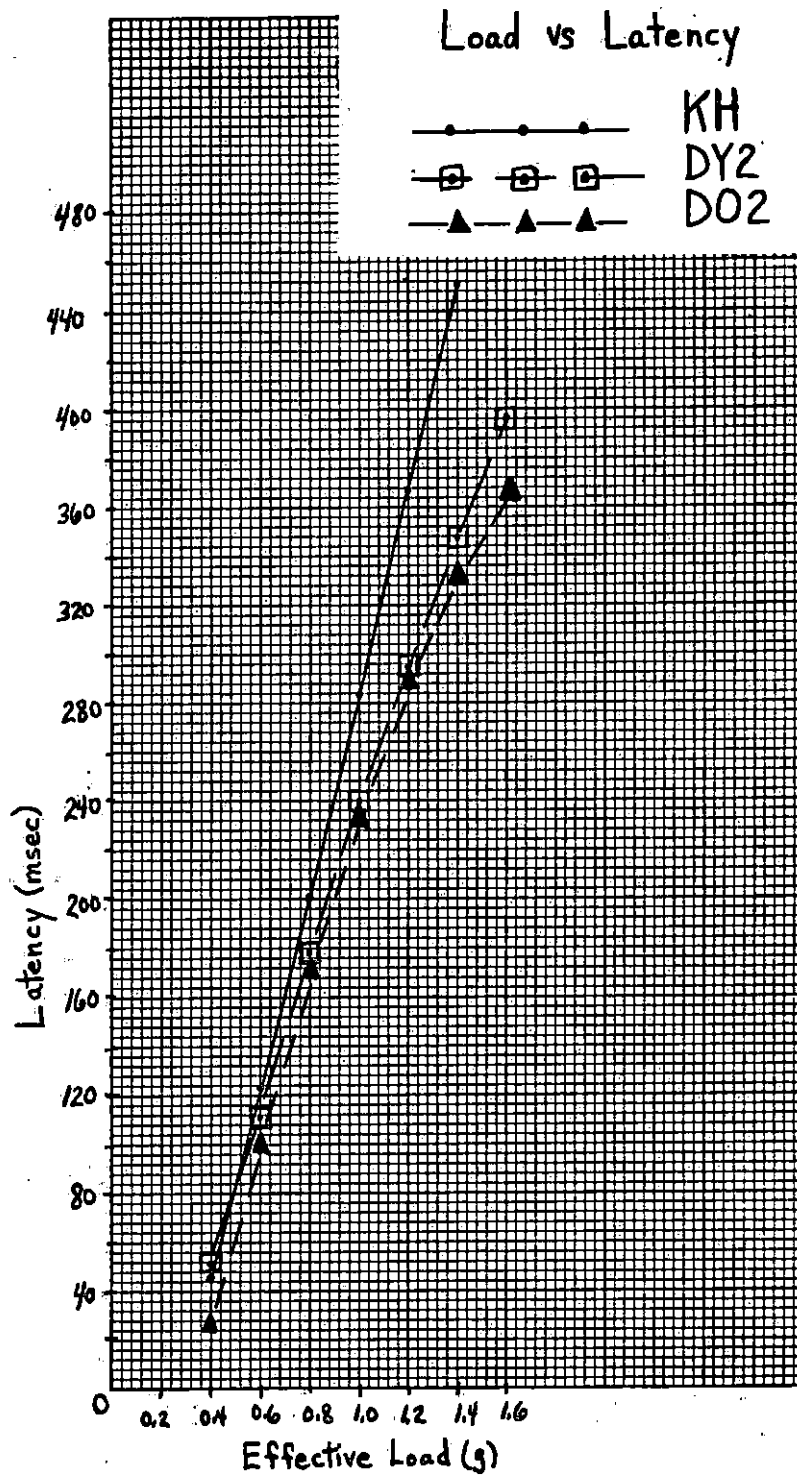
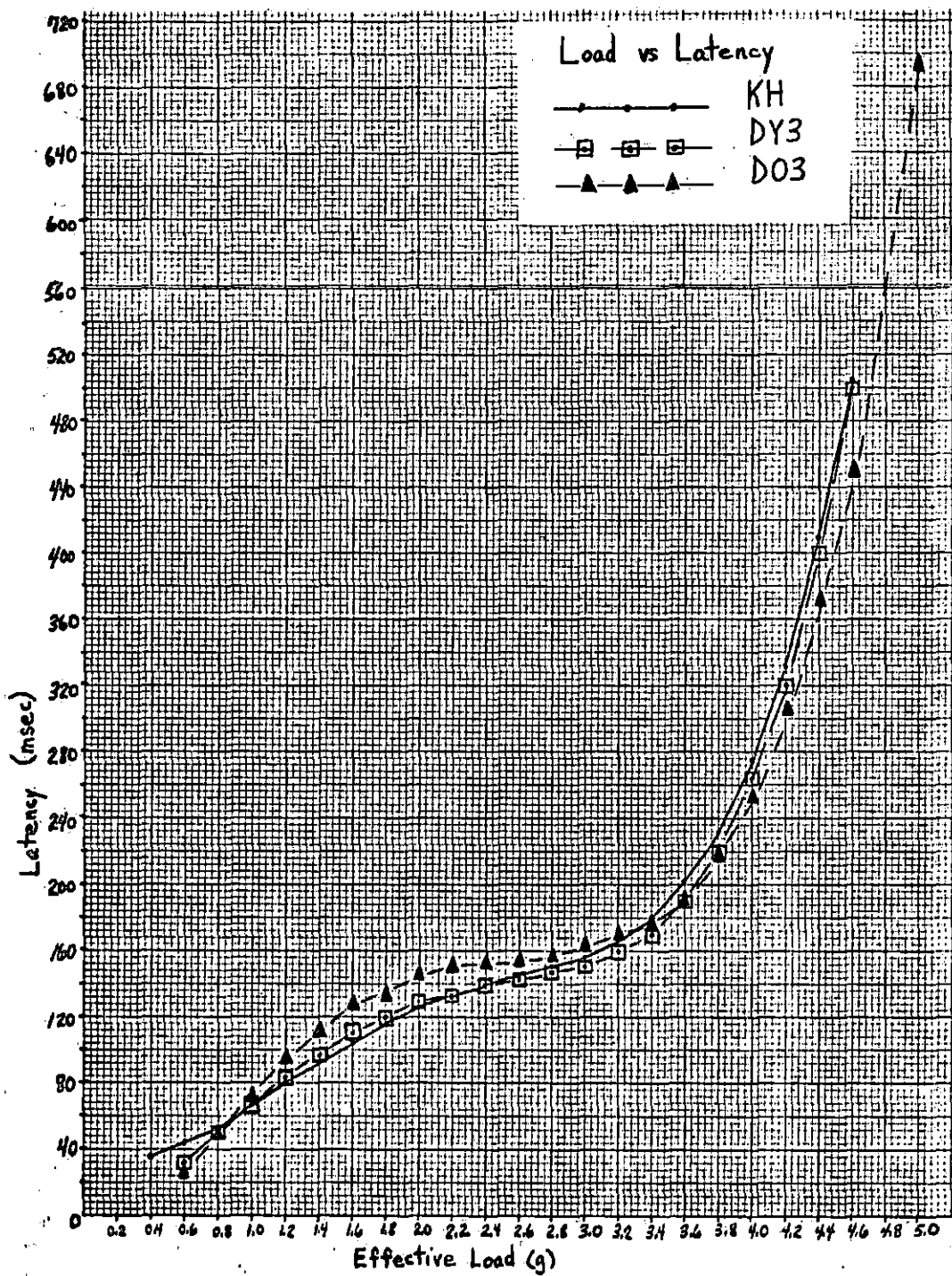


Figure 48. Load-latency curve

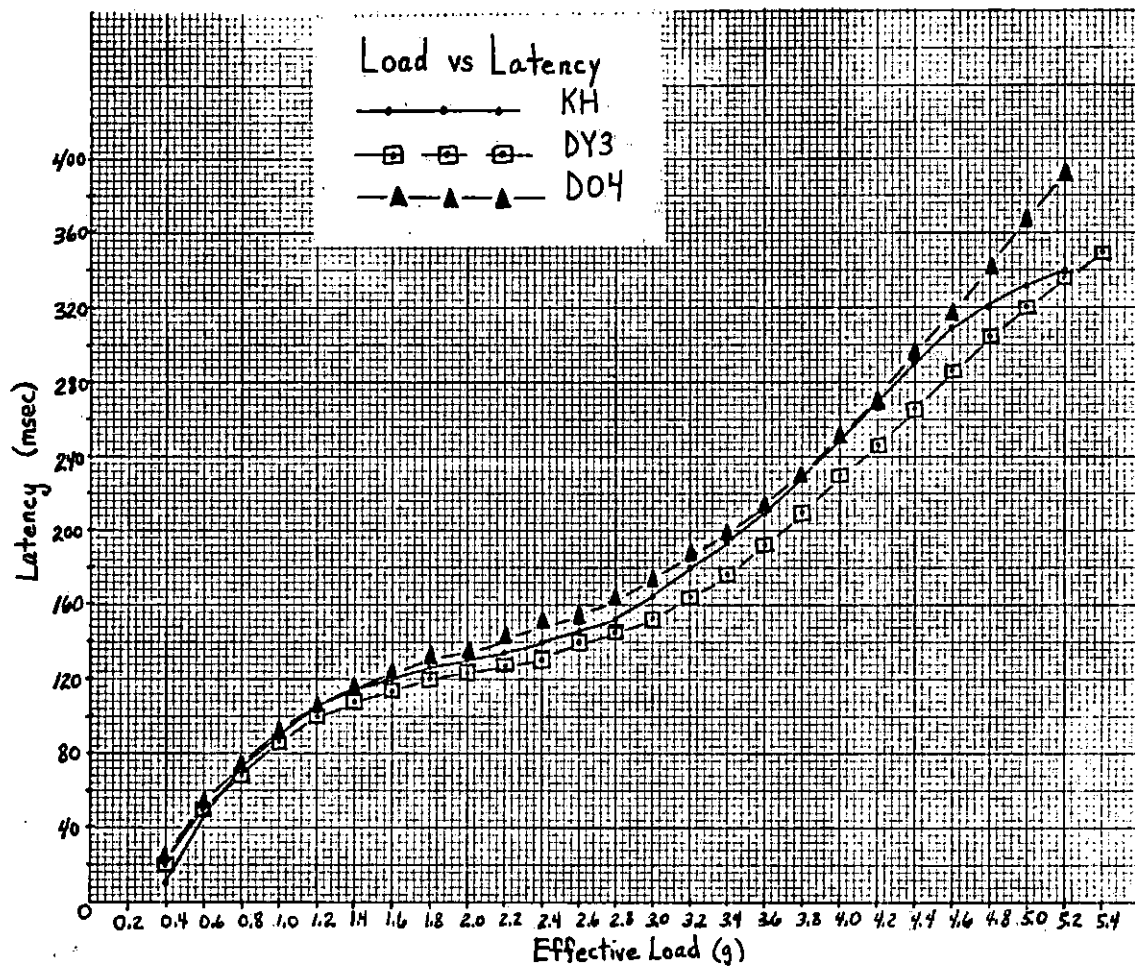
—•—•—•— KH: Krebs-Henseleit solution  
—□—□—□— DY3: Peak D, Young dog #3  
—▲—▲—▲— DO3: Peak D, Old dog #3

Fourth power equation curve.

The slope of the curve for peak D of plasma from an old dog was less than the slopes of the K-H curve and the curve for peak D of plasma from a young dog, but was not significantly different.







—●— KH: Krebs-Henseleit solution  
 —□— DY3: Peak D, Young dog #3  
 —▲— DO4: Peak D, Old dog #4

Fourth power equation curve.

The slope of the K-H curve decreased with peak D of plasma from the young dog, and then increased and exceeded the slope of the K-H curve with peak D of plasma from the old dog. There was no significant difference between peak D of plasma from the young dog and peak D of plasma from the old dog.

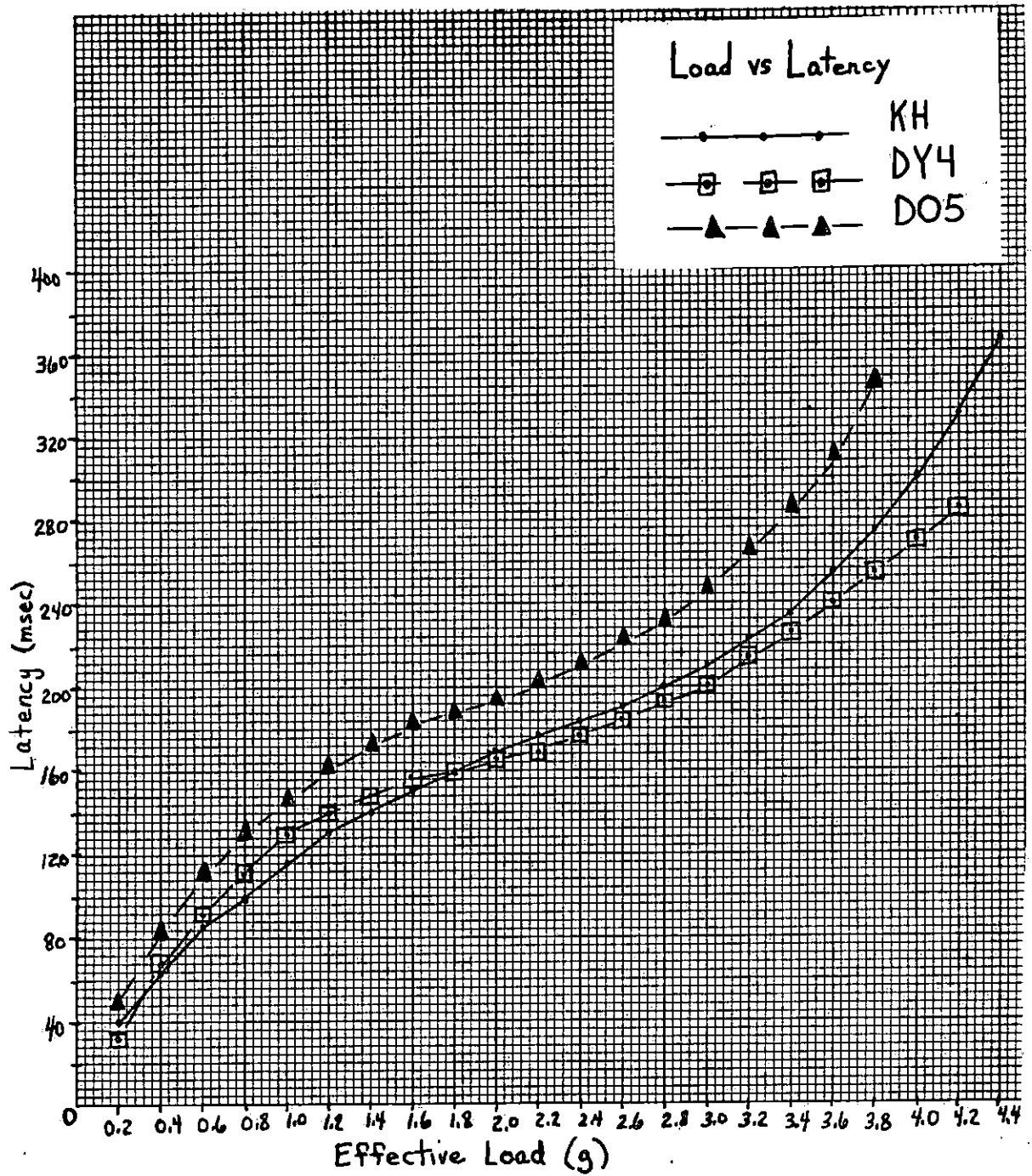
Figure 49. Load-latency curve

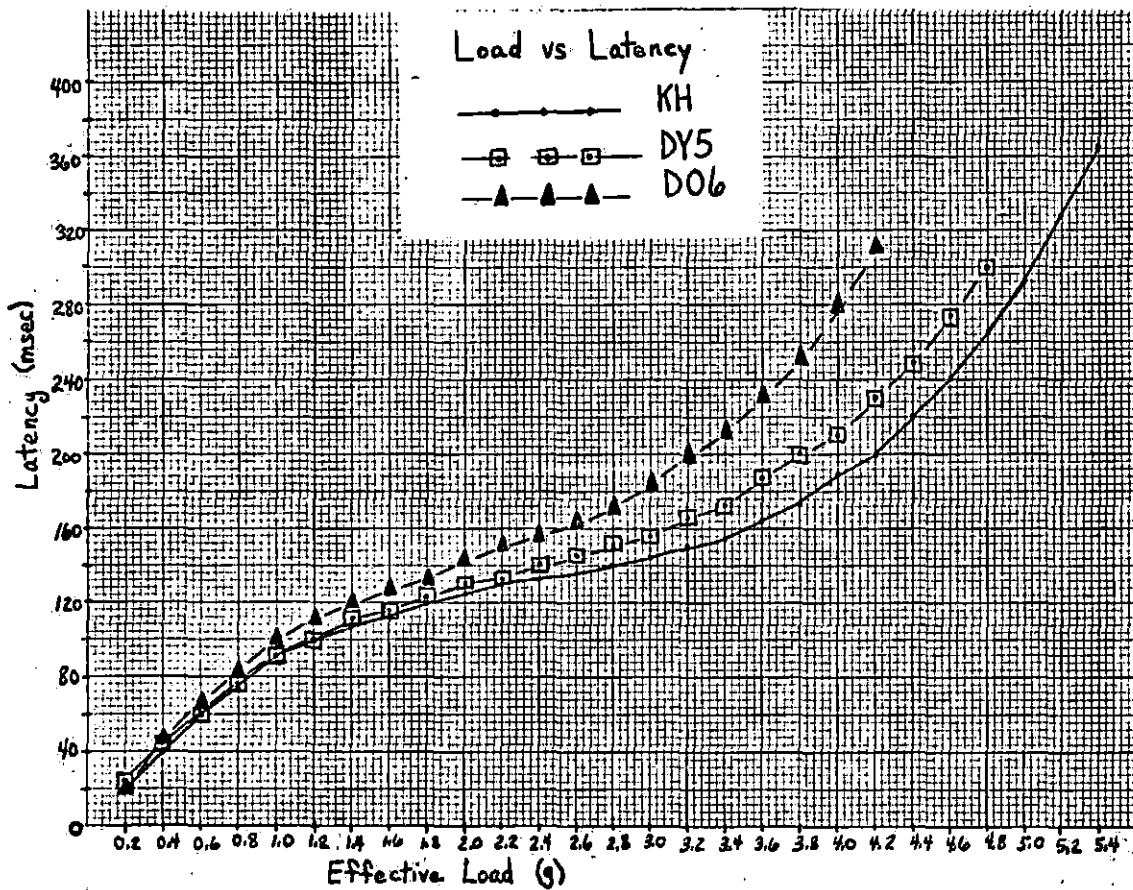
Figure 50. Load-latency curve

—•—•—•— KH: Krebs-Henseleit solution  
—□—□—□— DY4: Peak D, Young dog #4  
—▲—▲—▲— DO5: Peak D, Old dog #5

Fourth power equation curve.

The slope of the K-H curve decreased with peak D of plasma from the young dog, and then increased and exceeded the K-H curve slope with peak D of plasma from the old dog. The difference between peak D of plasma from the young dog and peak D of plasma from the old dog was not significant.



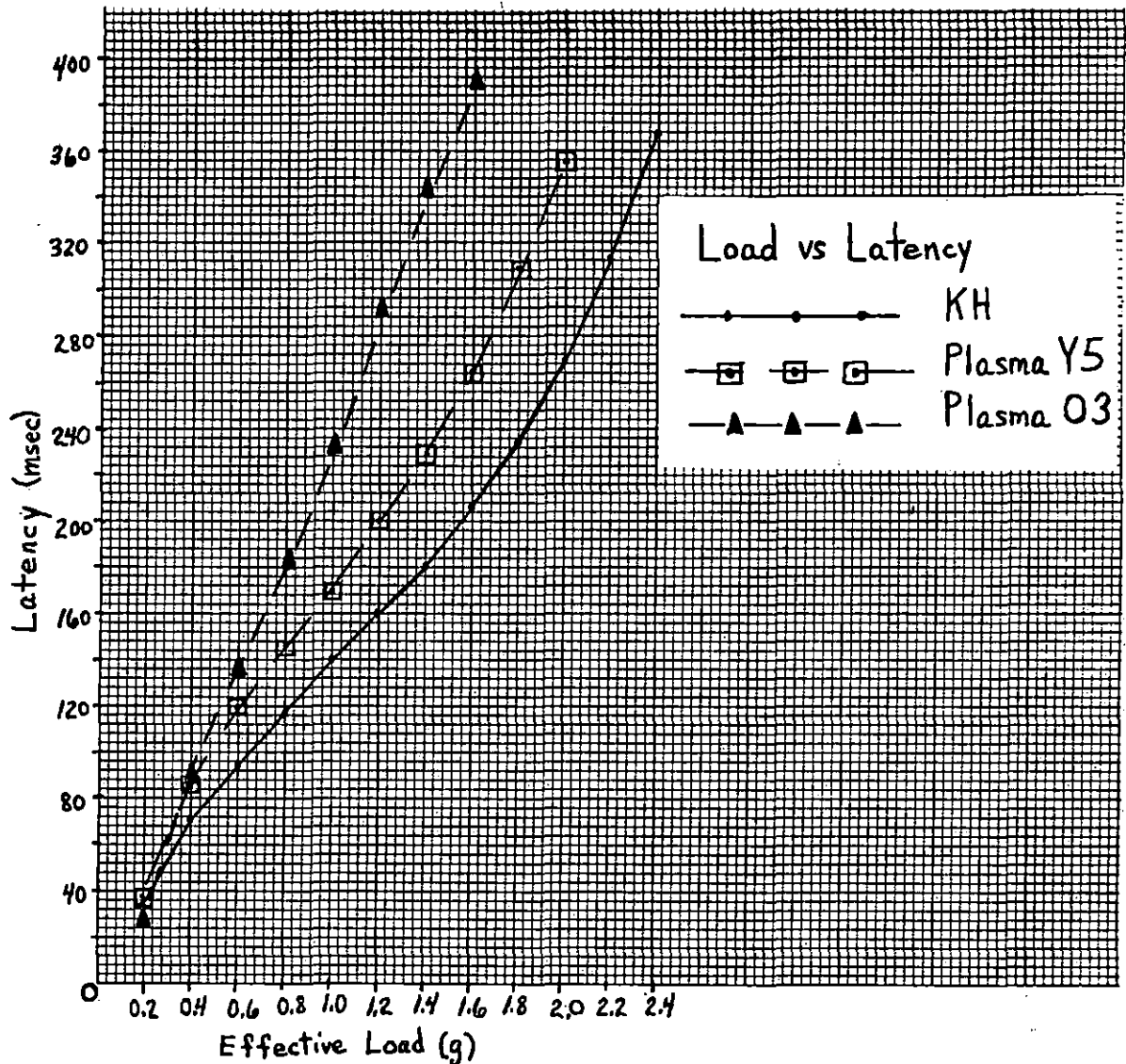


●—●—●— KH: Krebs-Henseleit solution  
 □—□—□— DY5: Peak D, Young dog #5  
 ▲—▲—▲— D06: Peak D, Old dog #6

Third power equation curve.

The slope continually increased as Krebs-Henseleit was replaced with peak D of plasma from the young dog and then with peak D of plasma from the old dog. The difference between peak D of plasma from the young dog and peak D of plasma from the old dog was not significant.

Figure 51. Load-latency curve



- KH: Krebs-Henseleit solution
- Plasma Y5: Plasma, Young dog #5
- ▲—▲—▲— Plasma O3: Plasma, Old dog #3

Fourth power equation curve.

The slope continually increased as Krebs-Henseleit was replaced with whole plasma from the young dog and then with whole plasma from the old dog. There was a significant difference between whole plasma from the young dog and whole plasma from the old dog ( $\alpha=0.05$ ).

Figure 52. Load-latency curve

Figure 53. Load-latency curve

—●—●—●— KH: Krebs-Henseleit solution  
—□—□—□— Plasma Y4: Plasma, Young dog #4  
—▲—▲—▲— Plasma O2: Plasma, Old dog #2

Fourth power equation curve.

The slope for whole plasma from the old dog was less than the slope for K-H and whole plasma from the young dog. There was no significant difference between whole plasma from the young dog and whole plasma from the old dog.

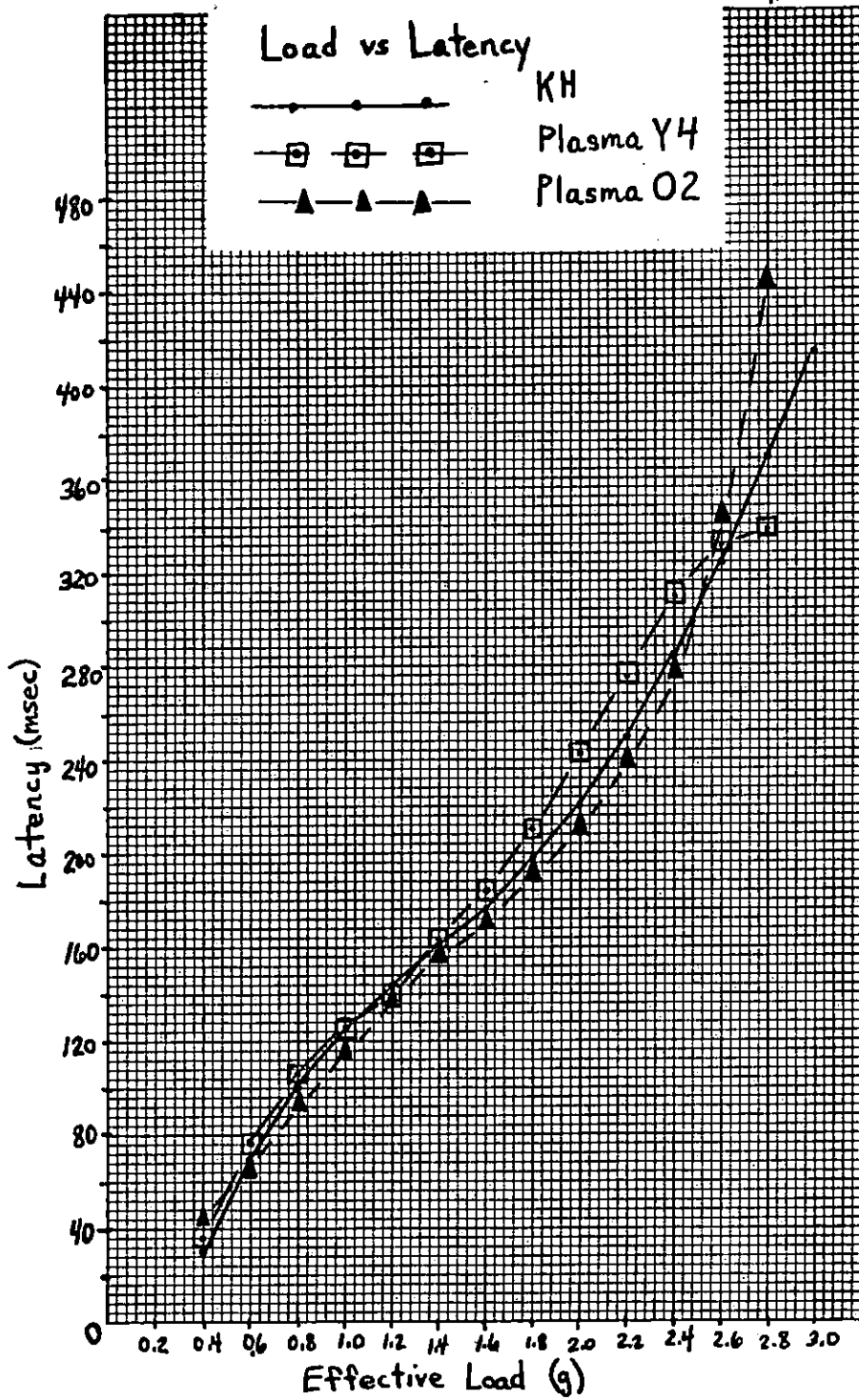


Figure 54. Load-latency curve

—•—•—•—•— KH: Krebs-Henseleit solution  
—□—□—□—□— Plasma Y5: Plasma, Young dog #5  
—▲—▲—▲—▲— Plasma O5: Plasma, Old dog #5

Third power equation curve.

There was no significant difference between whole plasma from the young dog and whole plasma from the old dog.



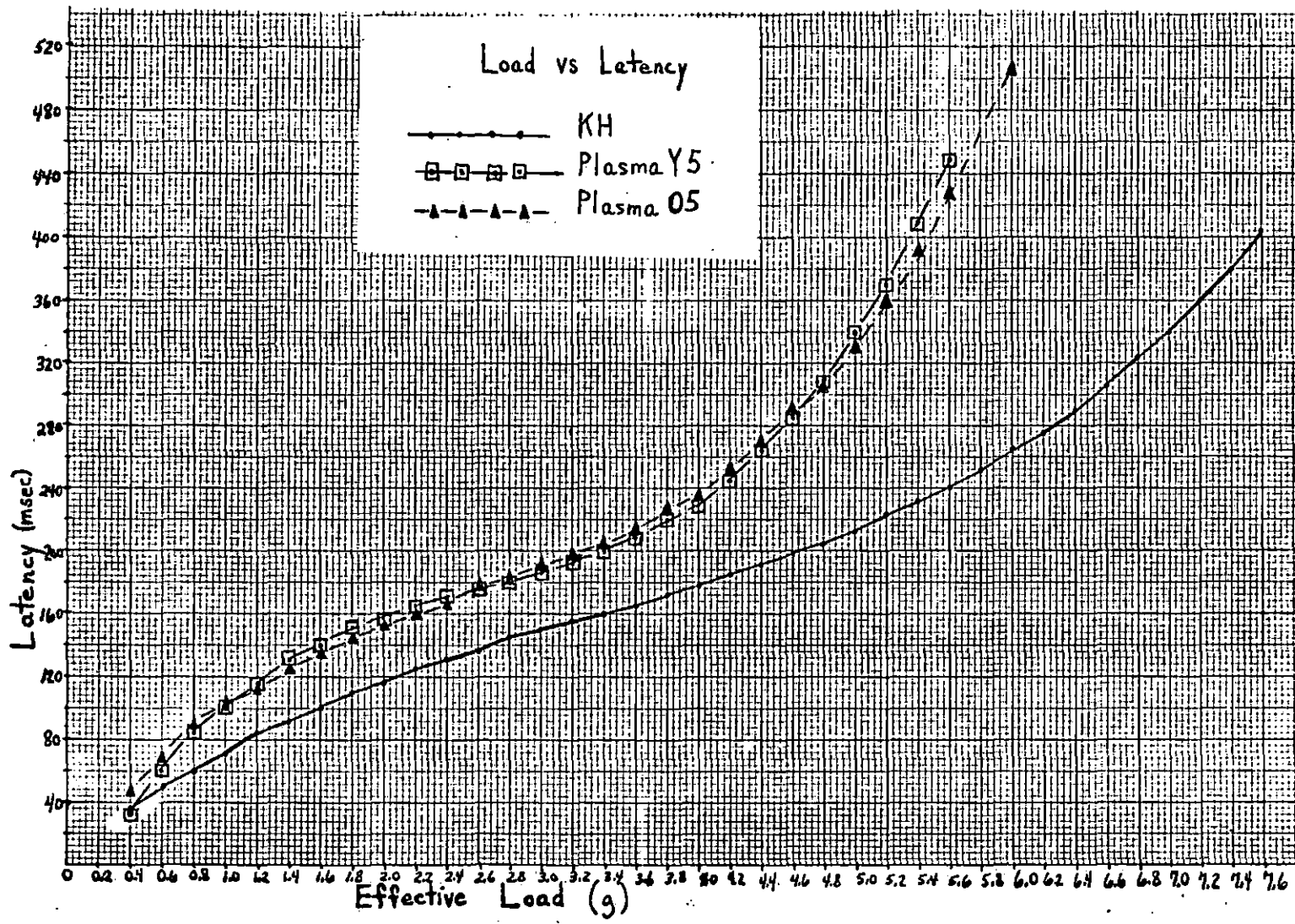


Table 5. F-values to test for method and age effects and age by method interaction

	Method effects		Age effects		Age by Method Interaction	
	$F_7^1$	Pr>F	$F_{14}^2$	Pr>F	$F_{14}^2$	Pr>F
Latency	0.14	0.723	0.06	0.940	3.63*	0.054
$P_o$	0.01	0.930	3.60*	0.055	2.47	0.120
$V_{max}$	1.07	0.334	0.61	0.557	1.58	0.240
$V_{max}$ /cross-sectional area	0.66	0.442	1.93	0.182	0.13	0.881
Active tension	0.24	0.639	3.84**	0.047	1.08	0.367

\* Approaching significance at 10% level ( $\alpha=0.10$ ).

\*\* Significance at 5% level ( $\alpha=0.05$ ).

The critical  $F_{7}^1$  value ( $\alpha=0.05$ ) = 5.59. The  $H_0$ : method 1 = method 2 was not rejected at  $\alpha=0.05$ , nor at  $\alpha=0.25$ . There were no significant method differences or effects on any of the five parameters: latency,  $P_0$ ,  $V_{max}$ ,  $V_{max}$  per unit of cross-sectional area, active tension.

The critical  $F_{14}^2$  value ( $\alpha=0.05$ ) = 3.74. The  $H_0$ : age 1 = age 2 = age 3 was not rejected at  $\alpha=0.05$ , nor at  $\alpha=0.25$ , and no significant age effects on latency or  $V_{max}$  were claimed to exist. The  $H_0$ : age 1 = age 2 = age 3 was not rejected at  $\alpha=0.05$ , nor at  $\alpha=0.10$ ; there were no significant age differences on  $V_{max}$  per unit of cross-sectional area. The  $H_0$ : age 1 = age 2 = age 3 was not rejected at  $\alpha=0.05$ ; there were no significant age effects on  $P_0$ . However, the  $H_0$ : age 1 = age 2 = age 3 was rejected at  $\alpha=0.10$ , and an age effect on  $P_0$  was claimed to approach significance. The  $H_0$ : age 1 = age 2 = age 3 was rejected at  $\alpha=0.05$  and a significant age effect on active tension was claimed to be present.

Overall, age effects were significant for active tension and approached significance for  $P_0$ . The  $H_0$ : age 1 = age 2 = age 3 was not rejected at  $\alpha=0.05$ , nor at  $\alpha=0.10$  for latency,  $V_{max}$ , or  $V_{max}$  per unit of cross-sectional area.

The  $H_0$ : all B's (slopes) are equal was not rejected at  $\alpha=0.05$ , nor at  $\alpha=0.25$ ; there was no significant age by method interaction for active tension. The  $H_0$ : all B's are

equal was not rejected at  $\alpha=0.05$ , nor at  $\alpha=0.10$ , and no age by method interaction was claimed to be significant or to approach significance for  $P_o$ . This indicated that the age effect on active tension and  $P_o$  was the same for methods 1 and 2.

There were no age effects on latency,  $V_{max}$ , or  $V_{max}$  per unit of cross-sectional area, so it was not necessary to assess any age by method interaction.

The critical value for  $t$ , 14 d.f.,  $\alpha=0.05$  is 1.761. The  $H_o: \mu_2 = \mu_3$  was not rejected at  $\alpha=0.05$ . There was no significant difference in  $P_o$  or active tension ( $n=9$ ) between young age treatment #2 and old age treatment #3. The LSD also indicated that there was no significant difference between young and old.

The  $H_o: \mu_1 = \frac{1}{2}(\mu_2 + \mu_3)$  was rejected at  $\alpha=0.05$ , and the standard, K-H treatment #1, was claimed to be different from the mean of young and old age treatments for  $P_o$  and active tension ( $n=9$ ).

An age effect approached significance for  $P_o$  and was significant for active tension. This age effect, however, was determined over three treatments: K-H, Y, O. It is necessary to determine where this age effect is occurring; thus two appropriate comparisons were made. There was no significant difference in  $P_o$  or active tension between young and old demonstrated by comparison 1 and the LSD. The

Table 6. Means

Analysis of Variance Procedure <sup>a</sup>							
Means							
<u>M</u> <sup>b</sup>	<u>N</u>	<u>Y1</u>	<u>Y2</u>	<u>Y3</u>	<u>Y4</u>	<u>Y5</u>	
1	18	172.529333	3.41955556	5.06705556	7.28577778	4.86922222	
2	9	143.344778	3.53322222	3.49422222	3.15622222	3.27133333	
<u>A</u> <sup>c</sup>	<u>N</u>	<u>Y1</u>	<u>Y2</u>	<u>Y3</u>	<u>Y4</u>	<u>Y5</u>	
1	9	161.705667	3.71477778	4.74166667	6.47400000	4.64200000	
2	9	160.195556	3.43788889	4.46222222	5.74166667	4.35111111	
3	9	166.502222	3.21966667	4.42444444	5.51211111	4.01666667	
<u>M</u>	<u>A</u>	<u>N</u>	<u>Y1</u>	<u>Y2</u>	<u>Y3</u>	<u>Y4</u>	<u>Y5</u>
1	1	6	191.708500	3.50916667	5.11283333	7.95000000	5.06116667
1	2	6	162.922667	3.49183333	4.91683333	7.03783333	5.00416667
1	3	6	162.956833	3.25766667	5.17150000	6.86950000	4.54233333
2	1	3	101.700000	4.12600000	3.99933333	3.52200000	3.80366666
2	2	3	154.741333	3.33000000	3.55300000	3.14933333	3.04500000
2	3	3	173.593000	3.14366667	2.93033333	2.79733333	2.96533333

<sup>a</sup>Y1 refers to latency; Y2 refers to P; Y3 refers to  $V_{\max}$ ; Y4 refers to  $V_{\max}/$  cross-sectional area; Y5 refers to active tension; M = method; A = age sub-treatment (1 = K-H (Krebs-Henseleit solution), 2 = Y (plasma from young dogs), 3 = O (plasma from old dogs)); N = number of observations in a mean.

<sup>b</sup>The first set of means M1,2 consists of method means.

<sup>c</sup>The second set of means A1,2,3 (n=9) consists of age means over both methods. The third set consists of age means for each method.

Table 7. Comparison of the means<sup>a</sup>

	n	comparison 1 =	comparison 2 =	LSD <sup>b</sup>
		( $\bar{y}_2. - \bar{y}_3.$ )	( $2\bar{y}_1. - \bar{y}_2. - \bar{y}_3.$ )	
		t-value	t-value	
latency	9	0.337	0.101	32.966 ++
	6	0.001	1.449*	40.375 ++
	3	0.581	2.225**	57.099 +
P <sub>o</sub>	9	1.178	2.405**	0.326 +
	6	1.032	0.683	0.399 ++
	3	0.58	3.203**	0.564 +
V <sub>max</sub>	9	0.121	1.099	0.553 ++
	6	0.663	0.206	0.677 ++
	3	1.146	1.609*	0.957 +
V <sub>max</sub> /cross-sectional area	9	0.45	1.914**	0.90 +
	6	0.268	1.837**	1.102 ++
	3	0.398	0.716	1.559 ++
Active tension	9	1.478*	2.343**	0.398 +
	6	1.671*	1.203	0.487 +
	3	0.205	2.360**	0.689 +

<sup>a</sup>Comparison 1 =  $\bar{y}_2. - \bar{y}_3.$ ; comparison 2 =  $2\bar{y}_1. - \bar{y}_2. - \bar{y}_3.$ .  $\bar{y}_1., \bar{y}_2., \bar{y}_3.$  refer to the means of all the observations in the K-H, young age, and old age treatments, respectively. LSD refers to the Least Significant Difference. Note that when n=9, we are studying the age means over both methods which is valid since there are no significant method differences.

<sup>b</sup>+ LSD is greater than the difference between the young and old age treatment means. ++ LSD is greater than the difference between any two of the three age treatment means: K-H, Y, O.

\*Approaching significance at 10% level ( $\alpha=0.10$ ).

\*\*Significance at 5% level ( $\alpha=0.05$ ).

standard, K-H treatment, was significantly different from the mean of the young and old age treatments (comparison 2). It can be concluded that it was the first treatment (K-H) that was separate from the young and old age treatments which, as a pair, were not significantly different from each other. Thus, the age effect exhibited for  $P_0$  and active tension could be attributed to the standard (K-H treatment) differing significantly from both the young and old age treatments which did not differ from each other.

The  $H_0: \mu_2 = \mu_3$  was not rejected at  $\alpha=0.05$ ; there was no significant difference in latency,  $V_{\max}$ , or  $V_{\max}$  per unit of cross-sectional area ( $n=9$ ) between young age treatment #2 and old age treatment #3. This was in agreement with the LSD.

The  $H_0: \mu_1 = \frac{1}{2}(\mu_2 + \mu_3)$  was not rejected at  $\alpha=0.05$ ; the standard was not significantly different from the mean of the young and old age treatments for latency and  $V_{\max}$  ( $n=9$ ). The  $H_0: \mu_1 = \frac{1}{2}(\mu_2 + \mu_3)$  was rejected at  $\alpha=0.05$ , and K-H was claimed to be significantly different from the mean of young and old for  $V_{\max}$  per unit of cross-sectional area ( $n=9$ ). An age effect on  $V_{\max}$  per unit of cross-sectional area was not significant when all three treatments were considered. However, when treatment #1 (K-H) was separated out and compared with the mean of treatments #2 (Y) and #3 (O), there was a

significant difference which was masked when all three treatments were considered together in determining age effects. This masking was probably due to the closeness of the values for Y and O age treatments (Table 6).

Although no significant method differences were present, comparisons of the young with the old age treatment, and the standard with the mean of the young and old age treatments were made for each method ( $n=6$ ,  $n=3$ ).

The  $H_0: \mu_2 = \mu_3$  was not rejected at  $\alpha=0.05$ ; there was no significant difference in latency,  $P_O$ ,  $V_{max}$ ,  $V_{max}$  per unit of cross-sectional area or active tension between young and old age treatments for methods 1 or 2.

The  $H_0: \mu_1 = \frac{1}{2}(\mu_2 + \mu_3)$  was not rejected at  $\alpha=0.05$ ; there was no significant difference between the standard (K-H) and the mean of the young and old age treatments for latency,  $P_O$ ,  $V_{max}$ , or active tension ( $n=6$ ). The  $H_0: \mu_1 = \frac{1}{2}(\mu_2 + \mu_3)$  was rejected at  $\alpha=0.05$ , and a significant difference between K-H and the mean of Y and O was claimed to be present for  $V_{max}$  per unit of cross-sectional area ( $n=6$ ). Again, this difference was probably masked by the closeness of the values for Y and O (Table 6), since no significant age effects were present for this parameter.

The  $H_0: \mu_1 = \frac{1}{2}(\mu_2 + \mu_3)$  was not rejected at  $\alpha=0.05$ ; there was no significant difference between the standard and the mean of Y and O for  $V_{max}$  or  $V_{max}$  per unit of cross-

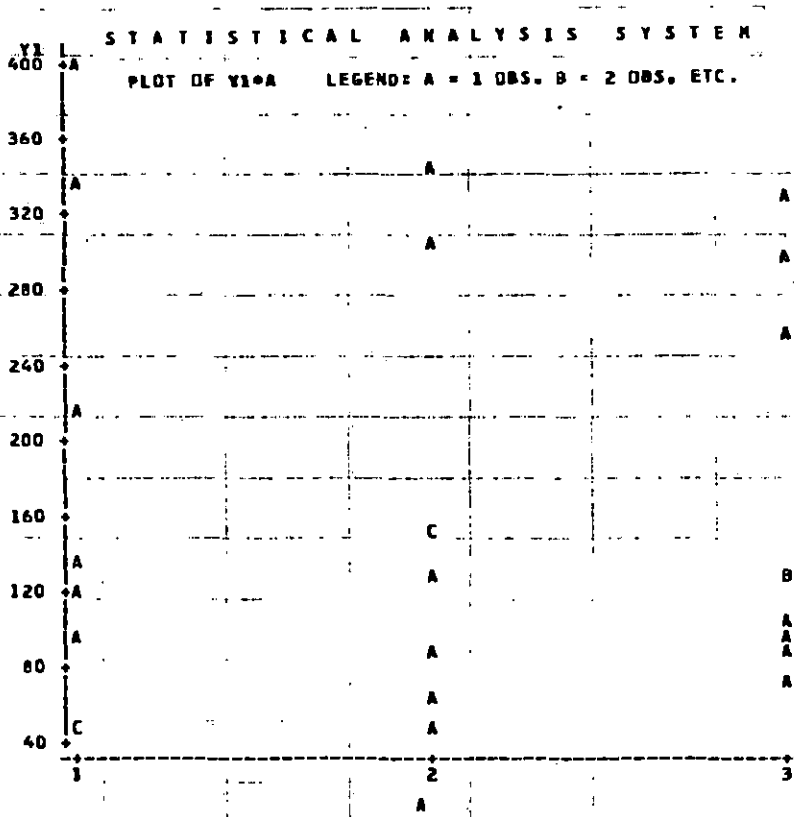


sectional area ( $n=3$ ). The  $H_0: \mu_1 = \frac{1}{2}(\mu_2 + \mu_3)$  was rejected at  $\alpha=0.05$ , and a significant difference between the standard (K-H) and the mean of the young and old age treatments was claimed to be present for latency,  $P_0$ , and active tension ( $n=3$ ). These significant differences in  $P_0$  and active tension were expected since age effects were demonstrated for these parameters, and were actually due to the K-H treatment differing from the young and old age treatments which did not differ from each other. The significant difference between K-H and the mean of Y and O for latency became apparent when the means over both methods 1 and 2 ( $n=9$ ) were subdivided into individual method means ( $n=6$  and  $n=3$ ). K-H was then seen to differ from Y and O which did not differ at all from each other for method 1, and differed only slightly from each other relative to the K-H value for method 2 (Table 6).

To conclude, there was no significant difference between plasma from young and old dogs. Any significant age effect could be attributed to the first age treatment (K-H) differing from both the young and old age treatments which, as a pair, did not significantly differ from each other.

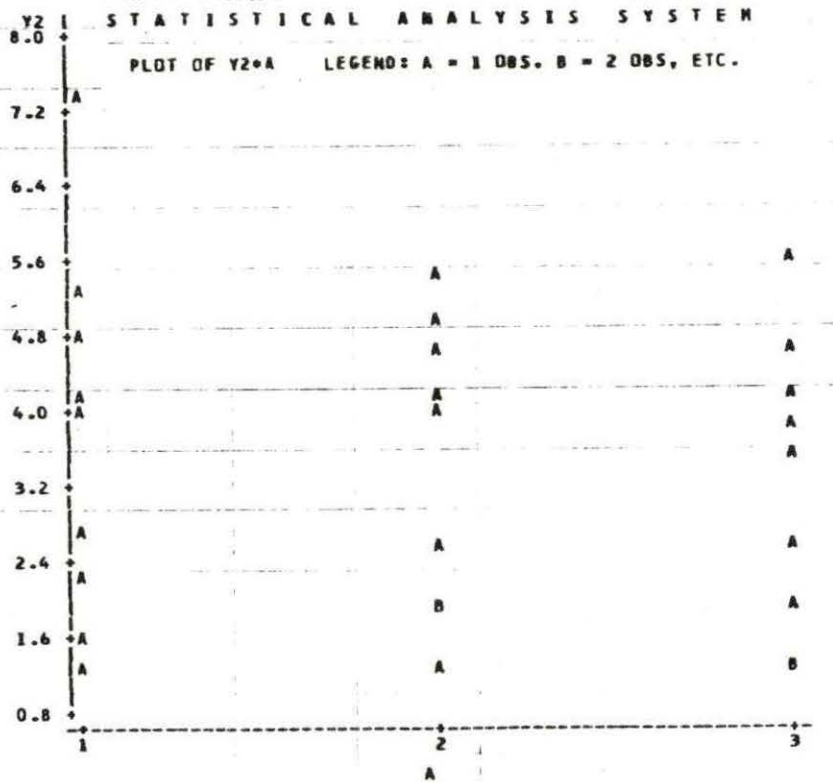
Table 8. Correlation coefficients

	latency	$P_o$	$V_{max}$	$V_{max}/\text{cross-}$ $\text{sectional}$ $\text{area}$	active tension
age	0.019	-0.126	-0.062	-0.059	-0.061
latency		-0.487	-0.719	-0.628	-0.656
$P_o$			0.566	0.488	0.674
$V_{max}$				0.729	0.679
$V_{max}/\text{cross-}$ $\text{sectional}$ $\text{area}$					0.938



Latency values are in msec/g.  
 Age treatments 1, 2, 3 correspond to Krebs-Henseleit (K-H) solution, Young (Y) (plasma, processed or unprocessed, from young dogs), and Old (O) (plasma, processed or unprocessed, from old dogs), respectively.

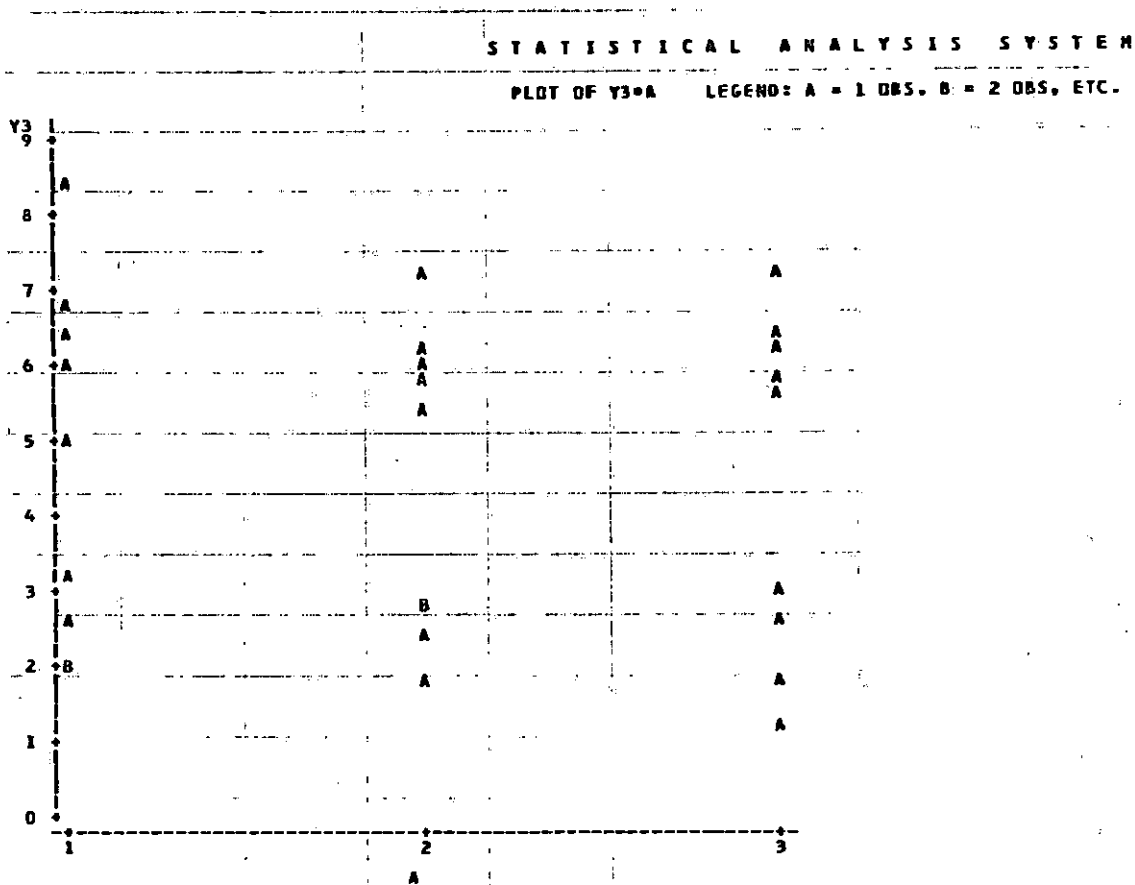
Figure 55. Latency (slope) and age



$P_o$  values are in grams.

Age treatments 1, 2, 3 correspond to Krebs-Henseleit (K-H) solution, Young (Y) (plasma, processed or unprocessed, from young dogs), and Old (O) (plasma, processed, or unprocessed, from old dogs), respectively. Note that the scatter of observations is similar for the young and old age treatments.

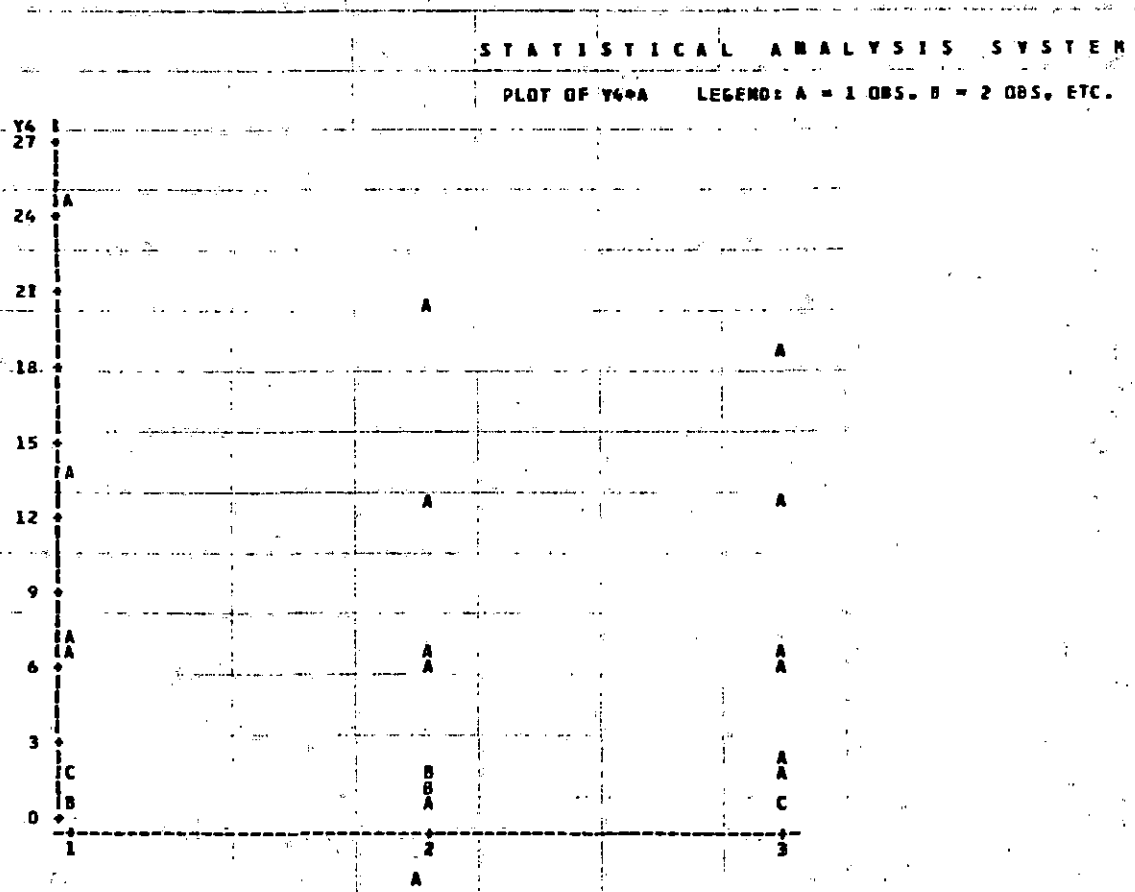
Figure 56.  $P_o$  and age



$V_{\max}$  values are in mm/sec.

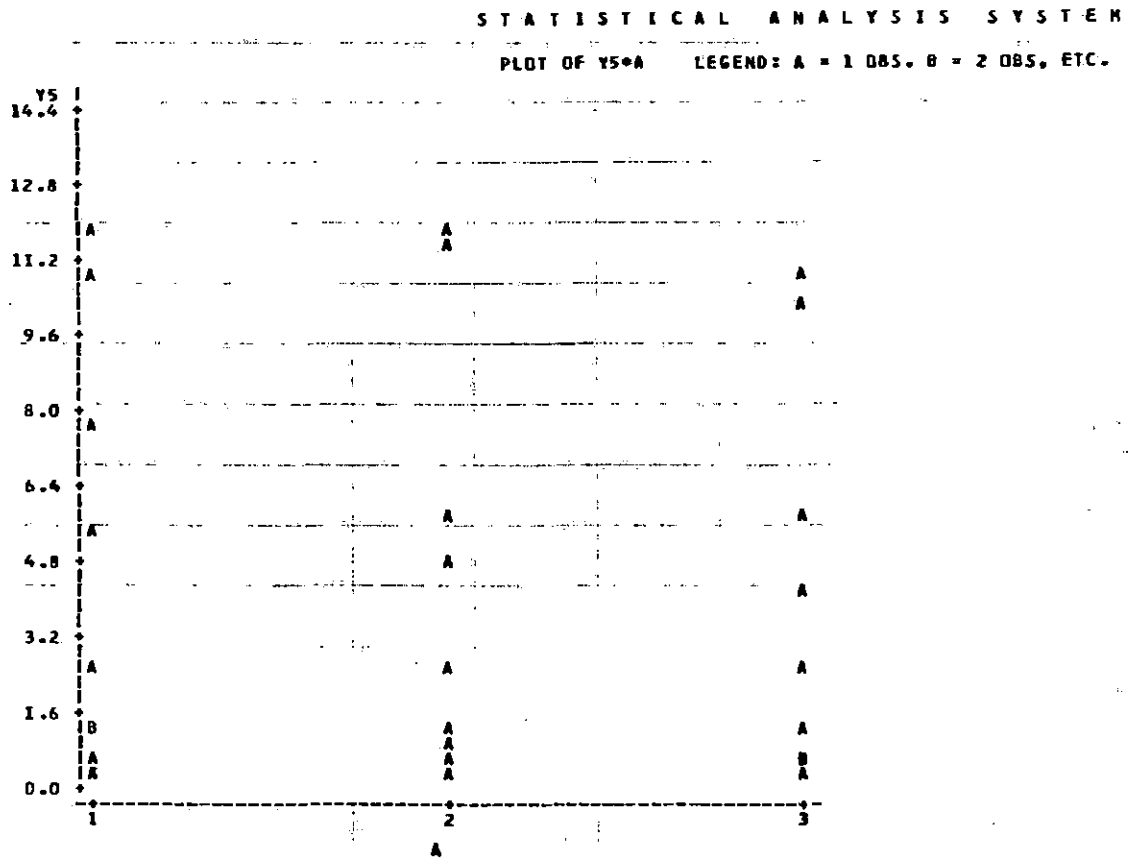
Age treatments 1, 2, 3 correspond to Krebs-Henseleit (K-H) solution, Young (Y) (plasma, processed or unprocessed, from young dogs), and Old (O) (plasma, processed or unprocessed, from old dogs), respectively. Note that the scatter of observations is similar for the young and old age treatments.

Figure 57.  $V_{\max}$  and age



$V_{\max}$ /cross-sectional area values are in  $(\text{mm}\cdot\text{sec})^{-1}$ . Age treatments 1, 2, 3 correspond to Krebs-Henseleit (K-H solution, Young (Y) (plasma, processed or unprocessed, from young dogs), and Old (O) (plasma, processed or unprocessed, from old dogs), respectively. Note that the scatter of observations is similar for the young and old age treatments.

Figure 58.  $V_{\max}$  per unit of cross-sectional area and age



Active tension values are in  $\text{g}/\text{mm}^2$ .  
 Age treatments 1, 2, 3 correspond to Krebs-Henseleit (K-H) solution, Young (Y) (plasma, processed or unprocessed, from young dogs), and Old (O) (plasma, processed or unprocessed, from old dogs), respectively. Note that the scatter of observations is similar for the young and old age treatments.

Figure 59. Active tension and age

Table 9. t-values for latency,  $P_o$ ,  $V_{max}$ ,  $V_{max}/cross-sectional\ area$ , and active tension for individual muscle experiments<sup>a</sup>

	latency	$P_o$	$V_{max}$	$V_{max}/cross-sectional\ area$	active tension
DY1-DS	-0.857	3.652****	1.890**		2.370***
AS-DS	-1.079	0.820	-0.046		1.177
DY1-DO1	0.671	0.0	-1.385*	-0.258	0.0
DY2-DO2	-0.373	-0.076	-0.735	-0.085	-0.012
DY3-DO3	0.932	-0.076	0.268	0.053	-0.019
DY3-DO4	-0.224	0.483	-0.216	-0.282	0.905
DY4-DO5	-0.402	0.895	0.752	1.425*	2.115**
DY5-DO6	-0.607	1.305	-0.307	-0.194	1.103
DY6-DO2	0.995	-0.112	0.008		-0.013
Plasma Y5- Plasma O3	-1.862**	1.079	1.696*	0.507	0.428
Plasma Y4- Plasma O2	0.405	0.187	0.029	0.017	0.148
Plasma Y5- Plasma O5	0.450	-0.259	0.259	0.164	-0.223

<sup>a</sup>Note that the pooled variance for each of the five parameters determined by the analysis of variance was used in calculating t-values. There was a significant difference in  $P_o$ ,  $V_{max}$ , and active tension between processed shock plasma peak D and processed plasma peak D from young dog #1.

\* Approaching significance at 10% level ( $\alpha=0.10$ ).

\*\*Significance at 5% level ( $\alpha=0.05$ ).

\*\*\*Significance at 2.5% level ( $\alpha=0.025$ ).

\*\*\*\* Significance at 0.25% level ( $\alpha=0.0025$ ).



## DISCUSSION

## Discussion of Methods

Dialysis and gel filtration were the most significant steps in the preparation of purified depressant factor (MDF) activity, separating MDF from protein and salt in plasma.

Dialysis

The reason for freezing and thawing plasma prior to dialysis was to remove the cryoprecipitable proteins which, if not removed, would collect on the dialysis membrane and interfere with the filtration process. Pressure dialysis was chosen in lieu of other deproteinization techniques. Filtration gels and membranes for ultrafiltration tend to bind polypeptides and proteins. Higher yields of MDF activity are obtained with pressure dialysis than with trichloroacetic acid-ether treatment (Yamada and Pettit, 1977).

Column chromatography

It was necessary to remove the upper 1.0-1.5 cm layer of the gel bed between column separations. When a column is repeatedly used, the flow rate may decrease. The upper part of the gel bed may become clogged with fine particles from the buffer solution or sample. The removal of this unwanted debris helps to maintain the flow rate and resolution

of the column, and to diminish the tendency of the gel bed to become compressed during elution.

#### Papillary muscle sensitivity

Several variables can influence isolated papillary muscle performance: osmolarity, pH, temperature, oxygenation, sodium ion concentration and calcium ion concentration.

According to Goldfarb et al. (1978), an osmolarity range of 270-310 milliosmols/liter did not induce any cardio-depressant activity. This is not consistent with what I have found to occur. An osmolarity of 288 and above will damage the papillary muscle. The base line resting tension will rise upward and eventually, the amplitude of contraction will decrease until the muscle dies. An osmolarity change may be due either to salts and ion buildup in the tubing of the system or water removal from the bath solution.

Tension development undergoes sigmoidal depression with acidosis. Developed tension was depressed by a solution pH outside the range of 7.25-7.60 (Goldfarb and Weber, 1977b; Lefer and Blattberg, 1968). Any pH changes that occurred may be due to a drift in pH of the buffer, air entering the system through leaks in the tubing or valves, or muscle activity. If the muscle is dying, cellular contents are released into the bath solution which lowers pH.

All muscle experiments were run at 27C. It has been

shown that the velocity of shortening of preloaded isotonic contractions was not dependent on temperature (Parmley and Chuck, 1973). In another study, temperature was found to have an effect on peak active tension. The peak active tension was reduced fivefold as temperature was increased from 20C to 38C (Johnson et al., 1974). Although physiological temperature is approximately 38C, papillary muscle is studied at lower temperatures to slow the contractile processes. Since equipment has a slow reaction time, it would be best if the muscle contracted as slowly as possible during mechanical measurements.

A high sodium ion concentration depresses and calcium ion concentration stimulates tension development in a linear fashion. An adequate calcium ion concentration in the muscle bath solution is important for contraction. When mammalian myocardium was exposed to calcium-free perfusion fluid, contractile tension declined with a half-time of 15-60 seconds (Langer, 1971; Langer, 1977). The necessity of having the correct concentration of ionized calcium is unquestioned. Calcium at concentrations of 7.5 mM effectively counteracted the negative inotropic effect of MDF in isolated feline papillary muscle preparations (Lefer, 1978).

The activation of the mechanical response of papillary muscle is dependent on the influx of ionized calcium from the extracellular phase with depolarization of the cell

membrane. The source of the  $\text{Ca}^{++}$  for excitation-contraction coupling is the cellular surface. Acidic mucopolysaccharides in the basement membrane are capable of binding ionized calcium. The  $\text{Ca}^{++}$  which moves into the cell either directly activates the mechanical response or triggers the release of additional  $\text{Ca}^{++}$  from intracellular storage sites.

An increased intracellular  $\text{Ca}^{++}$  concentration results in the increased binding of  $\text{Ca}^{++}$  to troponin C which neutralizes the inhibitory action of troponin I on myosin ATP-ase. These changes in the regulatory protein system permit the interaction of actin and myosin.  $\text{Ca}^{++}$  is essential for  $\text{MgATP}^{-2}$  hydrolysis and contraction. The hydrolysis of ATP provides the energy for the activation of cross-bridges.

Calcium governs both the number of active cross-bridges between the actin and myosin filaments during tension development and the rate of turnover of cross-bridge formation (Brutsaert et al., 1971, 1973; Edman, 1977).  $P_0$  and shortening velocity were greatly enhanced when papillary muscle was subjected to high calcium ion concentrations (Brutsaert et al., 1973).

It was therefore imperative to know the calcium ion concentration in the solution bathing the papillary muscle, and to monitor the variables which affect isolated papillary muscle.

The  $\text{CaCl}_2$  concentration in the Krebs-Henseleit buffer was

increased from 2.58 mM to 3.25 mM when the buffer was to be used with the lyophilized test peak. The osmolarity of the lyophilized test peak in 23 ml of K-H buffer was much higher than 282, and required the addition of 6 ml of water. The addition of water, while adjusting the osmolarity to physiological range, would concomitantly alter the concentration of the important ion, calcium. This was avoided by starting with an initial concentration of 3.25 mM  $\text{CaCl}_2$ .

#### Papillary muscle selection

The young age of the dogs from which papillary muscles were taken had no negative effect on this study. These muscles served as effective experimental units. Papillary muscles from 4-6 week old dogs have been shown to be functional with respect to receptor development (Hembrough et al., 1978). Since papillary muscles of young dogs are thinner they are easier to oxygenate in solution. Since the effect of old age was studied, it was desirable to use muscles from young dogs.

The geometric shape of the papillary muscle is important in determining the usefulness of the muscle and in estimating the capability of the muscle to function for an extended period of time (8 hours). The ideal morphology of a papillary muscle is length and thinness.

It is speculated that more tubular invaginations of the

plasma membrane may extend into the cytoplasm of long muscle cells. The lumen of the tubules from the transverse-tubular system is continuous with the extracellular space. These tubular invaginations usually are observed at the level of the Z band. Thus, with longer muscle cells, more tubules may come in contact with the contractile component area, and a rapid distribution of excitatory stimulus is facilitated throughout the cell. A recruitment of more myofibrils from the depth of the fiber is a result of the spread of depolarization along the transverse-tubular system.

The sarcoplasmic reticulum lies close to the plasma membrane. Electron-dense feet protrude from the wall of the sarcoplasmic reticulum and may facilitate the direct transfer of information from the plasma membrane to the sarcoplasmic reticulum. It would be advantageous to decrease the diffusion distance for calcium ions to the myofibrils. The inner core of thick, triangular shaped papillary muscles becomes hypoxic in a few hours in the muscle chamber since the diffusion distance for oxygen and ions is large. The spread of depolarization along the T-system would, most likely, not reach the inner core of very thick muscles. There are more plasma membrane tubular invaginations which contact the inner core of long, thin muscles.

If only the outer core of the muscle is functional, then a thick, triangular shaped muscle has a wasted inner

core with a minimal outer functional area. A long, thin muscle has an extended outer core with larger functional area, and a smaller inner core. A long muscle is advantageous, since the total functional range of papillary muscle is approximately 25% of the muscle length (Ford and Forman, 1974). As muscle length is increased and cross-sectional area is decreased, oxygen diffuses more effectively into the central hypoxic core. The life of the muscle is extended.

According to Brutsaert et al. (1971), developed force should exceed resting force by a ratio of 5 or 6 to 1 in adequately functioning feline papillary muscle preparations. Smaller ratios usually reflect mechanical damage to the muscle preparation. Feline papillary muscle is usually longer and thinner than canine papillary muscle. A long, thin muscle develops more force since the outer core of the muscle is functional. The  $P_o$  is higher in feline papillary muscle. Thus, the ratio of active tension to resting tension in feline papillary muscle is larger than the ratio in canine papillary muscle.

Based on Brutsaert's guideline ratio, a ratio of 4.5:1 was used as the primary criterion for canine papillary muscle. The mean ratio for eleven canine papillary muscles was 4.57 (Table 3). Caution should be exerted when interpreting the results of papillary muscles from other species, since species

differences do exist.

Five papillary muscles did not satisfy this initial criterion but did satisfy other criteria. Papillary muscles with ratios smaller than 4.5, but with  $P_o$ 's larger than 2 were used in age experiments: 3 and 8. The  $P_o$  steadily increased with time in age experiments 1, 2, 3, and in shock experiment 2. The only exception was the expected decrease in  $P_o$  with shock plasma peak D. Three papillary muscles had a cross-sectional area larger than the criterion value of  $2.1 \text{ mm}^2$ . The  $P_o$  was large and/or steadily increased with time for these muscles in age experiments: 1, 2, 3. Based on these criteria (active tension to resting tension ratio,  $P_o$ , cross-sectional area), eleven out of twelve muscles were acceptable.

The five muscles whose active to resting tension ratios were smaller than 4.5 were not omitted. The secondary criteria, large  $P_o$  and/or a steadily increasing  $P_o$ , are indicators of an adequately and continuously functioning muscle preparation. Mechanical damage to the muscle would not be reflected by a steadily increasing  $P_o$ . A muscle with a large  $P_o$  was usually indicative of a muscle with the potential to exhibit true clearcut differences between test samples, if differences existed. A small  $P_o$  indicated less developed force, and possibly a weak muscle which was very sensitive to minor differences between test samples. There



is the uncertainty, however, with small  $P_{O_2}$ -muscles, that any depression exhibited may very well be due to the deterioration of the weak muscle and not due to the presence of a depressant factor in the test sample.

The papillary muscle which was subjected to peak DY6 and peak DO2 was not used. The cross-sectional area was too large ( $6.73 \text{ mm}^2$ ), the muscle length was too short, and the  $P_{O_2}$  was greatly depressed after the buffer solution was replaced with peak D of plasma from young dog #6 (Figure 31, Table 4). Mechanical damage to the muscle was assumed to be responsible for this depression; the papillary muscle system was initially not circulating well. This was indicated by an improvement in amplitude of muscle contraction with the addition of oxygen directly to the muscle, and difficulty in stabilizing pH. This muscle experiment did serve to reconfirm the lack of difference between peak D of plasma from young and old dogs, despite the difference of peak D of plasma from both young and old dogs from the standard (K-H buffer solution). Peak D of plasma from the same old dog (O2) was repeated in age experiment 2 (Figure 26).

One final justification for the inclusion of three muscles with cross-sectional areas larger than the criterion value is the evidence in an experiment performed by Lundgren et al. (1976). There were no statistically significant

differences in the responses of thin and thick rabbit papillary muscles to plasma. He concluded that cross-sectional area was of no significance in relation to muscle responses. Again, it should be remembered that a different species was used, and also that the hypoxic core effect with thick muscles is only a hypothesis. The value of establishing criteria for muscle selection is an attempt to include only select stable muscle preparations with high potential for contractility.

#### Prestretching the muscle

The papillary muscle was prestretched with a heavy load for two contractions prior to each preload during the generation of a preload curve. Cardiac muscle contracts more vigorously when stretched. At an optimal length, the degree of overlap of thick and thin filaments will permit the generation of a large force. According to Noble and Else (1972), stretching the muscle during contraction overcomes the inhomogeneity of muscle and maintains the central sarcomeres at the desired length.

Prestretching the muscle with the same heavy weight prior to each preload weight places the muscle in the same condition with respect to thick and thin filament overlap for each test preload weight. This reduces the variability of the muscle during the generation of the curve.

Prestretching the muscle increases the length and permits a transient decrease in cross-sectional area of the muscle which subsequently increases oxygenation of the inner core. As the muscle is prestretched, the increased oxygenation aids the muscle to contract maximally for each preload weight. Any decline in amplitude of contraction during the generation of a preload curve cannot be due to a hypoxic inner core, since the muscle core continuously receives a "burst" of increased oxygen with each prestretch.

#### Basis for selecting the preload weight

The selected preload weight was ~92.5% of the preload weight that would produce a maximal contraction ( $L_{max}$ ). The selected preload thus produced a percentage of  $L_{max}$  between 90 and 100.

A preload producing a high percentage of  $L_{max}$  was used for a specific reason. When muscle length was increased from 90%  $L_{max}$  up to  $L_{max}$ , there was an immediate increase in isometric force due to the Starling mechanism. This was followed by a gradual secondary increase in force which occurred during the subsequent ten minutes (Parmley and Chuck, 1973). Parmley and Chuck (1973) conducted their study with 99%  $L_{max}$ .

The question as to whether the heart functions at the top of the length-tension curve or at 10% below  $L_{max}$  has been

a point of contention. According to Sonnenblick (1974), the heart functions between 2.0 and 2.2  $\mu\text{m}$ . At sarcomere lengths shorter than  $L_{\text{max}}$ , the resting tension declines exponentially to zero at  $\sim 85\% L_{\text{max}}$ . A positive filling pressure distends the heart, and therefore, the heart must work at sarcomere lengths greater than  $85\% L_{\text{max}}$ .

In all cases,  $V_{\text{max}}$  increased with increasing muscle extension even in the range of physiological muscle length from  $85\% L_{\text{max}}$  to  $L_{\text{max}}$  (Gulch and Jacob, 1975a; Minelli et al., 1975; Donald et al., 1972). Brutsaert et al. (1971), however, claimed that  $V_{\text{max}}$  remained constant between  $L_{\text{max}}$  and  $87.5\% L_{\text{max}}$ . The inhomogeneity and variation in sarcomere length was reduced by using a high preload, a resting tension close to  $L_{\text{max}}$  (Brutsaert et al., 1973).

By using a preload which produced a high percentage of  $L_{\text{max}}$ , the resting tension was set at a level just below that which would yield a maximal contraction. This places the muscle in an optimum state with respect to sarcomere length, and permits the muscle to respond with its full potential. Any change in contractility which may be induced by MDF signifies the sensitivity of the muscle to this depressant factor, since the muscle was functioning at an optimum point along the ascending limb of the length-tension curve.

### Generating preload and afterload curves backwards

Preload and afterload curves were generated backwards, beginning with the heaviest load and serially replacing it with lighter loads. This was done to avoid overstretching and fatiguing the muscle with time. Maximum velocity of shortening ( $V_{\max}$ ) is determined only by the total load, and not by the sequence of length changes or the mode of unloading to zero load (Brutsaert et al., 1971).

### Composite force-velocity curves

Velocity was plotted against  $P/P_0$  where  $P$  = load and  $P_0$  = maximum isometric force at zero velocity in the composite force-velocity curves (Figures 35-41). Dividing  $P$  by  $P_0$  normalized the force of all muscles, thereby eliminating differences in the size of the papillary muscles. The total number of activated myosin cross-bridges for each muscle was standardized.

Velocity per unit of cross-sectional area was plotted against  $P/P_0$  in the composite force-velocity curves (Figures 42, 43) to eliminate differences in cross-sectional area. Thus, all muscles were normalized with respect to both force and velocity per unit of cross-sectional area.

## Discussion of Results

Although I have confirmed the presence of MDF in the plasma of a canine with experimental pancreatic vessel ischemia, and have resolved the controversy between Lefer and Wangenstein, many questions concerning the nature of MDF still remain.

MDF is undoubtedly a peptide, since it is ninhydrin-positive and absorbs ultraviolet light at a wavelength of 230 nm, which is the optimum wavelength for peptide bonds. Based on calibration of the columns with molecular weight markers, MDF is estimated to have a molecular weight between 700 and 850 (Table 2). This small range has not been reported. Canine MDF exerted a negative inotropic effect on canine papillary muscle.  $V_{max}$ ,  $P_o$ , and active tension values were depressed significantly (Figure 23, Table 9). There was no significant effect on latency which was determined as the time from the beginning of stimulation to the beginning of contraction. This is consistent with other reports; MDF (two-hour shock) exerted no significant effect on latency which was determined as the time to peak tension.

Several investigators have reported the presence of MDF in shock plasma at concentrations in the nanomolar and picomolar range. Since MDF could not be completely isolated, and no calculations or descriptions on the determination of

these concentrations were provided, these concentrations should be considered only as estimates. There was no way to precisely measure the concentration of MDF in the eluate or lyophilized samples. However, it was possible to demonstrate the potential of MDF activity and the sensitivity of the papillary muscle bioassay to a 58.8-fold dilution of MDF from the original starting material (Figure 2).

The dilution of plasma during gel filtration should be considered when determining MDF bioassay parameters. A direct linear relationship between the concentration of the sample and the percentage inhibition of papillary muscle contraction was reported. Thus, the sensitivity of the papillary muscle bioassay was demonstrated for MDF, since a significant depression in contractility was observed with a 58.8-fold dilution of the original shock plasma. Thus, in actuality, the depressed values for  $V_{max}$ ,  $P_0$ , and active tension for MDF-treated muscles represent a higher depressant capability of MDF, since the MDF was diluted 58.8-fold from the original shock plasma sample. This is consistent with the high absorbance readings for peak D of shock plasma which, while in the eluate, was diluted 18.8-fold from the original starting material. Low absorbance readings for peak D of plasma from young and aged dogs were matched with expected contractility responses which indicated insignificant MDF activity in comparison to shock MDF activity.

It is impressive that the elution volume for MDF, which was found in peak D of shock plasma, was very similar to the elution volume for peak C of plasma from both young and old dogs. Peak D of plasma from both young and old dogs was found at a later elution volume than that for peak D of shock plasma. Peak C contains a normal component of plasma which has moderate negative inotropic activity (Lefer and Martin, 1970a). However, the negative inotropic effect of peak C was not seen in shock plasma when both peaks C and D were present. Only the effect of peak D (MDF) was observed. It is hypothesized that the active component(s) of peak C and peak D (MDF) may act on the same receptor site. Peak C would then have a weaker affinity for the receptor since the negative inotropic effect of peak C was not observed in shock plasma when MDF (peak D) was present. MDF probably saturated the available receptors and prevented the effect of the peptide in peak C from being expressed.

It is possible that peaks C and D-peptides compete for the same receptor site, since myocardial depressant activity was demonstrated with peak C of normal plasma, but not of shock plasma. Depressant activity was demonstrated in shock plasma with peak D. Similar elution volumes for peak C of plasma from young and old dogs and peak D of shock plasma imply that MDF has the same molecular weight as the peptide in peak C of normal control plasma from young and old dogs.



Peak D of normal control plasma from young and old dogs appeared at a later elution volume than MDF and did not have a large absorbance peak like MDF. No depression of papillary muscle in any fashion which was quantitatively similar to MDF was demonstrated.

The combination of isolated canine papillary muscle with canine processed and unprocessed plasma eliminated muscle-plasma interactions due to species differences and permitted the study of a species-specific (canine) MDF. The effects of MDF on isolated canine papillary muscle have not been reported. In the past, canine MDF was assayed on feline and rabbit papillary muscle, and the possible effect of species differences had to be considered with the effect of MDF.

Experiments were designed in such a manner that each muscle would serve as its own control. This removed the effect of muscle differences and eliminated the inconsistencies between muscles that arise from differences in muscle length, cross-sectional area, or in the state of contractility.

Two very large and similar peaks, peak A and peak D are depicted in each of the column elution patterns for a dog with experimental pancreatic vessel ischemia (Figures 5, 6). Significant MDF activity was present in peak D of the chromatogram in Figure 5 (Figure 23). Peaks A and D of the chromatogram in Figure 6 were then tested with another

papillary muscle to differentiate between the two large peaks and to confirm the presence of MDF in peak D (Figure 24).

Although there was a depression in  $P_0$  with peak D of shock plasma in the AS-DS muscle experiment (Figure 24), it was not significant. The response of the muscle in terms of  $V_{max}$  was unexpectedly different from the response of the muscle in Figure 23. There are several possible explanations as to why the expected significant differences between shock plasma peaks A and D did not occur.

When the muscle was subjected to shock plasma peak A, the immediate response was an increase in the amplitude of contraction. Although this initial increase in amplitude was observed for every test peak, the increase for shock plasma peak A was definitely much larger; so large, that the sensitivity on the dynograph recorder had to be reduced. It was therefore unusual that the  $P_0$  value for peak A was not larger than it was.

In reevaluating the situation, peak A from shock plasma should not be considered to be equivalent to either peak A or peak D of control plasma from a young dog not in shock. Although MDF was reported to be only in peak D of shock plasma, the possibility that a negative depressant factor may be aggregated to a large peptide or protein in peak A of shock plasma cannot be ruled out, especially since

the formation of MDF is only hypothesized. There may be large molecules in peak A which have combined temporarily with some residual MDF.

Peak A contains large peptides and protein which are beneficial to the muscle. This has been shown by a very large increase in amplitude of contraction. However, there may have been a competitive action between the large peptides in peak A which exert a positive effect on the papillary muscle and the hypothesized aggregated depressant factor which would prevent the expected significant increase in  $P_0$ . The effects of shock in plasma peak A should have been ascertained by testing an individual muscle with peak A of plasma from normal and shock-induced dogs.

The absence of a significant depression of  $P_0$  with shock plasma peak D following shock plasma peak A must be explained, since shock plasma peak D (Figure 23) contained significant MDF activity. It is possible that the beneficial supplementary protein found in peak A stabilized the muscle such that the reaction time for MDF (peak D) was slowed past the thirty-minute period for induction of a response. Thus, the exhibition of the negative effects of MDF were only delayed because the papillary muscle was stabilized with peak A.

Another point is that this one muscle experiment constitutes a small sample size, even though a pooled variance determined by the analysis of variance was used to test this

particular experiment for significance.

That the  $V_{\max}$  value for DS (Figure 24) was greater than the  $V_{\max}$  values for both AS and K-H is not consistent with the DS response in Figure 23. The incongruity of the  $V_{\max}$  value with  $P_0$  is also demonstrated in Figures 25 and 30.

The  $P_0$  values of the papillary muscle subjected to peak D of plasma from a young and old dog were identical (Figure 25). However, the  $V_{\max}$  value was larger for peak D of plasma from the old dog. In Figure 30, the  $P_0$  of the muscle subjected to peak D of plasma from an old dog was depressed, but the  $V_{\max}$  value was larger than the  $V_{\max}$  value for the preceding bath, peak D of plasma from a young dog.

Four explanations for this biological incongruity are presented. First, the validity of  $V_{\max}$  was questioned by several researchers. The possibility of an intrinsic load is not considered when  $V_{\max}$  is extrapolated from the force-velocity curve to zero load. There is no way of knowing whether unidentified internal forces are negligible or not, or whether they are consistent or changing in a muscle. It is possible that the  $V_{\max}$  values do not represent the maximum velocity of muscle shortening at zero load. Unexpected values for  $V_{\max}$  for particular muscle baths may be attributed to the presence of changing internal forces which would increase or decrease  $V_{\max}$  as they decreased or increased, respectively.

Second, there is some subjectivity in the selection of a particular polynomial to fit the experimental data points of a force-velocity curve by the method of least squares. The data points of all force-velocity curves were fit to 2nd, 3rd, and 4th order polynomials by the method of least squares and correlation coefficients were compared. The predicted y values (velocity) for chosen x values (load) were compared with experimental y values. The polynomial which gave y values as close as possible to experimental values was selected. The polynomial chosen for fitting the data points was the same for all three muscle baths within one muscle experiment. The polynomial which was used could vary from one muscle experiment to another.

Extrapolated  $V_{\max}$  values differed for all three polynomials, and therefore the polynomial had to be carefully selected.

Third, the incongruity lies within the extrapolation itself. When the  $P_0$  of a muscle is large and the afterload curve is generated backwards, the velocity changes gradually along a semi-plateau similar to a sigmoidal curve (K-H curve, Figure 30). A large number of data points may be entered into the computer, programmed to extrapolate  $V_{\max}$ , when the  $P_0$  value is large. The points along the plateau part of the curve influence the  $V_{\max}$  value. However, when

the  $P_0$  value of a muscle is small, the velocity changes more rapidly as the load is decreased. There is usually no plateau. The  $V_{\max}$  value is extrapolated from a smaller number of data points which can only force the  $V_{\max}$  value to a much higher value than is biologically possible. This occurs because the velocity points are changing faster over a smaller range of loads than in the sigmoidal curve where the  $P_0$  is large.

Fourth, since a high percentage of  $L_{\max}$  was produced by the selected preload, it is possible that the muscles were potentiated by a high resting tension and were closer to their ceiling of contractility. This may partially explain why some  $V_{\max}$  values remained high and were not easily depressed, assuming that  $V_{\max}$  is length-dependent.

The use of particular molecular weight markers for Bio-Gel P-2 should be discussed. Glycylglycine (molecular weight 132.1) was consistently found in the eluate at a mean elution volume of 110-131 ml ( $n=4$ ) which does not correlate with the molecular weight. There are two possible reasons. First, the exclusion limit for Bio-Gel P-2 is 200-1600 (Lefer, 1970). The elution volume for a substance will not be linear beyond the exclusion limits of the beads. Glycylglycine is below the cutoff point of the fractionation range. The other possible explanation is that the

glycylglycine stock material was not really the dimer, and therefore came off the column at a position which corresponded to a larger molecular weight substance.

Glycylglycine was used as a molecular weight marker for Bio-Gel P-2 by one research group (Lefer and Martin, 1970a), which prompted me to include it with the other molecular weight markers. Although Lefer (1970) acknowledged that the lower end of the exclusion range for Bio-Gel P-2 was 200, glycylglycine was still used as a marker. Glycylglycine in my separations consistently appeared in the eluate at a position which corresponded to a molecular weight of about 1200. It is believed that the molecular weight of glycylglycine is too low to satisfactorily calibrate Bio-Gel P-2 columns with this peptide.

Hexaglycine was used instead of glycylglycine, since the molecular weight (360.3) was larger than the low cutoff point for separation by Bio-Gel P-2. However, hexaglycine introduced a different problem, that of dissolution. This peptide would not dissolve unless it was heated in 1N HCl. A precipitate formed when the solution cooled to room temperature. Although hexaglycine was absorbed into the top layer of the gel bed, there was no assurance that hexaglycine was not precipitating within the column. This was substantiated by the poor resolution of the hexaglycine peak in the composite

chromatogram for molecular weight markers (Figure 21). Thirty milligrams of hexaglycine instead of fifty mg was dissolved in the same amount of acid and was reapplied to a column. Although the warm solution of 30 mg of hexaglycine in 1N HCl would still precipitate when cooled to 25C, it was layered on the column. The 30-mg hexaglycine peak was not as broad as the 50-mg hexaglycine peak, but the existence of a shoulder on the high molecular weight side of the 30-mg hexaglycine peak may indicate poor resolution. This probably means that hexaglycine was still precipitating as it passed through the column. The elution volumes at the peak height of both 50-mg and 30-mg hexaglycine peaks were similar (177.0 and 173.5 ml). Hexaglycine was not an ideal marker and may only serve as a rough estimate for the position of a 360.3 molecular weight substance.

Angiotensin III inhibitor (molecular weight 896) was found at an elution volume corresponding to a molecular weight of about 1375 (Figure 21). This peptide may have aggregated and passed through the column as a heavier particle. If this peptide combined as a dimer, it would appear in the eluate at an elution volume corresponding to twice the molecular weight. It would then be found in the void volume. A possible explanation for the position of angiotensin III inhibitor in the eluate is that there was some nonspecific "sticking" which altered the molecular



weight properties of the peptide. Angiotensin III inhibitor did not seem to have a monomeric weight when applied to Bio-Gel P-2.

The faster the flow rate, the sooner is the appearance of the peak in the eluate. This was evident with angiotensin II (molecular weight 1225). When the column flow rates were identical (9.2 ml/hr), two of the peaks were found in similar elution volumes. When the flow rate was increased to 11.2 ml/hr, the peak appeared sooner in the elution volume, but overlapped with two later peaks at the slower flow rate (Figure 21).

The column flow rate was constant throughout an entire run and varied only slightly, if at all, between runs for any one of the four columns. Differences in flow rates occurred when columns were repacked.

The different elution volumes for MDF (peak D of shock plasma) that are reported by different researchers may be explained by altering characteristics of the column. Any variance in column size, length, eluant or flow rate may shift the elution volume of peak D.

According to Lefer and Martin (1970a), all eluted peaks of shock plasma were ninhydrin-positive except peak B. My ninhydrin test results agree with those of Okuda and Fukui (1974); all eluted peaks including peak B were ninhydrin-positive (Table 2). The results of the ninhydrin assay,

which is indicative of total proteolysis, were consistent with absorbance readings at 230 nm for each of the peaks.

Several trends and consistencies may be suggested from the column elution patterns for young and old dogs (Figures 7-19):

In the chromatograms for young dogs, peak D was consistently smaller than peak C except for young dogs #2 and #4. In the chromatograms for old dogs, peak D was consistently larger than peak C except for old dogs #2 and #4 where peaks C and D were similar. A tradeoff in activity between peaks C and D was observed when shock plasma was compared with control plasma. The activity of peak C of control plasma diminished in shock plasma where peak D would be very active.

Although peak DY1 was smaller than peak CY1, and peak DO1 was larger than peak CO1, no depression of the papillary muscle resulted (Figure 25). There was even a continual increase in  $V_{max}$  and a continual decrease in the slope of the latency curve (Figure 46) as Krebs-Henseleit buffer was replaced first with peak D of plasma from the young dog and then with peak D of plasma from the old dog.

The medical history of old dog #1 (O1) made this dog an interesting subject. The 15-year old dog had mitral valve failure, renal failure and was being treated for Cushing's syndrome. An increased concentration of glucocorticoids

would be present which would stabilize lysosomal membranes. This would counteract the production of MDF if MDF was associated with old age. If large peak D's were found in the plasma of the other aged dogs, but not old dog #1, then the hypothesis that lysosomal enzymes are important in MDF formation would be valid.

Peak DO2 was not larger than peak CO2 and a continual increase in muscle performance resulted (Figure 26).

Although peak DY3 was smaller than peak CY3, and peak DO3 was larger than peak CO3, the  $P_o$  value of the muscle steadily increased as buffer was replaced with peak D of plasma from the young dog and then with peak D of plasma from the old dog (Figure 27). The slope of the latency curve for peak D of plasma from the old dog was the smallest (Figure 48).

Although peak DY3 of the second column elution pattern for young dog #3 was not much different than peak CY3, just as peak DO4 was similar to peak CO4, the  $P_o$  and slope of the latency curve improved with peak D of plasma from the young dog and worsened with peak D of plasma from the old dog. The changes, however, were only slight (Figure 28).

The depression of the papillary muscle subjected to peak DY4 and peak DO5 (Figure 29) should be considered. Peak DY4 was larger than peak CY4, and there was a slight initial depression in  $P_o$  and  $V_{max}$  when K-H was replaced with

peak D of plasma from the young dog. The column elution pattern for old dog #5 (Figure 18), the oldest dog in the study, was different from the chromatograms of the other dogs (young, old, and shock dogs) with respect to the size of peak A.

The possibility that the large peptides or protein contained in peak A were lost was considered at each step in the procedure (Figure 2). Freshly obtained blood from the 17-year old dog was completely processed again and a similar elution profile was produced (Figure 60, Appendix). This was repeated a third time, but peak A remained small (Figure 61, Appendix), unlike the peak A's from every other dog. There is a similarity of the peaks and the relationship between peaks C, D, and E for all three column elution patterns (Figures 18, 60, 61).

A decrease in sensitivity of the spectrophotometer was even considered, since peaks A and D were of the same size in shock plasma. If peak A was reduced by a decrease in sensitivity of the spectrophotometer, then peak D would also be reduced. However, peaks B, C, E, and F were no smaller than those for other dogs, so this step of the procedure was ruled out. The dialysis procedure was suspect because fibrin might adhere to the membrane if it was not completely removed from the plasma. This might prevent large proteins from passing into the ultrafiltrate. However, it is

extremely unlikely that the large peptides in peak A were lost during the procedure at three separate times for one particular dog. No explanation for small peak A for old dog #5 can be offered at present, unless some deficiency in the blood is exhibited by this small peak.

It should be noted that peak D05 was larger than peak C05, and a depression of  $P_o$ ,  $V_{max}$  and an increase in the slope of the latency curve resulted (Figures 29, 50).

Peak DY5 was smaller than peak CY5 and peak D06 was larger than peak C06. A continual depression in  $P_o$  and a continual increase in the slope of the latency curve resulted (Figures 30, 51).

Whole plasma was used instead of processed plasma peak D for three muscle experiments (Figures 32, 33, 34). Plasma Y5 caused a depression of  $P_o$ ,  $V_{max}$ , and an increase in the slope of the latency curve (Figures 32, 34, 52, 54). This is consistent with peak DY5 (Figure 30) which also caused a depression of  $P_o$ ,  $V_{max}$  and an increase in slope of the latency curve. This suggests that some common factor in peak D might also be present in the whole plasma of young dog #5. The elution pattern of the plasma from this dog does not differ from the others with the exception that peak E is larger than usual. However, this would not affect the response elicited by peak D. The depression elicited by young dog #5 may be traced to the anesthetic which was

administered to the dog in order to obtain a sufficient amount of blood.

According to Lundgren et al. (1976), the depression in developed tension elicited by whole plasma from control cats was due to the presence of pentobarbital in the plasma.

Plasma O3 (Figure 32) depressed  $P_O$ ,  $V_{max}$ , and increased the slope of the latency curve; however, these responses were not due to any anesthetic. Note that the response elicited by peak D03 (Figure 27) was different from whole plasma. The medical history of this 14-year old Weimaraner may be considered when explaining the depression in contractility. Although there was no history of a heart condition, there may very well have been some component in the blood which would cause the observed depression. This component could not be of the same molecular weight as the substance which is found in peak D.

$P_O$  and  $V_{max}$  were depressed with plasma Y4 (Figure 33) and peak DY4 (Figure 29) in a similar manner. No anesthetic was administered to young dog #4. However, there was a discrepancy in the effect on the slope of the latency curve. The slope increased with plasma Y4 (Figure 53), while the slope decreased slightly from the K-H slope value with peak DY4 (Figure 50). There is no explanation for the biological inconsistency concerning the slope of the latency curve.

The relationship of the plasma O2 force-velocity curve (Figure 33) to the plasma-young force-velocity curve was very similar to the relationship of the peak DO2 curve to the peak D-young curves (Figures 26, 31).

The  $P_o$  value of the muscle subjected to plasma O5 (Figure 34) was slightly larger than the  $P_o$  value for plasma from the young dog. This is in contrast to peak DO5 which depressed the  $P_o$  value from the value for peak D from the young dog (Figure 29). The curves for peak D from a young dog and peak DO5 were similar to the curves for whole plasma, except for a decrease in  $P_o$  when peak D from the old dog was used.

The probable reason why plasma O5 decreased the slope of the latency curve from the value for the plasma-young curve while peak DO5 increased the slope of the latency curve from the value for the peak D-young curve is that the large increase in slope which was caused by plasma from the young dog was due to the presence of the anesthetic in the whole plasma. Although both plasma O5 and peak DO5 increased the slope of the latency curve from the Krebs-Henseleit value, the effect of plasma O5 was not as detrimental as the effect of the anesthetic present in plasma Y5 (Table 4).

The  $P_o$  value increased when whole plasma from old dog #5 was used, but decreased when peak DO5 was used. There may be components of whole plasma which are beneficial and

absent in peak D which may be responsible for the improvement in  $P_0$  value.

There is a possible contributing factor for the depression of the force-velocity curves from processed plasma peak D samples when compared with the K-H force-velocity curves. The activity of the column eluate (Krebs-Henseleit minus glucose after passing through the column) was reported to be slightly myocardial depressant (Lefer, 1970; Lefer and Martin, 1970b). This may account for some of the depression which was observed with the peak D samples (Figures 28, 29, 30, 31).

However, the peak D samples used in Figures 25, 26, 27 improved muscle performance beyond the performance of the muscle with K-H buffer solution.

Another possible explanation for the depression with whole plasma when compared with the Krebs-Henseleit buffer is the lower free calcium ion concentration in the plasma relative to the Krebs-Henseleit solution. Protein-bound calcium which is nondiffusible represents about 30-55% of the total serum calcium (Moore, 1971).

One point should be clarified in interpreting the composite force-velocity curves (Figures 35-43). The total number of activated myosin cross-bridges for each muscle is corrected for with  $P/P_0$ . The force of all muscles is



normalized and differences in the size of the papillary muscle are eliminated. The force measurements along the x-axis should then range from 0 to 1 since  $P_o/P_o$  for each muscle is 1.

The points along the x-axes larger than 1 are the points extrapolated by the computer which is programmed to calculate the force where velocity is zero.

From the composite Krebs-Henseleit, peak D-young and peak D-old force-velocity curves (Figure 40) where velocities are the means of the velocities for the nine K-H curves, six DY curves and six DO curves, the overall effect may be demonstrated. The curves for DY and DO are very similar, and the peak D-old curve has a larger  $V_{max}$  value than that for peak D-young or K-H curves. A general trend of improved muscle performance as K-H was replaced with peak D of plasma from young dogs and then with peak D of plasma from old dogs is depicted.

A different trend is depicted in the composite with whole plasma from young dogs and whole plasma from old dogs (Figure 41). There was a general depression as buffer was replaced with plasma from young dogs and then with plasma from old dogs. However, two points must be considered. First, the sample size for whole plasma experiments was 3. Second, plasma from the same young dog was used in two of these experiments. The muscle depression which occurred

was probably due to the presence of anesthetic in the plasma.

The difference between the plasma-young curve and the plasma-old curve may be attributed to one muscle experiment (Figure 32) where the difference in  $V_{\max}$  between plasma Y5 and plasma O3 approached significance ( $\alpha=0.10$ ) (Table 9). Thus, this composite is representative of only three experiments in which it is very easy for just one experiment to shift a curve either toward or away from the K-H curve.

The composites in Figures 42 and 43 include a further normalization of the papillary muscles with respect to force and velocity per unit of cross-sectional area. The close similarity between peak DY and peak DO, and the improvement in muscle performance above the performance of the muscle with K-H buffer is again present.

The only difference between Figures 40 and 42 is that in Figure 42, it appears that peak DY was more beneficial to the muscle than peak DO in terms of  $V_{\max}$  per unit of cross-sectional area.

The effect of normalizing the three muscles subjected to whole plasma with respect to velocity per unit of cross-sectional area (Figure 43) was to approximate the plasma-young and plasma-old curves which indicates a similarity between whole plasma from young and old dogs.

A comparison should always be made with a constant

standard, such as modified Krebs-Henseleit solution, because of the components and unknown variables present in plasma. As it was concluded in the statistical analysis section of the RESULTS, there was no significant difference between plasma (processed or unprocessed) from young and old dogs. Any significant age effect could be attributed to the first age treatment (K-H) which differed from both the young and old age treatments. As a pair, the young and old age treatments did not significantly differ from each other.

#### Conclusions

The question still remains: Is MDF present in the plasma from aged dogs? Blood containing MDF was collected directly from the pancreas via the hepatic portal vein from a shock dog (pancreatic vessel ischemia). The blood from aged dogs was obtained via the jugular vein. If MDF was present in the aged animal, this peptide would not accumulate in concentrations which are present during shock or the aged animal would die. However, a low-grade concentration of MDF circulating within the aged animal is possible, since depressed reticuloendothelial and kidney systems are not uncommonly found in aged animals. Two possibilities should be considered when comparing the chromatograms from shock plasma with plasma from aged dogs. Peak D of shock plasma, which unquestionably contained MDF, was larger than

peak D of plasma from old dogs. The first hypothesis is that MDF could not be present at the same concentration in an aged dog as in a shock dog for survival reasons alone. Thus, the optical density readings for this peptide, which was found in the eluate at peak D, could not be similar for age and shock. The second possibility, which is only a mere thought, is that in an aged dog with poor circulation, if blood is not collected directly from the source of MDF, how certain can we be that MDF is present in detectable and undiluted concentrations in the peripheral circulation at any given time.

Basal amounts of MDF may always be present in the pancreas of a normal animal, young or old. Relatively low MDF activity was indicated in a chromatogram of sham-shock cat pancreas. Low MDF concentrations could be present in the normal animal and be continuously eliminated from the body. Only when the systems are depressed during shock does MDF accumulate and exert its actions in a vicious positive feedback cycle.

Thus, if MDF were to be detected in the plasma of an aged animal, the systems of the aged animal would have to malfunction to the same degree of severe depression as in the shock state.

A major problem inherent in the study of aging animals

should be realized. As a population ages, a continual selection occurs as members are removed by death. If MDF accumulates with age, but the animals die before the plasma MDF concentration is detectable, the study of surviving aged dogs will yield misleading results.

There is a possibility that MDF is present in the aged animal. MDF was not present in the six aged animals selected for the study at a detectable concentration with the procedures used. MDF, if present in these aged dogs, was certainly not present at the same concentration as MDF of shock plasma. There is a good possibility that the concentration of MDF may be increased by performing a series of lyophilizations of the initial 10-ml aliquot of peak D. Physiological osmolarity would have to be maintained without altering calcium and other ion concentrations. Low levels of MDF could then be detected in the aged animal with the bioassay. The other option would be to develop a more sensitive bioassay, although significant sensitivity has been demonstrated with the papillary muscle system.

Another alternative to the procedure of concentrating MDF would entail twelve or thirteen repeated column separations of plasma from the same aged dog to yield twelve or thirteen peak D's. These would then be pooled, lyophilized together and reconstituted to 24 or 26 ml.

Osmolarity would have to be adjusted without altering

the calcium ion concentration. No K-H buffer would be used since the muscle chamber holds 25 ml, or varied proportions of pooled peak D's and K-H could be used for the muscle bath.

A third alternative is to further purify peak D with a Dowex-50 ion exchange column.

Although the effects of each young dog can be explained, the value of using different young dogs as controls might be reevaluated. It was informative to study as many column elution patterns from young dogs as from old dogs. However, with the papillary muscle bioassay, each sample from a different aged dog was being tested against a sample from a different young dog. If this additional variable (young dog differences) was eliminated by repetitively using plasma samples from the same young dog on every papillary muscle, only muscle differences and differences between aged dogs would be present. The advantage of using samples from different young dogs was to observe the effects of plasma from young dogs compared with K-H buffer, in addition to using the young dogs as controls for aged dogs. The disadvantage of using one young dog for all aged dogs is that a young dog may be randomly chosen which has an unusual plasma component which may influence the papillary muscle to respond to plasma from all aged dogs in a particular way. The only way to fairly represent a population is to randomly sample

young dogs. If plasma samples from several young dogs are pooled, there may be interactions between different dog plasma which might also influence the papillary muscle to respond to plasma from all aged dogs in a certain way. It is possible to test a concentrated test solution of peak D of an aged dog (pooled from 12-13 identical column separations) against a series of different young dogs whose peak D solutions would be equally concentrated (12-13 column separations of plasma ultrafiltrate from each young dog).

Variabilities are high in mechanical studies of isolated muscles (Heller and Whitehorn, 1972). The bioassay technique has limitations. The number of samples which can be assayed at one time is limited by the viability of the papillary muscle utilized. The papillary muscle is extremely sensitive to pH and osmolarity changes, and a stable system must first be established. A noteworthy consideration is that it is very difficult to obtain large quantities of blood from aged dogs which makes it difficult to replicate steps in the procedure.

## REFERENCES

- Andrew, Warren. 1971. The anatomy of aging in man and animals. Grune and Stratton, New York.
- Blattberg, B., and M. N. Levy. 1966. Some properties of the reticuloendothelial-depressing substance of the dog. *Am. J. Physiol.* 210:312-314.
- Bloom, S. R., T. E. Adrian, M. G. Bryant, and J. M. Polak. 1978. Pancreatic polypeptide: A marker for Zollinger-Ellison Syndrome? *Lancet* 1 (8074):1155.
- Brady, A. 1965. Time and displacement dependence of cardiac contractility: Problems in defining the active state and force-velocity relations. *Federation Proc.* 24:1410-1420.
- Brady, A. 1967. Mechanics of isolated papillary muscle. Pages 53-64 in R. Tanz, F. Kavalier, and J. Roberts, eds. *Factors influencing myocardial contractility.* Academic Press, New York.
- Brand, E. D., and A. M. Lefer. 1966. Myocardial depressant factor in plasma from cats in irreversible post-oligemic shock. *Proc. Soc. Exp. Biol. Med.* 122:200-203.
- Brand, E. D., R. Cowgill, and A. M. Lefer. 1969. Further characterization of a myocardial depressant factor present in hemorrhagic shock. *J. Trauma* 9(3):216-226.
- Braunwald, E., and J. Ross. 1964. Applicability of Starling's law of the heart to man. *Circ. Res.* 15:169-178.
- Brutsaert, D., V. Claes, and E. Sonnenblick. 1971. Velocity of shortening of unloaded heart muscle and the length-tension relation. *Circ. Res.* 29:63-74.
- Brutsaert, D., V. Claes, and M. Goethals. 1973. Effect of calcium on force-velocity-length relations of heart muscle of the cat. *Circ. Res.* 32:385-392.
- David, D., and S. Rogel. 1976. Mechanical and humoral factors affecting cardiac function in shock. *Circ. Shock* 3(1):65-75.



- Detweiler, D. 1973. Mechanical activity of the heart. Pages 3-86-3-98 in J. R. Brobeck, ed. Best and Taylor's physiological basis of medical practice. 9th ed. The Williams and Wilkins Company, Baltimore, Maryland.
- Donald, T., K. Unnoppetchara, D. Peterson, and L. Hefner. 1972. Effect of initial muscle length on  $V_{\max}$  in isotonic contraction of cardiac muscle. *Am. J. Physiol.* 223(2):262-267.
- Dougherty, J. H., and L. S. Rosenblatt. 1965. Changes in the hemogram of the beagle with age. *J. Gerontol.* 20(2):131-138.
- Edman, K. A. 1977. The instantaneous force-velocity relationship as an index of the contractile state in cardiac muscle. *Basic Res. Cardiol.* 72:94-101.
- Edman, K. A., and E. Nilsson. 1972. Relationship between force and velocity of shortening in rabbit papillary muscle. *Acta Physiol. Scand.* 85:488-500.
- Ewing, K. L., and O. E. Tauber. 1964. Hematological changes in aging male C57BL/6 Jax mice. *J. Gerontol.* 19:165-167.
- Falsetti, H., R. Mates, D. Greene, and I. Bunnell. 1972.  $V_{\max}$  as an index of contractile state in man. *Circulation* 45:927.
- Finch, C. E., and L. Hayflick. 1977. Handbook of the biology of aging. Van Nostrand Reinhold Company, New York.
- Fisher, W. D., C. S. McArdle, M. Maddern, and I. McA. Ledingham. 1973a. A circulating myocardial depressant factor after shock. *Brit. J. Surg.* 60(4):308-309. (Abstr.)
- Fisher, W. D., D. W. Heimbach, C. S. McArdle, M. Maddern, M. M. Hutcheson, and I. McA. Ledingham. 1973b. A circulating depressant effect following canine hemorrhagic shock. *Brit. J. Surg.* 60(5):392-394.
- Floyd, J. C., S. S. Fajans, S. Pek, and R. E. Chance. 1977. A newly recognized pancreatic polypeptide; plasma levels in health and disease. *Recent Progr. Horm. Res.* 33: 519-570.

- Flynn, J., and A. M. Lefer. 1977. Beneficial effects of arachidonic acid during hemorrhagic shock in the dog. *Circ. Res.* 40:422-428.
- Ford, L., and R. Forman. 1974. Tetanized cardiac muscle. Page 142 in R. Porter and D. Fitzsimons, eds. *The physiological basis of Starling's law of the heart.* Associated Scientific Publishers, New York.
- Frolkis, V. V., N. V. Verzhikovskaya, and G. V. Valueva. 1973. The thyroid and age. *Exp. Gerontol.* 8:285-296.
- Galvin, M. J., and A. M. Lefer. 1978a. Actions of dopamine in splanchnic artery occlusion shock. *Am. J. Physiol.* 234(1):H1-H6.
- Galvin, M. J., and A. M. Lefer. 1978b. Effects of cysteine on the pathogenesis of cardiogenic shock. *Federation Proc.* 37:369. (Abstr.)
- Glenn, T. M., and A. M. Lefer. 1970. Role of lysosomes in the pathogenesis of splanchnic ischemia shock in cats. *Circ. Res.* 27:783-797.
- Goldfarb, R. D., and P. Weber. 1977a. The chemical nature of a pancreatic cardiodepressant factor. *Circ. Shock* 4:95-100.
- Goldfarb, R. D., and P. Weber. 1977b. Separation of pancreatic cardiodepressant activity into peptide and salt activity. *Proc. Soc. Exp. Biol. Med.* 156:219-222.
- Goldfarb, R. D., P. Weber, and J. E. Estes. 1978. Characterization of circulating shock-induced cardiodepressant substances. *Federation Proc.* 37(13):2724-2728.
- Goll, D. E., M. H. Stromer, R. M. Robson. 1977. Skeletal muscle. Page 523 in M. J. Swenson, ed. *Dukes' physiology of domestic animals.* 9th ed. Comstock Publishing Associates, Cornell University Press, Ithaca, New York.
- Gomez, O., and W. F. Hamilton. 1964. Functional cardiac deterioration during development of hemorrhagic circulatory deficiency. *Circ. Res.* 14:327-336.

- Greene, L. J., R. Shapanka, T. M. Glenn, and A. M. Lefer. 1977. Isolation of myocardial depressant factor from plasma of dogs in hemorrhagic shock. *Biochim. Biophys. Acta* 491:275-285.
- Grimm, A., and B. Wohlfart. 1974. Sarcomere lengths at the peak of the length-tension curve in living and fixed rat papillary muscle. *Acta Physiol. Scand.* 92:575-577.
- Grood, E., R. Mates, and H. Falsetti. 1974. A model of cardiac muscle dynamics. *Circ. Res.* 35:184-196.
- Gulch, R., and R. Jacob. 1975a. Length-tension diagram and force-velocity relations of mammalian cardiac muscle under steady-state conditions. *Pflugers Arch.* 355:331-346.
- Gulch, R., and R. Jacob. 1975b. The effect of sudden stretches on length-tension and force-velocity relations of mammalian cardiac muscle. *Pflugers Arch.* 357:335-347.
- Guyton, A. C. 1976. Textbook of medical physiology. 5th ed. W. B. Saunders Company, Philadelphia, Pennsylvania.
- Haglund, U. 1973. The small intestine in hypotension and hemorrhage. *Acta Physiol. Scand.* 88:3-31.
- Haglund, U., and O. Lundgren. 1978. Intestinal ischemia and shock factors. *Federation Proc.* 37:2729-2733.
- Hakim, A. A. 1975. Effects of digitoxin on "acute burn serum inhibitor" depressed human heart papillary muscles. *Pharm. Acta Helv.* 50(6):178-184.
- Harden, T. K., and R. L. Garrett. 1973. Depression of atrial contractility by peptides isolated from normal and shock plasma. *Proc. Soc. Exp. Biol. Med.* 144:56-59.
- Harman, D. 1960. The free radical theory of aging: The effect of age on serum mercaptan levels. *J. Gerontol.* 15(1):38-40.
- Harman, D. 1965. The free radical theory of aging: The effect of age on serum copper levels. *J. Gerontol.* 20(2):151-153.

- Harman, D. 1968. The free radical theory of aging: The effect of free radical reaction inhibitors on the mortality rate of male LAF mice. *J. Gerontol.* 23(4): 476-482.
- Harman, D., and L. Piette. 1966. The free radical theory of aging: Free radical reactions in serum. *J. Gerontol.* 21(4):560-565.
- Heller, L. J., and W. V. Whitehorn. 1972. Age-associated alterations in myocardial contractile properties. *Am. J. Physiol.* 222(6):1613-1619.
- Hembrough, F. B., A. Anderson, R. Tang, and D. D. Draper. 1978. Potential of papillary muscle from young dogs for use in various diagnostic studies. *Am. J. Vet. Res.* 39(12):1936-1942.
- Johnson, E. A., E. Sonnenblick, and L. Ford. 1974. Temperature. Pages 236-237 in R. Porter and D. Fitzsimons, eds. *The physiological basis of Starling's law of the heart.* Associated Scientific Publishers, New York.
- Kababji, V. M., W. Westphal, and E. Bauereisen. 1974. Temperature dependence of myocardial length-tension-relation. The effect of stretching: Recruitment or inotropism. *Basic Res. Cardiol.* 69:47-57. (Abstr.)
- Kabat, E. A. 1961. Estimation of protein with the biuret and ninhydrin reactions. Pages 559-563 in E. A. Kabat and M. M. Mayer, eds. *Experimental immunology.* 2nd ed. Charles C. Thomas Publisher, Springfield, Illinois.
- Kohn, R. 1971. *Principles of mammalian aging.* Prentice-Hall, Inc., Englewood Cliffs, New Jersey.
- Kosugi, I. 1974. The myocardial depressant factor in hemorrhagic and endotoxic shock in dogs. *Excerpta Medica Anesthesiol.* 9.6:347-348. (Abstr.)
- LaBella, F., and G. Paul. 1965. Structure of collagen from human tendon as influenced by age and sex. *J. Gerontol.* 20(1):54-59.
- Langer, G. A. 1971. The intrinsic control of myocardial contraction-ionic factors. *N. Engl. J. Med.* 285:1065-1071.

- Langer, G. A. 1977. Ionic basis of myocardial contractility. *Ann. Rev. Med.* 28:13-20.
- Lefer, A. M. 1970. Role of a myocardial depressant factor in the pathogenesis of circulatory shock. *Federation Proc.* 29(6):1836-1847.
- Lefer, A. M. 1973. Blood-borne humoral factors in the pathophysiology of circulatory shock. *Circ. Res.* 32(2): 129-139.
- Lefer, A. M. 1978. Properties of cardioinhibitory factors produced in shock. *Federation Proc.* 37(13):2734-2740.
- Lefer, A. M., and Y. Barenholz. 1972. Pancreatic hydrolases and the formation of a myocardial depressant factor in shock. *Am. J. Physiol.* 223(5):1103-1109.
- Lefer, A. M., and B. Blattberg. 1968. Comparison of the effects of two factors present in plasma of shocked animals. *J. Reticuloendothel. Soc.* 5:54-60.
- Lefer, A. M., and T. M. Glenn. 1973. Editorial comments: Controversy over myocardial depressant factor in shock. *J. Trauma* 13(8):746-747.
- Lefer, A. M., and T. F. Inge. 1973. Differentiation of a myocardial depressant factor present in shock plasma from known plasma peptides and salts. *Proc. Soc. Exp. Biol. Med.* 142:429-433.
- Lefer, A. M., and J. Martin. 1970a. Relationship of plasma peptides to the myocardial depressant factor in hemorrhagic shock in cats. *Circ. Res.* 26(1):59-69.
- Lefer, A. M., and J. Martin. 1970b. Origin of myocardial depressant factor in shock. *Am. J. Physiol.* 218(5): 1423-1427.
- Lefer, A. M., and M. Ogletree. 1978. Prostacyclin: A potentially valuable agent for preserving myocardial tissue in acute myocardial ischemia. *Science* 200(7): 52-54.

- Lefer, A. M., and J. A. Spath. 1975. Pancreatic hypoperfusion and the production of a myocardial depressant factor in hemorrhagic shock. *Excerpta Medica Anesthesiol.* 10.2:63. (Abstr.)
- Leffler, J. N., Y. Litvin, Y. Barenholz, and A. M. Lefer. 1973. Proteolysis in formation of a myocardial depressant factor during shock. *Am. J. Physiol.* 224(4): 824-831.
- Leyton, R., H. Spotnitz, and E. Sonnenblick. 1971. Cardiac ultrastructure and function: Sarcomeres in the right ventricle. *Am. J. Physiol.* 221(3):902-910.
- Litvin, Y., J. N. Leffler, Y. Barenholz, and A. M. Lefer. 1973. Factors influencing the *in vitro* production of a myocardial depressant factor. *Biochem. Med.* 8:199-212.
- Loeffler, L., III, and K. Sagawa. 1975. A one-dimensional viscoelastic model of cat heart muscle studied by small length perturbations during isometric contraction. *Circ. Res.* 36:498-512.
- Lovett, W. L., S. L. Wangenstein, T. M. Glenn, and A. M. Lefer. 1971. Presence of a myocardial depressant factor in patients in circulatory shock. *Surgery* 70(2):223-231.
- Lundgren, O., U. Haglund, O. Isaksson, and T. Abe. 1976. Effects on myocardial contractility of blood-borne material released from the feline small intestine in simulated shock. *Circ. Res.* 38(4):307-314.
- Minelli, R., C. Reggiani, R. Dionigi, and V. Capelli. 1975. Cardiac muscle models for both isotonic and isometric contractions. *Pflugers Arch.* 359:69-80.
- Moore, E. 1971. Studies with ion exchange calcium electrodes. *Gastroenterology* 60(1):43-53.
- Munnell, J. F., and R. Getty. 1968. Rate of accumulation of cardiac lipofuscin in the aging canine. *J. Gerontol.* 23:154-158.
- Nayler, W. G. 1975. Contraction and relaxation in the myocardium. Academic Press, London.

- Noble, M. 1974. Force-velocity relation at different muscle lengths. Pages 133-136 in R. Porter and D. Fitzsimons, eds. The physiological basis of Starling's law of the heart. Associated Scientific Publishers, New York.
- Noble, M., and W. Else. 1972. Reexamination of the applicability of the Hill model of muscle to cat myocardium. *Circ. Res.* 31:580-588.
- Okada, K., I. Kosugi, Y. Yamaguchi. 1974. The myocardial depressant factor in hemorrhagic or endotoxin shock in dogs. *Excerpta Medica Anesthesiol.* 9.4:208. (Abstr.)
- Okada, K., I. Kosugi, T. Kitagaki, Y. Yamaguchi, H. Yoshikawa, and Y. Senoh. 1977. Pathophysiology of shock. *Jap. Circ. J.* 41:346-360.
- Okuda, M., and T. Fukui. 1974. Myocardial depressant factor - a peptide: Its significance in cardiogenic shock. *Jap. Circ. J.* 38:497-508.
- Okuda, M., Y. Yamada, and K. Hosono. 1973. Characterization of a myocardial depressant factor isolated from cardiogenic shock (in Japanese). *Jap. Circ. J.* 37(8): 1009-1017.
- Parmley, W. W., and L. Chuck. 1973. Length-dependent changes in myocardial contractile state. *Am. J. Physiol.* 224(5):1195-1199.
- Parmley, W. W., D. Brutsaert, and E. Sonnenblick. 1969. Effects of altered loading on contractile events in isolated cat papillary muscle. *Circ. Res.* 24:521-532.
- Parmley, W. W., L. Chuck, and E. Sonnenblick. 1972. Relation of  $V_{max}$  to different models of cardiac muscle. *Circ. Res.* 30:34-43.
- Riegler, G. D., and J. E. Nellor. 1966. Changes in blood cellular and protein components during aging. *J. Gerontol.* 21:435-438.
- Rogel, S., and H. Hilewitz. 1978. Cardiac impairment and shock factors. *Federation Proc.* 37(13):2718-2723.

- Sonnenblick, E. 1974. Heart function and the length-tension curve. Page 232 in R. Porter and D. Fitzsimons, eds. The physiological basis of Starling's law of the heart. Associated Scientific Publishers, New York.
- Sonnenblick, E., and W. W. Parmley. 1967. Active state in heart muscle: Force-velocity-length relations, and the variable onset and duration of maximum active state. Pages 65-81 in R. Tanz, F. Kavalier, and J. Roberts, eds. Factors influencing myocardial contractility. Academic Press, New York.
- Strehler, B. L. 1964. On the histochemistry and ultra-structure of age pigment. Adv. in Gerontol. Res. 1: 343-383.
- Tate, E. L., and G. H. Herbener. 1976. A morphometric study of the density of mitochondrial cristae in heart and liver of aging mice. J. Gerontol. 31(2):129-134.
- Taylor, I. L., J. Rotter, J. H. Walsh, and E. Passaro. 1978. Is pancreatic polypeptide a marker for Zollinger-Ellison Syndrome? Lancet 1(8069):845-848.
- Thalinger, A. R., and A. M. Lefer. 1971. Cardiac actions of a myocardial depressant factor isolated from shock plasma. Proc. Soc. Exp. Biol. Med. 136:354-358.
- Trachte, G. J., and A. M. Lefer. 1978. Protective action of angiotensin converting-enzyme-inhibitor (CEI) in hemorrhagic shock. Federation Proc. 37:369. (Abstr.)
- Vaisrub, S. 1974. Myocardial depressant factor (MDF) in cardiogenic shock. J. Am. Med. Assoc. 228(4):500.
- Wangensteen, S. L., J. D. deHoll, S. F. Kiechel, J. Martin, and A. M. Lefer. 1970. Influence of hemodialysis on a myocardial depressant factor in hemorrhagic shock. Surgery 67(6):935-943.
- Wangensteen, S. L., W. G. Ramey, W. W. Ferguson, and J. R. Starling. 1973a. Plasma myocardial depressant activity (shock factor) identified as salt in the cat papillary muscle bioassay system. J. Trauma 13(3):181-194.



- Wangensteen, S. L., W. G. Ramey, W. W. Ferguson, and J. R. Starling. 1973b. Controversy over myocardial depressant factor in shock. *J. Trauma* 13(8):747-751.
- Wangensteen, S. L., R. S. Crampton, and W. W. Ferguson. 1974. Myocardial depressant factor in cardiogenic shock. *J. Am. Med. Assoc.* 228(13):1638-1639.
- Weber, K., and J. Janicki. 1977. Instantaneous force-velocity-length relations in isolated dog heart. *Am. J. Physiol.* 232:H241-H249.
- Wilkinson, J. H. 1976. The principles and practice of diagnostic enzymology. Year Book Medical Publishers, Inc., Chicago, Illinois.
- Williams, L. F., A. H. Goldberg, B. J. Polansky, and J. J. Byrne. 1969. Myocardial effects of acute intestinal ischemia. *Surgery* 66(1):138-144.
- Wilson, P. 1973. Enzyme changes in aging mammals. *Gerontology* 19:79-125.
- Yamada, T., and G. W. Pettit. 1977. Modified paper chromatographic method for assay of myocardial depressant factor. *Circ. Shock* 4:379-386.

## ACKNOWLEDGMENTS

I would like to express my warmest thanks to both Dr. Malcolm H. Crump and Dr. Frederick B. Hembrough who introduced me to this field of research and instilled in me curiosity and excitement to continue research in physiology. Their support, guidance, and sincere interest was appreciated.

I would like to thank both Dr. Franklin A. Ahrens and Dr. Richard L. Engen for their generosity in lending me valuable equipment, and Dr. Robert W. Carithers who was extremely helpful in making aged dogs available for this study.

APPENDIX

Figure 60. Bio-Gel P-2 column elution pattern of processed plasma ultrafiltrate obtained from an aged female beagle (17 years) (05)

The peaks are designated A through F in order of decreasing molecular weight. The column flow rate was 11.2 ml/hr (5.6-ml fractions). Fractions 1 through 9 had optical density readings of 0.02.

<u>Peaks</u>	<u>Elution volume (ml)</u>	<u>Location of peak height (ml)</u>
A	61.7-84.1	72.9
B	100.9-123.3	123.3
C	128.9-145.7	134.5
D	145.7-156.9	151.3
E	168.1-179.3	173.7
F	218.5-257.7	252.1

Optical density (230 nm)

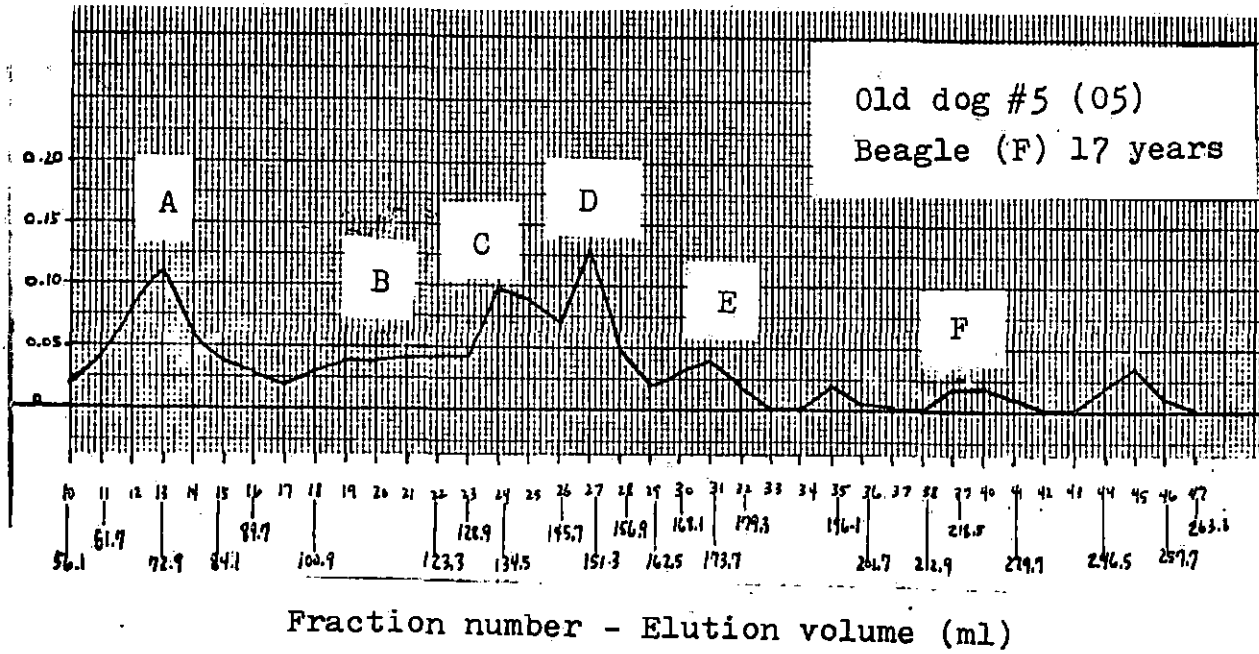


Figure 61. Bio-Gel P-2 column elution pattern of processed plasma ultrafiltrate obtained from an aged female beagle (17 years) (05)

The peaks are designated A through F in order of decreasing molecular weight. The column flow rate was 11.2 ml/hr (5.6-ml fractions). Fractions 1 through 10 had optical density readings of 0.02.

<u>Peaks</u>	<u>Elution volume (ml)</u>	<u>Location of peak height (ml)</u>
A	65.8-88.2	71.4
B	105.0-121.8	121.8
C	127.4-144.2	138.6
D	144.2-161.0	149.8
E	177.8-200.2	194.6
F	217.0-261.8	250.6

